THE UNIVERSITY
of EDINBURGH

Functional MRI in *FMR1* premutation carriers: A cross-sectional study of neurodegeneration and neurodevelopment

Stephanie S. G. Brown

PhD in Psychiatry, University of Edinburgh, 2017

Declaration

I hereby authorise the University of Edinburgh to publish the abstract of this thesis, and to authorise others to do so, for scholarly purposes and with proper acknowledgement of authorship.

I hereby authorise Edinburgh University Library to copy my thesis for the purposes of supplying copies, on request, to libraries and individuals, subject to their signing the appropriate copyright declaration which will be preserved in Edinburgh University Library.

I certify that this thesis has been composed by myself and that, as part of a larger research group, I have properly acknowledged the contribution of others where appropriate.

Stephanie S. G. Brown

14/04/2017

Abstract

Expansion of the CGG repeat region of the *FMR1* gene from less than 45 repeats to between 55 and 200 repeats is known as the *FMR1* premutation. Carriers of *the FMR1* premutation may develop a neurodegenerative disease called fragile X-associated tremor/ataxia syndrome (FXTAS), which involves progressive symptoms of tremor, ataxia and cognitive decline. Evidence also suggests that premutation carriers experience other psychiatric difficulties throughout their lifespan.

The present study aimed to investigate and delineate neurodegenerative and neurodevelopmental aspects of the premutation utilising primarily fMRI, clinical assessments and molecular measurements in 17 premutation carrier participants and 17 age-matched control participants, aged between 20 and 70 years. The functional imaging protocol included a motor task and an emotional processing task. A battery of clinical and neuropsychological tests outside of the scanner and blood-based measurements of *FMR1* CGG repeat length, FMRP levels and *FMR1* mRNA levels were also carried out.

In the motor task, premutation carriers demonstrated significantly less cerebellar activation than controls during sequential versus random finger tapping ($FWE_{corr}<0.001$). In addition, there was a significant age by group interaction in the hippocampus, inferior parietal cortex and temporal cortex originating from a more negative relationship between brain activation and age in the carrier group compared to the controls ($FWE_{corr}<0.001$). Quantative real-time PCR analysis revealed that mean age-matched *FMR1* mRNA levels display a trend towards being higher in carriers and clinical testing of motor skills additionally showed significantly worse tremor and co-ordination scores in non-FXTAS carriers. No significant associations were seen between these measurements and neuroimaging data.

During the emotional processing task, carriers exhibited significantly lower activation compared to controls ($FWE_{corr}<0.001$) at the bilateral superior parietal lobe, bilateral Brodmann Area (BA) 17 (V1), right intraparietal area and right BA18 (V2) when comparing high arousal and low arousal conditions. Group by age interaction analyses indicated no significant between group differences at a whole brain level. Clinical assessment revealed that carriers displayed significantly worse symptoms of obsessive-compulsiveness, anxiety, global severity of psychiatric symptoms, facial emotion recognition and autistic traits compared to controls and FMRP levels were comparable between groups. No significant associations were seen between these measurements and neuroimaging data.

Here, we present for the first time functional imaging-based evidence for early movement-related neurodegeneration in Fragile X premutation carriers. These changes pre-exist the diagnosis of FXTAS and are greatest in older carriers suggesting that they may be indicative of FXTAS vulnerability. Additionally, we show significantly altered emotional processing at neuropsychological, clinical and functional neuroimaging levels in carriers compared to controls, which appear to display stability over age. Overall, we present new evidence in keeping with possible neurodegenerative and neurodevelopmental traits in *FMR1* premutation carriers.

Acknowledgements

I would like to give my heart-felt thanks for the support and direction of this project from my supervisors Andrew Stanfield and Heather Whalley. I would also like to sincerely thank Peter Kind and his lab for their invaluable help in carrying out the lab-based work for this project.

All data collection, MRI analyses, statistical analyses, *FMR1* mRNA and FMRP quantification was carried out by myself.

My thanks also go to the Helen Maud-Garfit fund, which funded this work into the *FMR1* premutation.

Most importantly, I would like to thank the individuals who took part in this study and their families, who generously gave their time and energy to make this work possible.

Table of contents

Chapter 1: An introduction to the Fragile X premutation

1.1 Neurodegeneration in the Fragile X premutation and the neurological clinical presentation of FXTAS

The Fragile X-associated Tremor/Ataxia Syndrome (FXTAS) is one of the most prevalent neurodegenerative movement diseases with a known single gene causation (Tassone & Berry-Kravis 2010). The syndrome develops in approximately 40% of males and 8-16% of females who carry a repeat expansion mutation of the *FMR1* gene, which is known as the *FMR1* premutation. Specifically, the Fragile X premutation is an enlargement of the non-translated 5' CGG repeat island of FMR1 to between 55-200 repeats. The normal repeat range in the general population is anywhere up to 55 repeats (Dombrowski et al. 2002; Coffey et al. 2008). As of yet, there is no evidence-based, targeted treatment for FXTAS. However, treatment of the associated symptoms have proven effective for some affected people (Hall et al. 2006).

FXTAS presents classically as a late-onset disorder, usually in males above the age of 50 years. Patients typically experience progressive symptoms of gait ataxia, kinetic tremor and mild Parkinsonism. As the disease advances, tremor usually increases in amplitude, causing patients difficulty with every day activities that require fine motor control, such as eating and writing (Tassone, Adams, Elizabeth M Berry-Kravis, et al. 2007). Gait instability gradually worsens such that falling and loss of balance subsequently become more frequent in the later stages of the disease, often resulting in injury and causing FXTAS individuals to eventually become bed bound (Leehey et al. 2008). Features of Parkinsonism are also an important part of the FXTAS phenotype, with patients typically experiencing rigidity and hypomimia. Although these Parkinsonian symptoms are usually characterised as mild, it is estimated that over a quarter of FXTAS patients are initially misdiagnosed with Parkinson disease (Hall et al. 2005). Autonomic dysfunction, peripheral neuropathy and changes to normal endocrine functioning are also commonly found in patients with FXTAS (Tassone & Berry-Kravis 2010). Neuropathic signs in particular are thought to be linked to the presence of ataxia and increased severity has been found to positively correlate with larger CGG repeat expansions (Berry-Kravis, Goetz, et al. 2007). Moreover, electrophysiological findings in males both with and without FXTAS are found consistently to be abnormal, although this is much less significant in carriers without other neurological symptoms (Soontarapornchai et al. 2008). Autonomic dysfunction is frequently reported by older premutation carriers, with the majority of men with FXTAS experiencing urinary incontinence and some presenting with orthostatic hypotension (Jacquemont et al. 2003a).

Progressive cognitive decline also forms a major part of the FXTAS diagnosis. Approximately 40% of males with FXTAS will develop full dementia, although this frequency is likely to be an underestimate for those with late-stage FXTAS (Bourgeois et al. 2007). The percentage of women that develop dementia however is thought to be significantly lower (Hagerman et al. 2004). Clinical

reports have also suggested that subtle cognitive impairments may precede the onset of motor dysfunction in many FXTAS cases (Bourgeois et al. 2006).

The cognitive impairment in FXTAS is both cortical and subcortical, with involvement of the frontal and hippocampal structures and both cerebral and cerebellar white matter. This presents as deficits in attentional control, working memory, declarative learning and memory and information processing speed, which gradually worsen (Seritan et al. 2008). Many of these types of cognition come under the umbrella of executive functioning, which is the subset of cognitive processes that regulate planning, judgements, selective attention focussing and multi-tasking. In FXTAS, cognitive decline is primarily driven by executive dysfunction, and other deficits are thought to be largely secondary (Brega et al. 2008). An integral part of executive functioning is the autonomous initiation of purposeful behaviour and the inhibition of inappropriate activity. Dysregulation of this type of executive functioning, namely disinhibition, is a prominent deficit in individuals with FXTAS, and is one of the earliest signs of cognitive impairment for those with the Fragile X premutation. Evidence indicates that age plays a large a role in disinhibition for premutation carriers both with and without FXTAS, as the trajectory of inhibitory control appears to worsen over time (Cornish et al. 2008). Marked impairment in non-verbal intelligence, as measured by IQ scores, is also commonly seen in individuals with FXTAS, whereas verbal IQ functioning is much less affected (Hagerman et al. 2001). The executive functioning system is distributed widely across the whole brain, with many areas that feed into and out of it, nevertheless, given its integrative role of structuring goal-directed behaviour, the prefrontal cortex has been implicated as a region of interest for dysexecutive syndromes such as FXTAS (Yang et al. 2013).

It is notable that the phenotype of FXTAS is highly variable. Patients often present with varying degrees of disordered movement and cognitive impairment, with progression of the disease being extremely fast in some cases and much slower in others (Tassone & Berry-Kravis 2010). The reasons for such heterogeneity are unclear, however it is likely that both genetic and environmental factors play a role.

1.2 Neurodevelopmental disorders in Fragile X premutation carriers

Neurodevelopmental disorders such as autistic traits and psychiatric problems (including anxiety, depression, obsessive-compulsive behaviour and irritability) have been identified in Fragile X premutation carriers throughout their lifespan (Dorn et al. 1994). The manifestation of these disorders seems to be irrespective of FXTAS development, and it is possible that these neurodevelopmental abnormalities are functionally separate to neurodegeneration in carriers, representing a stable phenotype (Hagerman & Hagerman 2013).

Psychiatric checklist questionnaires have revealed that both male and female asymptomatic premutation carriers scored higher than control subjects for obsessive-compulsiveness and overall

symptom severity. Males and females with FXTAS exhibited a more severe psychiatric phenotype, with elevated scores for somatization, obsessive-compulsiveness, depression and overall symptom severity (Hessl et al. 2005). It is unclear however, whether this heightened level of psychiatric symptomatology is inherently part of FXTAS or whether existing problems are exacerbated by cognitive dysfunction and physical illness. Notably, whilst carriers commonly exhibit increased prevalence of symptoms of psychiatric disturbance, research does not suggest a link between the Fragile X premutation and clinically significant psychiatric illness (Bacalman et al. 2006). Carrier mothers that have a child with Fragile X Syndrome are especially affected with psychiatric symptomatology, with one study reporting a 55.7% lifetime incidence of mood disorders in this subset of individuals, of which 19.7% were classified as major depression disorder and 41% were classified as anxiety disorders. It is likely in these cases that stress and the lifestyle demands of caring for a disabled child with Fragile X play a large role in augmenting psychiatric difficulties (Franke et al. 1998). Recent evidence has also shown that premutation carriers have a significantly heightened risk of developing a social phobia, with lifetime prevalence in both male and female carriers being estimated at 34.2% compared with 12.6% in the general population (Bourgeois et al. 2011). Again, research is suggestive that these findings into social phobias in carriers may be a result of the interacting effects of social stress and genetic risk, given that approximately 18% of female carriers with a Fragile X child suffer from a social phobia, compared to 5.9% of female carriers without a Fragile X child (Franke et al. 1998).

The frequency of autism spectrum disorder (ASD) within in the Fragile X premutation carrier population has also been found to be significantly higher than in the general population, with an estimated 10-20% of carrier males and 1-7% of carrier females meeting the criteria for ASD, compared to less than 1% of males and females in the general population (Besterman et al. 2014; Hagerman & Hagerman 2016). Studies have shown that social deficits consistent with ASD in particular, such as poor social cognition, lowered accuracy in social perception and marked difficulty with interpersonal skills are frequently observed in carriers from a young age (Cornish et al. 2005).

Much like the neurodegenerative aspects of the Fragile X premutation, the psychiatric and neurodevelopmental problems experienced by some carriers are notably broad and heterogeneous. The genetic risk appears to be inclusive of many types of disorder or elevated symptomatology, and it is likely that environmental and socio-economic factors play a part in determining manifestation.

1.3 Molecular pathology of the premutation and FXTAS

In full Fragile X Syndrome, a CGG repeat expansion of the *FMR1* gene to above 200 repeats causes the gene to become heavily methylated, silencing its protein output by inhibiting transcriptional access to the gene (Brasa et al. 2016). However, in the Fragile X premutation, with an expansion of between 55-200 CCG repeats, the gene still produces a functional FMRP transcript. FMRP is

primarily a transcriptional regulator, and is at its highest concentrations within the brain, where it is an important regulator of synaptic plasticity and maturation (Tassone & Berry-Kravis 2010; Harlow et al. 2010). High FMRP expression levels are also observed in lymphocytes, placenta, teste, lung and kidney tissue (Hinds et al. 1993).

Studies into the molecular markers of the Fragile X gene have shown that *FMR1* mRNA levels are increased up to 8-fold the normal level in premutation carriers (Tassone, Hagerman, Taylor, Gane, et al. 2000). The reasons for this increase are as yet unclear, although it is highly likely that the expansion of the CGG repeat island alters the genetic chromatin structure, allowing improved access for transcriptional modulators of *FMR1* (Li & Jin 2012). Despite the premutation allele producing a functional protein transcript, it has also been shown that FMRP levels are slightly lower in carriers, especially when the numbers of CGG repeats are higher (Li & Jin 2012; J. M. Wang et al. 2012; Berry-Kravis & Hall 2011). The causation of these lower FMRP levels are uncertain, as given that *FMR1* mRNA levels are higher it would be reasonable to expect that FMRP levels would also be increased. However, it has been suggested that falls in FMRP may result from deficits in the mRNA translational efficiency, as an expanded CGG repeat island impedes ribosomal subunit migration to the start codon (Li & Jin 2012). It seems likely when considering the role of FMRP in both healthy brain development and Fragile X Syndrome, that small decreases in FMRP in carriers may be the driving force behind neurodevelopmental abnormalities, in particular autistic traits. Nevertheless, it is widely accepted that it is the large increases in *FMR1* mRNA that are the major causative factor in the development of FXTAS (Garcia-Arocena & Hagerman 2010).

The characteristic neuropathological hallmark of FXTAS is the presence of intranuclear inclusions, the formation of which is thought to be driven by an excess of *FMR1* mRNA. Studies investigating how high levels of *FMR1* mRNA may cause neurotoxicity in FXTAS have shown that intranuclear inclusions in neurones and astrocytes are formed regardless of the presence of encoding regions of the *FMR1* gene but do not form without the CGG repeat expansion (Hagerman & Hagerman 2004). Intranuclear inclusions that contain *FMR1* mRNA are found throughout the brain and brainstem of FXTAS patients (Greco et al. 2002; Greco et al. 2005). Exactly how these inclusions develop however is undetermined, but in keeping with the gain-of-function theory, the favoured opinion is that excess mRNA begins to sequester mRNA binding proteins, including histones, heat shock proteins and cytoskeletal proteins. In particular, neurofilament isoforms A and C have been shown to play a role in the formation of intranuclear inclusions, which is likely to cause neurofilament and trafficking dysregulation within neurones and could be a major contributing factor to peripheral neuropathy in carriers. Additionally, the direct effects of accumulation within cells are not the only facets to consider, as knock-on effects of sequestration such as inhibition of normal mRNA binding protein functions are entirely probable (Tassone, Hagerman, Taylor, Gane, et al. 2000; Greco et al. 2005).

Repeat Associated non-AUG initiated (RAN) translation has also been implicated in the molecular pathology of FXTAS. RAN translation is the process by which a protein is translated from outside of the open reading frame of a gene in association with an island of repeated base sequences, and here the expanded CGG repeat region triggers the production of a polyglycine-containing protein known as FMRpolyG (Oh et al. 2015). This protein product has been demonstrated to be toxic in multiple human cell lines, and accumulates in intranuclear inclusions in cell culture, mouse models of FXTAS and human patients. Evidence suggests that FMRpolgG is a significant contributor to neurodegeneration in premutation carriers as intranuclear inclusions in FXTAS are ubiquitin-positive in pathology studies, and the effects of this combined with RNA toxicity may be additive or synergistic. Moreover, RAN translation has become a more prominent focus in neurodegeneration research as a whole, as similar repeat associated proteins initiated outside of the open reading frame have been implicated in amyotrophic lateral sclerosis and frontotemporal dementias (Todd et al. 2013; Todd et al. 2010).

Recent findings have also found that antisense transcription plays a role in the molecular pathology of FXTAS. The antisense transcript *ASFMR1* overlaps the CGG repeat island of the *FMR1* gene, is transcribed in an antisense orientation and has been recently suggested to subsidise phenotypic variations associated with disorders arising from the expansion of *FMR1* (Khalil et al. 2008). The premutation allele causes *ASFMR1* mRNA to be upregulated, in a similar way to original *FMR1* mRNA upregulation, and both are silenced by the full Fragile X mutation. Alternative splicing of this gene product has been identified in carriers of the premutation, again suggestive of a neurodegenerative role in FXTAS (Ladd et al. 2007).

Despite a lack of exact molecular understanding of how toxic RNA gain-of-function, RAN translation and antisense transcription contribute to phenotypes of the premutation and FXTAS, it is likely that combined downstream effects of these genetic changes cause severe cellular stress and subsequent programmed cell death. This manifests at a tissue and whole brain level as the classical radiological findings and symptomatic presentation of FXTAS.

1.4 Genotype and phenotype relationships

Molecular measurements from the *FMR1* gene have been shown in a wealth of studies to have associations with various phenotypic features of FXTAS.

One of the most commonly drawn conclusions from study data is that occurrence and severity of FXTAS are associated with larger CGG repeat sizes in the *FMR1* gene (Leehey et al. 2008; Tassone, Adams, Elizabeth M Berry-Kravis, et al. 2007; Allen et al. 2008b). Of motor and nerve conduction symptomatology, it has been demonstrated that age of onset for tremor and ataxia, and peripheral neuropathy measurements are significantly correlated with size of the CGG repeat region (Tassone, Adams, Elizabeth M. Berry-Kravis, et al. 2007; Berry-Kravis, Goetz, et al. 2007). Cognitive FXTAS

phenotypes have also shown significant associations with CGG repeat length, with poorer scores of intelligence as measured by the Full Scale Intelligence Quotient (FSIQ), perceptual organisation, processing speed and executive functioning as measured by the Behavioural Dyscontrol Scale, the Controlled Oral Word Association Test and the Symbol Digit Modalities Test all demonstrating a significant association with larger repeat sizes (Hessl et al. 2005; Cohen et al. 2006; Grigsby et al. 2007). Poorer scoring for inhibitory control and cognitive impairment as measured by the Mattis Dementia Rating Scale also showed a relationship to a larger number of CGG repeats (Cornish et al. 2008; Sévin et al. 2009). Repeat size however has not proven to be a significant indicator of psychiatric illness or elevated psychiatric symptoms in premutation carriers, with no significant association with somatization, obsessive-compulsiveness, interpersonal sensitivity, depression, anxiety, hostility, phobic anxiety, paranoid ideation or psychoticism (Hessl et al. 2005). When considering radiological changes associated with FXTAS however, repeat size again shows some significant correlations. Voxel density of cerebellum, amygdala-hippocampal complex and thalamus and whole brain, cerebral, cerebellar and ventricular volume all significantly associated with length of the CGG repeat region, as may be expected given the phenotypic correlation between higher repeat sizes and more severe FXTAS symptomatology (Moore et al. 2004; Loesch et al. 2005; Cohen et al. 2006; Adams et al. 2007). In keeping with these findings, CGG repeat size also showed a positive correlation with percentages of neurons and astrocytes in brain pathology samples with intranuclear inclusions (Greco et al. 2006).

As demonstrated by the literature, CGG repeat size shows many significant phenotypic relationships. Investigation into these associations is very much supported by accurate genetic analysis techniques in determining base pair sequences, meaning that measurements obtained from peripheral blood samples are precise representations of repeat sizes (Tassone et al. 2008; Tzeng et al. 2005). It is also of note that for the development of some premutation or FXTAS phenotypes, those which show no or inconsistent relationships with CGG repeat length, that repeat expansion size may have little to no effect magnitude. However, more investigation into the molecular biology of the expanded *FMR1* CGG repeat island is required.

Measurements of *FMR1* mRNA also show some relationships to FXTAS and premutation phenotypes, as may be expected given the higher levels of *FMR1* transcription in carriers and links to gain-of-function toxicity. In premutation carriers only, levels of *FMR1* mRNA were observed to correlate with scores of peripheral neuropathy and nerve conduction (Berry-Kravis, Goetz, et al. 2007; Soontarapornchai et al. 2008). Significant associations were not identified however between mRNA levels and FXTAS rating scores (Tassone, Adams, Elizabeth M Berry-Kravis, et al. 2007). Cognitive measurements also showed no associations (Hessl et al. 2005; Cohen et al. 2006). Measures of psychiatric symptoms did show a relationship with *FMR1* mRNA levels, with somatization, obsessive-compulsiveness, interpersonal sensitivity, depression, anxiety, hostility, paranoid ideation

and psychoticism, but not phobic anxiety, exhibiting a significant correlation (Hessl et al. 2005). Most radiological features showed no significant association, except for hippocampal volume (Cohen et al. 2006; Adams et al. 2007; Moore et al. 2004).

It may be considered a somewhat surprising finding that almost all psychiatric measurements significantly associated with *FMR1* mRNA, as psychiatric symptomatology in carriers is thought to be primarily neurodevelopmental, and therefore would not be likely to correlate with a build-up of high levels of mRNA. However, given that many patients with neurodegeneration experience worsening psychiatric problems, it is likely that these significant associations are related to FXTAS pathology and are not developmental in nature (Kazui et al. 2016; Ismail et al. 2016). Studies to replicate these findings would also be beneficial to establish to robustness of such correlations. In addition, phobic anxiety did not show a relationship with *FMR1* mRNA, despite being reported as significantly worse in a FXTAS sample, and this may be due to it being a more stable, life-long trait in carriers (Hessl et al. 2005). Additionally, lack of associations between radiological changes associated with FXTAS and *FMR1* mRNA levels in some studies are also rather unexpected when considering the RNA gain-of-function toxicity hypothesis (Moore et al. 2004; Qurashi et al. 2011). This may be due to some radiological changes during the disease not being driven, at least primarily, by changes in RNA, however it is more likely that peripheral measurements of *FMR1* mRNA are not accurately representing brain expression. Implication of the hippocampus however may be indicative of a limbic vulnerability to the onset of molecular pathology and inclusion formation in FXTAS, in a similar manner to other neurodegenerative diseases and mechanisms of aggregate development (Hochgräfe et al. 2013; Nunomura et al. 2012; Kandiah et al. 2014). These studies demonstrate the complex nature of linking FXTAS pathology or premutation traits to *FMR1* mRNA levels, as results show inconsistency of expected correlations with neurodegenerative and neurodevelopmental traits. Aside from a complexity of molecular pathology that is not yet established, it may be possible that the reason for these discrepancies is that blood-based molecular measurements are not necessarily reflective of distinct expression profiles in the brain, or indeed may only reflect some areas of *FMR1* expression in the brain but not others.

Fewer studies have investigated FMRP levels in addition to *FMR1* mRNA and CGG repeat length, most likely due to the more difficult methodology of isolating and quantifying protein levels without brain tissue. Nevertheless, in studies that have investigated FMRP quantity and phenotypic relationship, no association was found between FMRP and cognition as measured by the FSIQ or any psychiatric symptom (Hessl et al. 2005; Cohen et al. 2006). A significant association was identified however between lower voxel density of the cerebellum, amygdala-hippocampal complex and thalamus in carriers and FMRP levels (Moore et al. 2004).

When considering the data that carriers have slightly lower levels of FMRP and the wealth of existing knowledge of the importance of FMRP during brain development, it may be expected that carriers have cognitive and neurodevelopmental differences that are driven in part by FMRP (Primerano et al. 2002; Lozano, Rosero, et al. 2014). However, findings have shown a lack of relationship between these variables as measured by the FSIQ and psychiatric checklists (Hessl et al. 2005; Cohen et al. 2006). Again, the reason for the lack of significant findings may be the difficulty in using peripheral blood for molecular investigation, but also, given that changes in FMRP in carriers are moderate at best and notably variable, it is likely that modest effect sizes may be missed. A significant association between the radiological measurements of voxel density at the cerebellum, amygdala-hippocampal complex and thalamus and FMRP has been established, and this brain phenotype exhibited no relationship to *FMR1* mRNA levels (Moore et al. 2004). This finding of lower brain voxel density in carriers therefore could possibly be considered to be linked to changes in regional brain structural integrity due to the vital role FMRP plays in early synaptic plasticity.

Overall, the use of regression analyses for establishing genotypic and phenotypic relationships in FXTAS and the premutation has been important for the field. However, a number of limitations, as previously discussed, may mean that underlying molecular pathology and its association to various clinical, cognitive, psychiatric or radiological phenotypes may be being understated.

1.5 The epidemiology of the Fragile X premutation and FXTAS

The prevalence of the Fragile X premutation is estimated to be between 1/150 to 1/300 in females and between 1/400 to 1/850 in males (Tzeng et al. 2005; Dombrowski et al. 2002; Hagerman & Hagerman 2016). Within the premutation population, it is estimated that over a third of males over the age of 50 exhibit both tremor and ataxia, meeting the criteria for a diagnosis of probable FXTAS. Penetrance further increases with age, with over half of premutation males showing signs of FXTAS above the age of 70 (Sébastien Jacquemont et al. 2004). Penetrance of FXTAS in female carrier populations appears to be significantly lower, in addition to symptoms of the disease often being much milder. It is estimated that approximately 8% of women who carry the premutation allele and are over the age of 40 exhibit signs of FXTAS (Coffey et al. 2008).

By combining data on the frequency of the *FMR1* premutation allele in the general population, and considering incomplete FXTAS penetrance within this group, FXTAS is estimated to affect 1/4,000 males over the age of 50 within the general population (Dombrowski et al. 2002). Direct population-based studies on FXTAS have yet to be conducted, given the rarity of the disease and the regularity of misdiagnoses of FXTAS as other types of movement disorder and cognitive neurodegeneration. In addition, other epidemiological facets of carrier status are yet to be defined, such as mortality rates or expansion quantifications of the CGG repeat island. Further epidemiological study into these aspects of the Fragile X premutation are likely to reveal significant and medically relevant insights into the

nature of carrier status and FXTAS, and may indeed demonstrate that *FMR1* repeat-associated disorders are not as uncommon as originally thought.

Since the Fragile X-associated Tremor/Ataxia Syndrome was identified in 2001, awareness of individuals and families affected by the condition has continued to increase, as has the understanding of the lifelong neurodevelopmental issues that also may affect carriers. The presence of the premutation allele is an important factor for families to consider, if, indeed, they are aware of it. This is because the premutation allele is known to expand in the CGG repeat island region over maternal transfer (Nolin et al. 2003). If the CGG repeat length exceeds the premutation range, which as previously mentioned, is between 55-200 repeats, and becomes longer than 200 repeats, then the *FMR1* gene becomes heavily methylated, inhibiting access for transcriptional regulator proteins and obstructing transcription. This DNA methylation silences the gene, blocking protein output and causes a severe neurodevelopmental disorder called Fragile X Syndrome, which is characterised by major intellectual disability, global developmental delay and autistic traits (Penagarikano et al. 2007). For reasons that are as yet unclear, the premutation allele does not tend to expand over paternal transfer. Therefore, given the sex-linked nature of the *FMR1* gene, males with the premutation will always pass on a stable carrier allele to their daughters, but never to their sons. Females with the premutation however, will have a 50% chance of passing on the allele to a child of either sex, with the likely possibility that the CGG repeat island of *FMR1* will also expand and the child will have Fragile X Syndrome (Nolin et al. 1996).

Penetrance of Fragile X-associated disorders differs significantly between men and women, and this is clearly seen in the premutation. Because of the presence of a second, functioning *FMR1* allele in women, the effects of the mutated allele are somewhat masked. This is not the case for males, who carry only one copy of *FMR1*. Within the female carrier population however, there is significant heterogeneity of phenotype (Hagerman et al. 2004; Franke et al. 1998). This heterogeneity stems from the natural process of X-inactivation within female cells, where one of the two X chromosomes in each cell is silenced at random to provide dosage compensation of X-related genes. X-inactivation in females with the premutation means that percentages of the active premutation allele can vary significantly between women, meaning that the severity of Fragile X premutation carrier symptomatology fluctuates to a large degree (Nolin et al. 2003; Nolin et al. 1996). In a similar way, X-inactivation plays a large role in protecting many girls and women with the full mutation from serious intellectual disability and autism, as females inheriting an *FMR1* CGG repeat length greater than 200 will have a 50-70% risk of showing features of Fragile X Syndrome, compared to virtually 100% of males (Keysor & Mazzocco 2002).

Taking into account the aforementioned problems in assessing the epidemiological presence of FXTAS and the Fragile X premutation, it is possible that their prevalence may be larger than current

data suggests. It is therefore of importance that the field pursue population, such as newborn, screening and understanding of the effects of carrying the premutation, in the hope that targeted treatments may be developed in the future and benefit a larger-than-expected clinical group.

Chapter 2: A systematic review of neuroimaging findings in Fragile X premutation carriers

2.1 Introduction

The neuroimaging techniques employed in premutation research to date have been magnetic resonance based structural, diffusion tensor and functional imaging. Neuroimaging has played a vital part in advancing our knowledge and understanding of the premutation and FXTAS. Much of the current research has served to elucidate FXTAS diagnostic criteria and to begin to unravel the complex pathology of both neurodevelopmental abnormalities and neurodegeneration in carriers. It is likely that in the future, neuroimaging studies will start to reveal more sophisticated measurements of subtle changes in the brain, allowing a greater understanding of the disease process and directing clinicians towards a clearer understanding of prognosis.

Structural magnetic resonance imaging (MRI) is a technique that images parts of the body, in this case the brain, using contrasts created by the magnetic properties of water molecules in the body. It is a favoured method of neuroimaging as it is safe and non-invasive, however an MRI scan is both costlier and more time-consuming than other types of medical imaging and can exacerbate anxiety and claustrophobia in patients or research participants (Eshed et al. 2007). Nevertheless, given that MRI has high-quality image resolution and effectively differentiates between tissue types within the brain, such as white matter and grey matter, it is one of the most utilised imaging modalities for medical research (Bigler 2015).

Diffusion tensor imaging (DTI) is a structural MRI technique that utilises the diffusion and movement of water molecules to produce contrasted brain images. As water molecules will not diffuse freely in brain tissue, the nature of their motion can reveal detailed insights into brain tissue architecture. The variation in the restriction of the diffusion of water molecules means that structural integrity of neuronal tracts can be reliably investigated in both control and patient groups. The drawbacks of this valuable experimental technique include the fact that DTI scans are very noisy and can cause discomfort for participants, especially in those who are claustrophobic or anxious. In combination with a long scan time to obtain detailed and usable DTI data, this means that participants can be prone to not completing the scan. However, these issues can be fairly easily managed with appropriate preparation and explanation for subjects undergoing a DTI scan (Garin-Muga & Borro 2014; Assaf & Pasternak 2008).

Functional MRI (fMRI) is a technique utilised in premutation research that measures functional brain activity by monitoring changes that are associated with blood flow. The technique is based upon a contrast known as the blood-oxygen-level dependant (BOLD) response, which is reliant on the MRI scanner identifying changes in the magnetic properties of blood in the brain. Because neuronal activity and blood flow are tightly coupled, when neuronal populations are active, blood flow to those specific areas increases (Buxton 2013). Consequently, fMRI can reliably display active regions of the

brain in response to sets of stimuli and is a frequently employed method in psychiatric and neurology research. There are however some problematic aspects to the use of functional imaging, one prominent issue being that head movement during scanning can result in artificial changes in activation signals in the brain. Another issue is ambiguous baseline conditions during testing, given that the brain is constantly active. This means that experimental design must carefully take baseline activity into account, and control or rest conditions within a task must be appropriate to the test conditions to minimise physiological noise. This type of problematic and unwanted brain activity must also be taken into consideration during image processing and data analysis. Task design is also a critical part of experimental legitimacy, and poorly designed scanner tasks can be significantly detrimental to valid results. For example, a task utilising a blocked design – one which groups stimuli together to allow for an additive hemodynamic response – must use a baseline condition suited to the task stimuli, and awareness of the fact that participants may experience boredom or predict parts of the task when blocks are not randomised is important. In contrast to block design, an event-related design of a scanner task may be used to minimise aspects of boredom and task prediction. This type of design uses short, randomised presentation of stimuli, and as such is considered to be a more realistic test of brain activation. However, as the BOLD response to stimuli presented in this manner is inherently low and event-related designs lack the robust statistical power that a block design possesses. If these issues are properly taken into account and managed however, fMRI can be a very insightful and useful imaging technique (Glover 2011; Eklund et al. 2016).

Here, the aforementioned imaging techniques utilised in investigation into individuals with the Fragile X premutation are reviewed with respect to the current published literature.

2.2 Methods

Medline, EMBASE and PsychINFO were searched for all English language studies published between January 1990 and December 2013 that reported imaging data in fragile X premutation carriers. Terms included in the search were as follows: “Fragile X” “Fragile X premutation” “premutation carriers” and related terms combined using the AND operator with “magnetic resonance imaging”. All abstracts resulting from the search were assessed for inclusion. There were 422 abstracts identified during the search, of which 385 were excluded due to lack of relevance to neuroimaging and/or the Fragile X premutation. There were 37 articles that remained, which were then assessed according to inclusion criteria individually in full text. Primary research articles were considered for inclusion if they were published by an English language peer-reviewed journal, used sample groups of fragile X premutation carriers with or without FXTAS and compared the group(s) to a group of healthy controls and included structural, functional or diffusion tensor MRI methodology. The process of selection of papers is summarised in Figure 2.1.

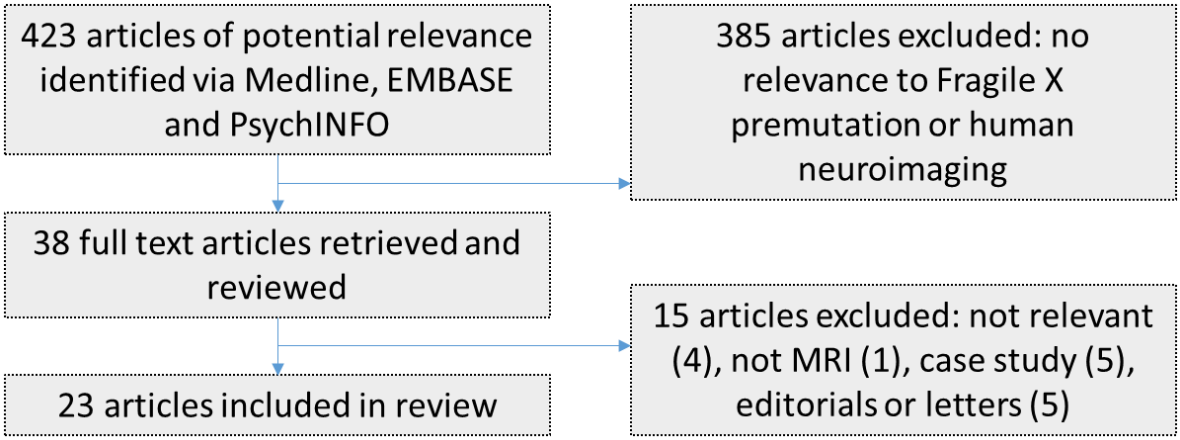

Figure 2.1. Inclusion and exclusion process of relevant literature.

2.3 Results

Studies utilising structural MRI techniques have identified substantial radiological changes in premutation carrier populations both with and without FXTAS in comparison to control subjects. A number of these structural brain abnormalities form important diagnostic criteria for FXTAS and can be particularly useful in differentiating between FXTAS and other similar neurological diseases.

To date, a total of 12 studies have used structural MRI in premutation carrier groups (these are summarised in Table 2.1). Of these studies, eleven utilised quantitative measurements and one used qualitative analysis techniques. A notable finding of these studies involves a hallmark radiological feature of FXTAS, which is a region of increased T2 signal intensity at the middle cerebellar peduncles (MCPs), commonly known as the MCP sign. The MCP sign is a primary diagnostic criterion for FXTAS, and its pathological basis is thought to originate from the development of spongiosis in the deep cerebellar white matter (Berry-Kravis, Abrams, et al. 2007). However, it is worth noting that presence of an MCP sign is not completely indicative of FXTAS, as it has been reported in other neurodegenerative disorders, such as multiple system atrophy. Similarly, it is estimated that the MCP sign is only present in 60% of male individuals with FXTAS and 13% of female individuals with FXTAS (Adams et al. 2007). The MCP sign was identified in FXTAS groups in all of the four studies that investigated this region. Cerebellar and cerebral atrophy is also found in virtually all patients with FXTAS, with 9 out these 12 studies both quantitatively and qualitatively identifying such volume loss. Carrier populations both with and without diagnosed FXTAS exhibited statistically significant decreases in volumes of the total brain, cerebrum, cerebellum and brain stem (Loesch et al. 2005; Cohen et al. 2006). Mild to moderate loss of volume was observed in 75% of carriers with signs of FXTAS, and 20% of patients showed loss of volume that was characterised as severe (Jacquemont et al. 2003a). Radiological findings were less pronounced and less frequent in FXTAS patients with milder symptomatology (Juncos et al. 2011). The corpus callosum is also an area of interest in FXTAS disease pathology, with thinning apparent from both qualitative and quantitative volumetric analysis in the majority of patients with a diagnosis (Brunberg et al. 2002). Changes in hippocampal and amygdala volume have also been noted in multiple studies, however these are less significant and findings have not been reliably replicated between research groups (Loesch et al. 2005; Cohen et al. 2006; Selmeczy et al. 2011).

Table 2.1: Structural Imaging Studies

Study	Participants	Methodology	Significant findings
(Brunberg et al. 2002)	17 male PMCs with signs of FXTAS (mean age 68) and 14 male controls	Molecular measures (CGG repeat size,	15/17 PMCs showed symmetrically decreased T1 and increased T2 signal intensities in cerebellar white matter 14/17 PMCs exhibited the MCP sign

	(mean age 66 years)	FMRP and FMR1 mRNA) Structural and volumetric MRI	Cerebellar cortical atrophy was present in 16/17 PMCs and cerebral atrophy was present in all PMC participants The corpus callosum was thinned in 14/16 PMCs and MCPs were atrophic compared to the control group
(Jacquemont et al. 2003b)	20 male PMCs with FXTAS (aged >50 years) and 20 matched controls. PMCs recruited through FXS families	Molecular measures (CGG repeat size, FMRP and FMR1 mRNA) Structural and volumetric MRI	Mild to moderate loss of cerebral cortical volume was present in 75% of patients. The volume loss was severe in 20% Increased T2 signal intensity in the subependymal and deep white matter of the frontal and parietal lobes was seen in 75% of patients
(Moore et al. 2004)	20 male PMCs and 20 male age matched controls. PMCs recruited through FXS families.	Molecular measures (CGG repeat size, FMRP and FRM1 mRNA) Structural and volumetric MRI	The PMC group had significantly less voxel density in several brain areas including the cerebellum, thalamus and amygdalo-hippocampal complex Aging, increased CGG repeat size and decreased FMRP were all associated with decreased voxel density Regional grey and white matter density is significantly affected in PMCs
(Loesch et al. 2005)	12 male PMCs (mean age 62.15) and 11 male matched controls (mean age 62.1). PMCs recruited through FXS families.	Structural and volumetric MRI Cognitive testing Molecular measures (CGG repeat size and FMR1 mRNA)	Variable MRI changes in PMCs classified as being 'neurologically affected', including cerebral, cerebellar atrophy and the MCP sign
(Cohen et al. 2006)	11 male PMCs without FXTAS, 25 male PMCs with FXTAS and 21 male matched controls. Aged	Structural and volumetric MRI (performed on segmented total cranial volume	No differences in radiological findings between unaffected PMCs and controls, except for a reduction in brainstem volume (the brainstem-cerebellar region extended from one slice inferior to the anterior commissure to the most inferior slice containing the cerebellar vermis;

	between 51-79. PMCs recruited through FXS families.	axial FLAIR images) Neurocognitive testing Molecular measures (CGG repeat size and FMR1 mRNA)	the inferior border of the cerebellar vermis was used as a tracing cut-off) Differences in all brain region volumes measured, except for hippocampus, between FXTAS affected and control groups CGG repeat length was associated with the volume of many areas including the cerebellum, ventricle and whole brain white matter hyperintensity IQ scores were significantly associated with volumes of multiple regions including whole brain, cerebrum, cerebellum, hippocampus, ventricles and whole brain white matter hyperintensity Higher CGG repeat lengths were correlated with lower IQ scores
(Adams et al. 2007)	15 female PMCs with FXTAS (age 59.5±10.3 years), 20 unaffected PMC females (age 43.3 ± 11.2 years), and 11 matched female controls (age 51.0 ± 10.3 years). 36 male PMCs with FXTAS (age 65.0 ± 5.6 years), 25 unaffected PMC males (age 53.5 ± 12.5 years) and 39 matched male controls (age 58.0 ± 15.0 years). PMCs recruited through FXS families.	Structural and volumetric MRI Clinical evaluation Molecular measures (CGG repeat size and FMR1 mRNA)	Less pronounced reductions of cerebellar volumes and less involvement of the MCP sign was seen in female PMCs compared to male PMCs Reduced brain volumes and increased white matter disease in PMC females compared to control females Significant associations between reduced cerebellar volume, increased severity of FXTAS symptoms and increased CGG repeat size

(Loesch et al. 2008)	24 male PMCs, aged above 33 years and 21 matched controls.	Structural and volumetric MRI	PMCs showed significant decrease in total brain and cerebrum volumes Volumes of right, left and total hippocampus were significantly increased in PMCs Significant correlation with decreased brain volume and increasing CGG repeat size
(Adams et al. 2010)	16 female PMCs with FXTAS (age 57.5 ± 12.46 years), 17 unaffected PMC females (age 44.94 ± 11.23 years), and 8 matched female controls (age 50.63 ± 11.43 years). 34 male PMCs with FXTAS (age 66.44 ± 6.77 years), 21 unaffected PMC males (age 52.38 ± 12.11 years) and 30 matched male controls (age 57.2 ± 14.12 years). PMCs recruited through FXS families.	Structural and volumetric MRI Clinical evaluation Molecular measures (CGG repeat size and FMR1 mRNA) Psychological symptoms	Significant negative correlation between total hippocampal volume and anxiety in female PMCs with and without FXTAS. This was driven by the significant negative correlation between right hippocampal volume and anxiety In male PMCs with and without FXTAS, only paranoid ideation negatively correlated with hippocampal volume Female PMCs also demonstrated a negative association between hippocampal volume and severity of anxiety-related symptoms Negative association between CGG repeat size and hippocampal volume, but this was not significant after adjustment
(Selmeczy et al. 2011)	49 PMC males (mean age 48.5 years) and 48 matched controls (mean age 47.9 years). PMCs recruited through FXS families.	Intelligence and psychological testing Molecular measures (CGG repeat size and FMR1 mRNA) Structural and volumetric MRI	No significant differences between groups in amygdala volumes Significant negative correlation between amygdala volume and the lower range of CGG repeat expansions, but not the higher range

(Juncos et al. 2011)	50 male PMCs, with and without FXTAS (mean age 65 years). PMCs recruited through FXS families	Testing for tremor, ataxia and cognitive defects Full neurologic evaluation, including clinical assessments and structural MRI	The majority of PMCs exhibited general volume loss and the MCP sign CGG repeat size did not seem to correlate with FXTAS severity Radiological changes were less severe and less frequent in participants with milder FXTAS symptomatology
(Hashimoto, Javan, et al. 2011)	31 male PMCs with FXTAS, 24 male PMCs without FXTAS and 28 male matched controls (aged between 40 and 80 years)	Molecular measures (CGG repeat size and FMR1 mRNA) Psychological and cognitive assessment Structural and volumetric MRI	Grey matter loss in cortical and subcortical regions was seen in FXTAS patients Significant associations between grey matter loss in the left amygdala and increased levels of obsessive-compulsive and depressive traits. Also significant associations seen between decreased grey matter in the left inferior frontal cortex and anterior cingulate cortex and poor working memory Significant negative effect of CGG repeat size on grey matter density in the dorsomedial frontal regions
(Wang, Hagerman, et al. 2013)	11 male PMCs without FXTAS, 36 male PMCs with FXTAS and 14 male controls (aged between 47-81 years)	Structural and volumetric MRI Clinical assessments for presence of FXTAS and psychiatric problems.	FXTAS group showed significant atrophy in the bilateral thalamus and putamen, left caudate and right pallidus compared to controls FXTAS group also showed significant DWI hypointensity in the bilateral thalamus, caudate, putamen and right pallidus compared to controls Volume measurements of the bilateral thalamus and putamen, and left caudate showed significant negative correlation with FXTAS stage
Abbreviations **PMC: premutation carrier; FXS: Fragile X Syndrome MCP: middle cerebellar peduncle**			

Four DTI studies in Fragile X premutation carriers have been published to date (these are summarised in Table 2.2).

Patients with FXTAS demonstrated significantly lower structural connectivity in motor, limbic, association and callosal white matter fiber tract categories (J. Y. Wang et al. 2012). As might be expected, motor fiber tracts were of particular interest, with carriers with established FXTAS displaying reductions in connectivity at the descending motor tract, the MCP, the superior cerebellar peduncle and the anterior body of the corpus callosum (Wang, Hessl, et al. 2013). Patients with FXTAS were also found to have reduced fractional anisotropy (FA) in multiple white matter tracts, including the MCPs, the superior cerebellar peduncles, the cerebral peduncle, the fornix and the stria terminalis. In this study, in carrier groups both with and without FXTAS, both axial and radial diffusivities were found to be significantly higher than controls at the MCPs (Hashimoto, Srivastava, et al. 2011).

Table 2.2: Diffusion Tensor Imaging Studies

Study	Participants	Methodology	Significant findings
(Hashimoto, Srivastava, et al. 2011)	35 PMC males with FXTAS, 16 PMC males without FXTAS and 20 matched male controls. Participants aged between 40 and 79 years.	Structural MRI: Diffusion tensor imaging, tract of interest (TOI) analysis Molecular measures (CGG repeat size, FMRP and FRM1 mRNA)	FXTAS group showed significant reductions in fractional anisotropy (FA) in multiple white matter tracts including the MCPs, superior cerebellar peduncle, cerebral peduncle, the fornix and stria terminalis Axial and radial diffusivities were significantly elevated in the MCP in both premutation groups U-shaped relationship between CGG repeat size and axial and radial diffusivities in the MCP
(J. Y. Wang et al. 2012)	15 PMCs aged under 45 years and 19 matched controls under 45 years (younger groups). 15 PMCs aged over 45 years with FXTAS, 11 PMCs aged over 45 years without FXTAS and 15 matched controls aged over 45 years (older groups). Participants were all male.	Structural MRI: Diffusion tensor imaging, tractography	Carriers with FXTAS showed reduced structural connectivity relative to controls in motor, limbic, association and callosal fiber tract catagories Carriers with FXTAS also showed greater age-related decline in structural connectivity in limbic, association and callosal fiber tracts Only groups with lesions in the MCP and corpus callosum exhibited significantly reduced structural connectivity

(Battistella et al. 2013)	30 PMC males and 37 male matched controls aged between 20-70 years. All participants had a family member with FXS.	Global cognitive assessment Neurologic evaluation Structural MRI: Diffusion tensor imaging, radial and mean diffusivity, FA and axial diffusivity maps Molecular measures (CGG repeat size)	Grey matter voxel based morphometry showed a lower grey matter volume in the anterior lobule VI of the cerebellum and bilateral thalamus in PMCs Radial diffusivity was increased at the MCPs, hippocampal fimbria/fornix and stria terminalis bilaterally MCP radial diffusivity showed interaction with age and CGG repeat size
(Wang, Hessl, et al. 2013)	36 male PMCs with FXTAS, 26 male PMCs without FXTAS and 34 male controls. PMCs were recruited via FXS families	Structural MRI: Diffusion tensor imaging, volume and average values of FA, MD and average DWI Molecular measures (CGG repeat size and FRM1 mRNA)	FXTAS group had significantly lower tract volume at the descending motor tract, the MCP, the superior cerebellar peduncle (SCP) and the anterior body of the corpus callosum CGG repeat length correlated negatively with the SCP tract volume in both PMC groups CGG repeat length also correlated negatively with SCP FA in the FXTAS group

Abbreviations

PMC: premutation carrier; MCP: middle cerebellar peduncle, FA: fractional anisotropy, MD: mean diffusivity, DWI: diffusion-weighted image

To date, there have been 7 publications of fMRI data in premutation carriers (these are summarised in Table 2.3). These considered multiple different types of cognition and processing, with one investigating numerical processing, two investigating social processing and four investigating various aspects of memory. In one study into working memory, premutation carrier groups both with and without FXTAS generally performed equally well in the scanner tasks compared to the control group. However, both premutation groups showed significant differences in activation during the task, with the right ventral part of the inferior frontal cortex (vIFC) and the left dorsal part of the inferior frontal

cortex and premotor cortex (dIFC/PMC) exhibiting a reduction in activation (Hashimoto, Backer, et al. 2011). Tasks requiring associative memory recall showed that carriers had reduced left hippocampal activation in comparison to controls, in addition to increased parietal activation patterns (Koldewyn et al. 2008). Premutation carriers also displayed a low level of temporoparietal activation during temporal working memory retrieval compared to spatial working memory retrieval, whereas controls exhibited higher levels (Kim et al. 2014). In a study involving a magnitude estimation task carried out in the scanner, the premutation group were found to have significantly decreased lower fronto-parietal activation, particularly at the bilateral inferior parietal lobule and the left inferior frontal gyrus (Kim et al. 2013). Emotional processing tasks have also reliably shown premutation carrier group activation differences in comparison to controls, with two studies finding a reduction in amygdala activation in response to emotional stimuli. In particular, the right and overall amygdala activations appear significantly lower (Hessl et al. 2007; Hessl et al. 2011). One study found additional significant reductions of activation at the bilateral superior temporal sulcus, the bilateral orbital gyrus and the bilateral insula during emotional processing, whereas these areas were reliably activated in the control population (Hessl et al. 2011).

Table 2.3: Functional Imaging Studies

Study	Participants	Methodology	Significant findings
(Hessl et al. 2007)	12 PMC males (mean age 42.9 years) and 13 male matched controls (mean age 39.8 years)	Psychological assessment (intelligence and psychological symptoms) Molecular genetic measures (CGG repeat size, FMR1 mRNA) Structural and functional MRI/face processing task Fear potentiated startle and skin conductance paradigms	In PMCs, psychological symptoms were significantly associated with decreased right amygdala volume PMCs showed an overall decrease in amygdala activation and varied activation patterns Unlike in controls, PMCs showed no significant activation in the bilateral superior temporal sulcus, bilateral orbital gyrus and bilateral insula PMCs showed a greater overall activation in response to calm faces
(Koldewyn et al. 2008)	11 PMC males (mean age 42.9 years) and 11	Psychological assessment (intelligence and	Groups did not differ in hippocampal volume PMCs showed reduced left

	matched male controls (mean age 39.8 years).	psychiatric symptoms) Molecular genetic measures (CGG repeat size, FMR1 mRNA) Structural and functional MRI/associative memory recall task	hippocampal activation and increased right parietal activation during memory recall task compared to controls Left hippocampal activation was negatively correlated with both FMR1 mRNA levels and psychiatric symptomatology in the PMC group
(Hashimoto, Backer, et al. 2011)	15 PMCs with FXTAS, 15 PMCs without FXTAS and 12 matched controls. Males and females aged between 33 and 75 years.	Functional MRI and working memory task	All groups performed equally on working memory task All groups had significant activation in bilateral hippocampus, inferior frontal cortex, premotor cortex, anterior cingulate cortex and supplementary motor area The right vIFC and left dIFC/PMC showed reduced activation in both PMC groups Regression analysis showed a significant negative effect of mRNA levels on vIFC activity
(Hessl et al. 2011)	23 PMC males (mean age 32.9 years) and 25 matched controls (mean age 30.1 years).	Molecular genetic measures (CGG repeat size, FMR1 mRNA and FMRP) Structural and functional MRI/emotional processing task	PMCs had significantly smaller right and left amygdala volumes PMCs had reduced right amygdala activation during emotional processing task Regression analysis revealed reduced FMRP levels to be a primary factor in the reduced amygdala activation There was no difference between groups on task accuracy
(J. M. Wang et al. 2012)	24 PMC males (mean age 32.6 years) and 25 male	Molecular measures (CGG repeat size, *FMR1* mRNA and	FMRP was 23% reduced in PMCs No difference in hippocampal/total cerebral volume between groups

	matched controls (mean age 30.1 years).	FMRP) Structural and functional MRI/memory encoding task Psychophysiological interaction analysis	Both groups had similar performance on encoding task No significant difference in activation amount or pattern between groups Functional connectivity analysis revealed that PMCs had significantly lower connectivity with the right prefrontal cortex and the right parahippocampal gyrus. This correlated with reduction in FMRP
(Kim et al. 2013)	16 female/12 male PMCs (mean age 32.3 years) and 14 female/15 male controls (mean age 30.6 years)	Functional MRI/magnitude estimation task Molecular measures (CGG repeat size and methylation, and *FMR1* mRNA) IQ assessment	The PMC group showed significantly reduced activation in the bilateral inferior parietal lobule and the left inferior frontal gyrus compared to controls for the distance effect in the task CGG repeat size was a primary factor in reduced fronto-parietal activation in the PMC group
(Kim et al. 2014)	20 asymptomatic PMCs (mean age 30.4 years, female:10) and 20 controls (mean age 29.7, female: 10)	Functional MRI/working memory task Molecular measures (CGG repeat size and methylation, *FMR1* mRNA) IQ assessment	The control group showed significantly greater activation at the right temporoparietal junction during temporal WM retrieval than in spatial WM retrieval. PMCs failed to show this increase at the temporoparietal junction during spatial compared to temporal WM retrieval Elevated *FMR1* mRNA predicted reduced temporoparietal activation in PMCs

Abbreviations

PMC: premutation carrier; vIFC: ventral part of the inferior frontal cortex; dIFC/PMC: dorsal part of the inferior frontal cortex and premotor cortex; FXS: Fragile X Syndrome; MCP: middle cerebellar peduncle WM: working memory

2.4 Discussion

Despite being integral to the FXTAS diagnosis criteria, structural MRI studies into FXTAS and the premutation reveal that MCP sign is not a solid indicator of the disease, as it is present in only approximately 60% of cases. Combined with its non-exclusivity, the radiological presence of the MCP sign can serve only as a likely indicator of FXTAS, but does not provide a definitive diagnosis (Loesch et al. 2008). Additionally, evidence is highly suggestive that asymptomatic carriers also exhibit milder and more infrequent radiological abnormalities, and while this strongly alludes to early signs of degeneration, it is unclear whether this is necessarily the case (Loesch et al. 2005). In a similar way to the MCP sign, thinning of the corpus callosum is thought to be one of the first radiological changes to occur in FXTAS and may precede onset of cognitive and motor symptoms, therefore meaning it could be a potentially useful predictor of disease onset. Changes at the amygdala and hippocampus are also often observed, however, interestingly, despite these areas intuitively being involved in premutation pathology, they do not seem to be as significantly affected as other regions of the brain. At the hippocampus, some groups have identified the region to be significantly increased in volume, whereas other groups have reported it to be not significantly different to control subjects. Similarly, volumetric studies into the amygdala have seen changes, but these were not statistically significant upon analysis (Loesch et al. 2005; Adams et al. 2010; Cohen et al. 2006).

Diffusion tensor studies are highly supportive of the notion that progressive loss of white matter structural integrity is fundamental to FXTAS disease pathology. Increases in radial and axial diffusivities at the MCPs in both asymptomatic carriers and those with FXTAS are further confirmation that changes at the MCPs are an early sign of degeneration that is likely to precede the outward manifestation of FXTAS (Hashimoto, Srivastava, et al. 2011). In addition, evidence suggests that only individuals with lesions at the MCPs and corpus callosum have significantly decreased structural connectivity at a whole brain level, again indicative of the MCPs and corpus callosum being potentially important areas for early disease pathology (J. Y. Wang et al. 2012).

Functional MRI research studies have indicated that in addition to structural changes, functional abnormalities of the brain also form part of the premutation and FXTAS phenotype. During associative memory recall tasks, increases in activation at the parietal cortex is suggestive of compensatory mechanisms within premutation carrier groups, given that performance in the task was not significantly different to control subjects (Koldewyn et al. 2008). This type of neural compensation may be important in the carrier phenotype, allowing individuals to counteract processing deficiencies and appear outwardly asymptomatic. Findings of reduced activation in the limbic system of carriers is also further evidence of the higher incidences of social and psychiatric problems in carrier populations, and may indeed be linked to structural findings, such as volume loss at the amygdala (Hessl et al. 2011). Additionally, during a scanner task that involved the presentation of neutral faces to participants, premutation carriers were observed to respond to this type of stimuli with greater overall brain activation, which again may be reflective of social difficulties and

neuropsychological abnormalities (Hessl et al. 2007). On the whole, fMRI in Fragile X premutation carriers has shown a reduction in the BOLD signal at multiple different brain regions in response to varied stimuli. However, the literature is not without conflicting results, and some research groups have demonstrated no significant differences in comparison to control groups during functional testing (J. M. Wang et al. 2012). This absence of differences between groups may arise for many different reasons, one such important reason being that the heterogeneity of the premutation phenotype and percentage of FXTAS penetrance may cause studied groups of carriers to vary considerably. In addition, groups using asymptomatic carriers require larger numbers of participants to allow for a more sensitive measure of what are likely to be small effect sizes, and given that known premutation carriers are infrequent within the general population, this is often difficult to achieve. Moreover, type of task used in the scanner, pre-scan training or practice and variation in the methods of analysis are all likely to affect results between groups of researchers.

Review of the current neuroimaging and premutation literature here establishes that there is a significant space for development in the research. Structural imaging has demonstrated both global brain changes in FXTAS and focal changes such as the possible early identifier of thinning of the corpus callosum and the frequently seen FXTAS hallmark, the MCP sign. DTI has moreover has shown reduced structural integrity in various brain regions of premutation carriers, both with and without FXTAS. The MCPs, motor tracts and limbic tracts appear to be the most highlighted regions of changes in diffusivity in DTI studies to date. Existing functional MRI studies have used emotional and working memory tasks in carriers both with and without FXTAS, establishing changes in BOLD response commonly at the amygdala, hippocampal formation, parietal regions and the inferior frontal cortex. An important part of the progression of the research into the *FMR1* premutation and FXTAS will be to replicate these results in larger populations and aim towards longitudinal multi-modal study of premutation carriers prior to and after the onset of illness. A combination of various neuroimaging techniques, out of scanner measurements of symptomatology and molecular measurements of *FMR1* gene products may be useful in linking the premutation genotype to FXTAS and other carrier phenotypes. Through this type of study, it may also be possible to further define the nature of FXTAS development and additionally to distinguish neurodevelopmental changes in carriers from later-life, neurodegenerative changes.

Chapter 3: Introduction to experimental sections

3.1 Introduction to current study

Reviewing of the existing neuroimaging literature on *FMR1* premutation carriers revealed that an important future study in the premutation and FXTAS field would be a longitudinal imaging study of premutation carriers without FXTAS with follow-up until possible development of neurodegeneration. Such a study would provide cross-sectional age-related insights into the premutation and using future follow-up investigation would allow for the mapping of phenotypes across time. Most pertinent to this investigation would be to delineate stable, neurodevelopmental traits of carriers from the degenerative processes of FXTAS. Cross-sectional and longitudinal data will also be important to further characterise the biological mechanisms and clinical presentation of FXTAS development and prognosis.

The first step towards such a study is to clarify whether premutation carriers show differences to brain function which predate the onset of frank FXTAS. In addition, it is possible to use cross-sectional data to provide preliminary evidence of a change over time, by examining whether there is a relationship between age and neuroimaging differences in carriers comparative to a control group.

We therefore set out to examine using fMRI whether premutation carriers without showed differences compared to controls even when they had not developed FXTAS. We also aimed to examine whether some features of the FXTAS phenotype were neurodevelopmental, such as psychiatric symptomology, social difficulties and autistic traits and whether some were neurodegenerative in nature, such as motor function. We chose to utilise two fMRI tasks, one hypothesised to relate to a neurodevelopmental feature of the premutation state (an emotional processing task) and another hypothesised to relate to a neurodegenerative characteristic of the premutation state (a finger-tapping task). In tandem with fMRI investigation, outside scanner measurements of these premutation characteristics were chosen to examine the presence and extent of clinical or neuropsychological phenotypes. Molecular measurements of *FMR1* gene products were also included in the study protocol, to allow insight into possible molecular influence on carrier phenotypic variables.

3.2 Neurodegeneration in the Fragile X premutation: Hypotheses

Part of the clinical presentation of FXTAS is the progressive loss of normal motor functioning (such as balance problems, tremor and ataxia). As mentioned, in the present study, the premutation carrier group will be asymptomatic for FXTAS to allow for examination of differences in carriers that exist in the absence of overt disease. We set out to utilise an fMRI based finger-tapping motor task to identify possible functional differences in the motor areas that are likely to be age-dependant in premutation carriers which may precede the overt clinical changes associated with FXTAS. In this

way, we would predict to observe mild functional differences that are synonymous to the early stages of FXTAS manifestation.

Previous literature in typically developing people utilising fMRI based finger-tapping tasks of variable complexity and frequency show main activations at the primary motor cortex, supplementary motor area and the superior parietal cortex (Minkova et al. 2015). When regressed against finger-taps, fMRI data also indicated a main significant cluster at the motor cortex (Murta et al. 2016) . When considering healthy aging, it appears qualitatively that older individuals exhibit different activation patterns during fMRI when performing simple movements compared to younger individuals (Hutchinson et al. 2002). Evidence also suggests that more of the brain is recruited during motor tasks in older individuals, including non-motor areas, which is suggestive of a necessity for higher processing and compensatory mechanisms (Zapparoli et al. 2013; Sharma & Baron 2014). Motor training and motor imagery or cognition also play a key part in differential functional brain responses to finger-tapping tasks in older cohorts, with training-specific BOLD response increases at the premotor cortex in individuals who performed motor training and increases at the secondary visual cortex in individuals who performed mental training (Boraxbekk et al. 2016). These findings highlight the importance mental processing, attentional regulation and changes during healthy aging suggestive of compensatory mechanisms during finger-tapping tasks.

There are currently no fMRI studies using motor tasks in FXTAS; however, considering such tasks in clinical neurodegeneration populations more generally, investigations into Huntington's disease have revealed a critical role for the dorsal premotor cortex in functional motor control in carriers of the Huntington gene without disease. Additionally, this research has indicated that impairment in the premotor cortex may cause compensatory recruitment of the parietal cortex in overt Huntington's disease, marking the premotor areas and compensatory activations as points of interest in early pathology (Bartenstein et al. 1997). In patients nearing clinical onset of Huntington's disease, involvement of the supplementary motor area has also been shown to be caudally over-recruited during higher frequencies and more demanding finger-tapping movements (Kloppel et al. 2009). In Parkinson's patients with tremor, cerebello-thalamo-cortical circuitry dysfunction is implicated in the development of tremor symptoms, with a poor suppression of tremor being linked to lower cerebellar neural activity (Deiber et al. 1993). Neuroimaging studies also suggest compensatory activity in the cerebellum in Parkinson's disease (Lewis et al. 2011). Lower cerebellar activation has also been implicated during a variable frequency finger-tapping task in Spinocerebellar Ataxia Type 3 (Duarte et al. 2016; Cleary & Ranum 2014).

Given evidence based on studies into healthy aging and neurodegenerative diseases, we would expect to see group differences in the fMRI finger-tapping task in this study at the premotor cortex, supplementary motor area and the cerebellum, in addition to other regional involvement of

compensatory mechanisms, possibly at more diffuse areas of higher function. Random finger-tapping driven by choice, compared to learned sequential tapping, has been shown to elicit stronger activation in classical motor regions as well as recruit areas of higher cognitive functioning, such as the dorsolateral prefrontal cortex (Gountouna et al. 2010). The chosen focus of finger-tapping task design for this study will therefore be centred around sequential and random finger-tapping to produce a similar variance in brain activation and task demand. By using a task design of this type, we hope to contrast the random and sequential tapping conditions to probe differences between asymptomatic carriers and controls concerning brain regions responsive to changes in task demand. This contrast between the sequential and random conditions, also focuses analysis on the compensatory activity and mental imagery that have been previously noted as sensitive to age (Boraxbekk et al. 2016). In addition to a classic between group imaging analysis, we will also consider whether the effect of age on brain activation during the finger tapping task differs between carriers and control individuals, which may implicate brain areas that are vulnerable to early development of FXTAS pathology.

In accordance with previous findings, we also expect molecular measurements of *FMR1* mRNA derived from peripheral blood samples to be higher in Fragile X premutation carriers (Tassone, Hagerman, Taylor, Gane, et al. 2000; Jacquemont et al. 2003a). It is also expected that due to altered RNA metabolism, *FMR1* mRNA may accumulate over time and higher levels may be associated with increasing age in carriers, which is supported by *FMR1* mRNA-mediated intranuclear inclusions in the brain becoming larger over time in individuals with FXTAS (Tassone, Hagerman, Taylor, Gane, et al. 2000; Sellier et al. 2010). Given the RNA toxic gain-of-function model for FXTAS, we would also expect to see functional brain changes that are likely neurodegenerative in nature to correlate with increasing *FMR1* mRNA levels in the carrier group.

Presence of sub-clinical levels of motor symptoms in carriers without overt FXTAS have been found to be variable, which is likely to be dependent on differences in sample age and future FXTAS penetrance (Allen et al. 2008a; Leehey et al. 2008; Tassone, Adams, Elizabeth M Berry-Kravis, et al. 2007). However, we expect to see some mild changes in tremor, co-ordination and balance, especially in older individuals. Previous research in premutation carriers has employed a computerised system called the CATSYS-2000 system to establish that carriers without FXTAS exhibit worse co-ordination scores and to generate estimates of age-related prevalence of tremor and ataxia in carriers (Allen et al. 2008b; Aguilar et al. 2008). Given this robust history of use in premutation carriers, the CATSYS-2000 system will be used in the present study to obtain measurements of participant tremor, balance and co-ordination and we would expect to see a subtle group differences in carriers of increased, yet not clinically significant motor symptomology in line with FXTAS development before frank clinical onset.

3.3 Neurodevelopment in the Fragile X premutation: Hypotheses

As previously discussed, premutation carriers are known to have an increased risk of psychiatric problems, such as depression, obsessive-compulsiveness and autistic traits. We therefore predict that carriers will show differences in emotional processing that link to these disorders (Jacquemont et al. 2004; Cornish et al. 2005). Moreover, we predict that these changes arise from the neurodevelopmental aspects of the Fragile X premutation, and as such will represent a stable trait as opposed to one that is involved in the neurodegenerative processes of FXTAS. We therefore aim in the present study to utilise an emotional processing fMRI task that uses photographic stimuli sourced from the International Affective Picture System (IAPS) to probe possible between group differences in emotional function. Multiple previous fMRI studies have used Ekman face-based tests using fearful faces, so the present study will use an IAPS-based paradigm with the aim of establishing novel emotional processing differences in premutation carriers on a more complex emotional spectrum than can be examined using fearful and neutral face tasks (Hessl et al. 2007; Hessl et al. 2011).

The pictures from the IAPS are defined according to valence and arousal parameters, in keeping with the dimensional model of emotion, which specifies that all emotions fall on spectra of valence (pleasant to unpleasant) and arousal (calm to excited) (Bonnet et al. 2015). Functional imaging using IAPS stimuli has shown that the intensity and extent of BOLD activation at the right and left amygdala is closely correlated to the increasing emotional intensity (arousal rating) of positive valence pictures (Bonnet et al. 2015). Additionally, only pictures deemed to be arousing (both unpleasant and pleasant) produced clusters of activity in certain regions, such as the occipital gyrus, the right fusiform gyrus and the superior parietal lobes (Lang et al. 1998). Positive linear relationships have also been found between activation in the amygdala and the arousing quality of visual stimuli and activation in the insula and prefrontal cortex and IAPS arousal ratings (Prehn et al. 2015; Sabatinelli et al. 2005). Distinct findings have also demonstrated that pleasurable visual stimuli preferentially activate the nucleus accumbens and medial prefrontal cortex (Sabatinelli et al. 2007). When grouped against neutral pictures, affective pictures of either pleasant or unpleasant stimuli were observed to produce more extensive activation in the visual cortex, especially the secondary association areas (Brodmann Areas 18 and 19) (Bradley et al. 2003). Unpleasant IAPS stimuli was observed to elicit positive peak BOLD responses that were greater relative to neutral stimuli at the primary visual cortex, the bilateral amygdalae and the right ventrolateral prefrontal cortex. This type of emotional discrimination was also found to follow a typical region-specific time course, whereby right amygdala responsiveness precedes that of the left amygdala, which in turn precedes that of the ventrolateral prefrontal cortex (Kohno et al. 2015). Another study identified significant BOLD activation during presentation of pleasant stimuli at the ventromedial prefrontal cortex, bilateral middle temporal gyrus and the right precuneus, whereas aversive stimuli prompted significant activation at the left amygdala and bilateral middle temporal gyrus. These patterns of valence associated activations were observed consistently across a range of healthy subjects and individuals

with various psychiatric disorders, including major depressive disorder and panic disorder, however there was no evident interaction between psychiatric diagnostic group and whole brain significant responses (Hägele et al. 2016). The occipito-temporal cortex and the amygdala-hippocampal complex were also highlighted as areas of non-specific emotion related activation, which increased in intensity during negative valence stimuli from the IAPS compared to pleasant stimuli (Radua et al. 2014).

Taken together, findings of task-based fMRI using the IAPS stimuli have identified the amygdala, hippocampal complex, the ventrolateral and ventromedial prefrontal cortex, the insula and the orbitofrontal cortex as brain regions associated with both high and low valence emotional processing, with associative links between some areas of regional BOLD intensity and image arousal ratings. fMRI studies using IAPS task design and psychiatrically affected groups have indicated that overall, BOLD responses are elevated in the limbic regions and prefrontal cortex, particularly during low valence conditions, and amygdala-prefrontal functional connectivity is attenuated in individuals with psychiatric disorders. Given that the previous literature utilising the IAPS demonstrates brain activation patterns in multiple populations that involve a connectome of brain regions that are likely to reflect an emotional processing system, we can hypothesise that the premutation group in this study, given their higher incidences of psychiatric problems, may show attenuated or heightened BOLD responses in areas previously described as altered in psychiatric populations. In keeping with previous commonalities in fMRI IAPS based tasks, the task to be utilised in the present study will be centred around spectra of valence and arousal in an event-related design. To ensure engagement with the task, participants will also be asked to indicate an arbitrary measure of picture content that does not explicitly involve ratings of either pleasure or arousal.

As previously mentioned, Fragile X premutation carriers are a high risk group for the development of autism spectrum disorder (ASD) and psychiatric symptomatology (Cornish et al. 2005; Dorn et al. 1994). In concordance with previous findings therefore, we would expect to see significantly different measurements of neuropsychological or psychiatric symptoms in carriers when compared to controls in tests conducted outside of the scanner. In studies of premutation carrier males, the self-report psychiatric questionnaire Symptom Checklist -90- Revised (SCL-90-R) (Pearson) has been used to characterise symptomatology of the following: somatization, obsessive-compulsiveness, interpersonal sensitivity, depression, anxiety, hostility, phobic anxiety, paranoid ideation, psychoticism and global severity index. Males without FXTAS were observed to have worse scores in obsessive-compulsiveness and global severity than controls as scored by the SCL-90-R (Hessl et al. 2005). Using this measure we would therefore hope to replicate these previous psychiatric findings. Symptoms of autism spectrum disorder in adults of normal intelligence can be self-reported using the Autism Quotient (AQ) and the Empathy Quotient (EQ) (Baron-Cohen et al. 2001). The AQ questionnaire involves assessment of participant social skills, attention switching, attention to detail, communication and imagination and has an 83% accuracy in positively predicting the presence of

autism spectrum disorder above a score of 26 (Woodbury-Smith et al. 2005; Baron-Cohen et al. 2001). The EQ assesses ability for empathic awareness in participants, and has an 81% accuracy of correctly identifying individuals on the ASD spectrum with scores lower than 30 (Baron-Cohen & Wheelwright 2004). EQ scores are also predictive of AQ scores (Wheelwright et al. 2006). Previous studies into ASD and the *FMR1* premutation have revealed that the incidence of ASD is significantly higher in premutation males (Saul & Tarleton 1993). Therefore, the use of the AQ and the EQ in the present study is hoped to reflect these previous findings. Other neuropsychological measurements, the Ekman Faces and Social Judgement tests, will also be included, to allow more thorough investigation of social and emotional processing and ability in tandem with the MRI scanner-based emotional task. Additionally, it will be of interest as to whether these psychiatric and neuropsychological variables exhibit correlational significance when regressed against data from between group brain imaging analyses from the emotional processing task.

In terms of possible molecular changes driving emotional and psychiatric differences in carriers, it is theorised that *FMR1* protein levels are key. FMRP is densely concentrated at the post-synaptic density, and is essential for healthy brain development, as is demonstrated by marked neurodevelopmental problems in Fragile X Syndrome and animal knock-out studies (Penagarikano et al. 2007). It therefore seems probable that slightly lowered levels of FMRP in carriers compared to controls may be causing subtle neurodevelopmental differences which manifest in the neuropsychological and psychiatric symptoms found in previous studies (Tassone, Hagerman, Taylor, Gane, et al. 2000; Allen et al. 2005). This study therefore aims to establish first whether FMRP is indeed lower in this male premutation population, and second whether levels of FMRP are associative with fMRI BOLD responses, as has been identified previously, where amygdala dysfunction was found to correlate with lower levels of FMRP in carriers (Hessl et al. 2011). Overall, we aim to use this combination of methodology to investigate the existence of carrier/control differences and to establish whether FMRP levels and symptomatology are associated with possible changes in BOLD response.

Chapter 4: Neurodegeneration in the Fragile X premutation: Methods

4.1 Participants and recruitment

Male carriers of the premutation and a group of healthy male age-matched control subjects were recruited. The age range for inclusion in the study was 20-70 years. Recruitment was carried out using the Patrick Wild Centre and Fragile X Registry email lists, which are contactable lists of potential participants held by the affiliated centre for Fragile X related clinical studies and 1000 mailings were sent out through the existing Fragile X family database held by the Fragile X Society. Potential premutation carrier participants were required not to have received a diagnosis of FXTAS and to have been genetically confirmed as a carrier prior to taking part in the study. Participants were not permitted to take part in the study if they were a member of a family with an identified individual with the Fragile X premutation or Fragile X Syndrome, but had not had a genetic test to confirm or deny carrier status. This was to minimise unexpected findings, and the ethical issues surrounding diagnosis of carrier status during the study. Both carrier and control participants were also not permitted to take part if they fell out with the age range of 20-70 years. All participants were given an Information Sheet at least 48 hours prior to taking part in the study, were given the opportunity to ask any questions they may have had and gave fully informed written consent on the day of testing. All participants were also screened for MRI eligibility and safety prior to taking part.

A power calculation was used to define an ideal sample population of 80 (40 controls and 40 premutation carriers). Dividing age in a 5-level factor (20-29, 30-39, 40-49, 50-59, 60-69) with group as a 2-level factor (control, carrier) and assuming an effect size for the interaction of eta sq = 0.18 (estimated from Cornish et al. 2008 and Cornish et al. 2009, who report findings consistent with an effect size of >0.18) a total sample of 60 participants would be required to give 80% power to detect an age interaction difference at a significance level of $p<0.05$. In addition, two previous neuropsychological studies in this area (Cornish et al. 2008, Cornish et al. 2009) examined 40 premutation carriers and identified differences between them and controls in terms of the relationship between age and cognitive function. Neuroimaging studies generally require smaller sample sizes than neuropsychological studies, therefore a sample size of 80 was deemed preferable and sufficient. However, recruitment of male premutation carriers for the study yielded a low response rate (<2% of Fragile X families contacted). Causes for this plausibly included the likely requirement for significant travel for participants, unwillingness or inability to take time off work, anxiety about an MRI scan and a relatively large length of testing time. In addition, male carriers of the premutation who have been genetically diagnosed are rare, and due to ethical issues surrounding confirming carrier status during the study, recruitment was unable to include individuals who were suspected to have the premutation but had not undergone genetic counselling. The sample size for the current study therefore was not as large as originally predicted.

The protocol was approved by the South East Scotland Research Ethics Committee and NHS Lothian Research and Development Office.

4.2 Imaging methods

All MRI data was acquired on a 3 Tesla Siemens MRI scanner using an 8 channel head coil. For the acquisition of functional images the TR was 1560ms, the TE (echo time) was 26ms, the flip angle was 66 degrees, the FOV (field of view) was 220mm, slice thickness was 5mm and slice number per volume was 26. Slice order was interleaved and bottom up in the axial orientation. Each participant also underwent a T1-weighted magnetization prepared rapid acquisition gradient echo (MPRAGE) sequence, for the purpose of image preprocessing. For the MPRAGE acquisition the TR was 2300ms, the TE was 2.98ms, the flip angle was 9 degrees, the FOV was 256mm, slice thickness was 1mm and slice number per slab was 160. Each participant also underwent a 12 minute DTI sequence which is not considered further in this thesis. The scanning protocol in total was approximately 50 minutes for each participant.

The finger-tapping motor task used for this study utilised a block design and consisted of three conditions (Fig. 4.1). In the sequential tapping condition, participants were asked to tap their thumbs and index fingers in a predetermined sequence in time with a flashing symbol. In the random tapping condition, participants were asked to tap their thumbs and index fingers in a random order in time to a flashing symbol. The final condition consisted of a flashing fixation cross, where participants were asked to simply rest and watch the screen. The flashing symbol appeared once every second, for a duration of 0.5 seconds. Each condition block had a total duration of 30 seconds (including a 2 second prompt screen) and was repeated 4 times during the task. The task was designed and ran using Presentation™ software. Participants were given written instructions for all of the tasks before entering the MRI scanner (Appendix 4.1), shown an example of each task on a laptop screen and given the chance to ask any questions they may have had. The tasks were visually presented to participants in the scanner using goggles that fit onto the scanner head coil.

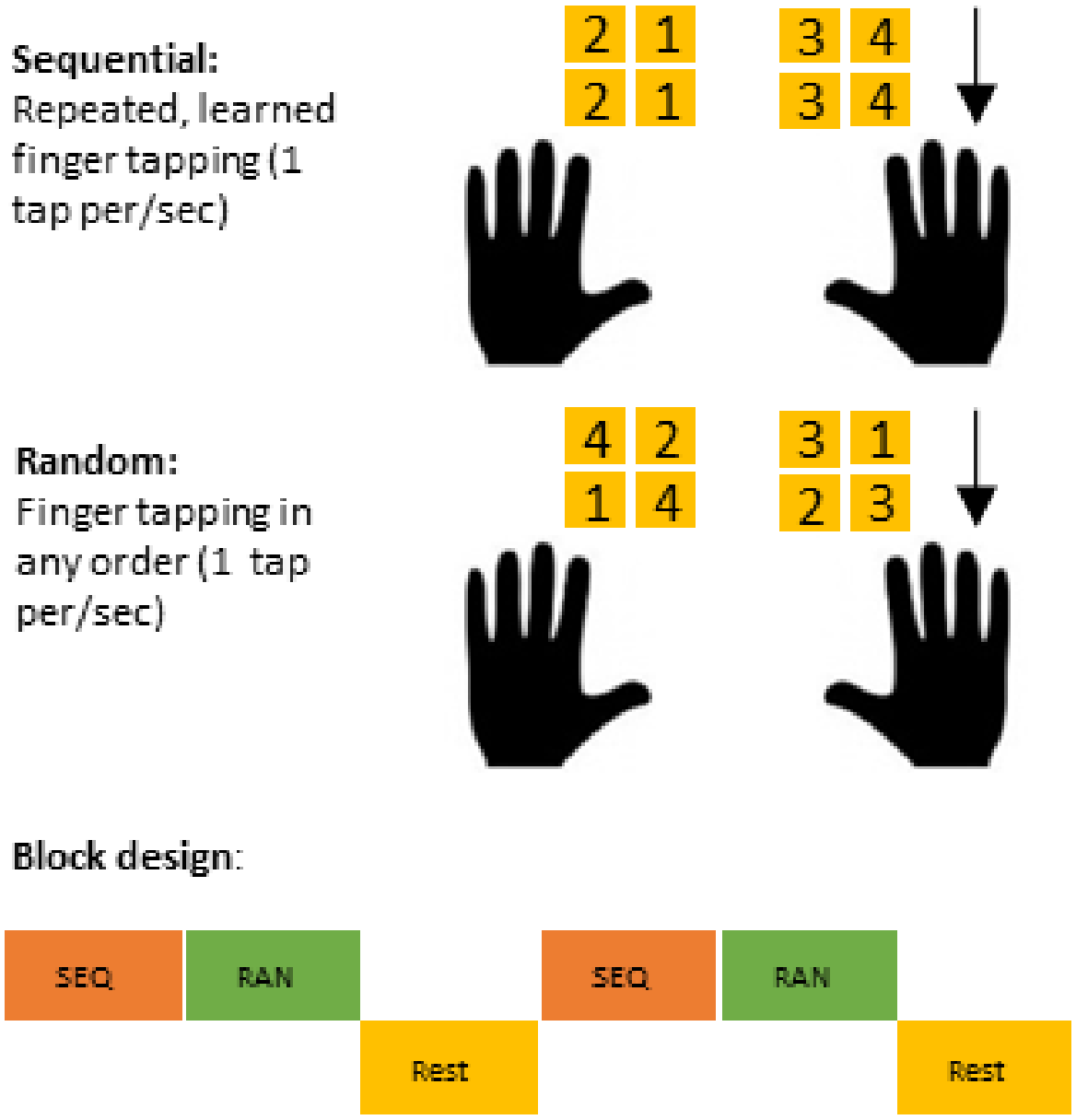

Figure 4.1 Finger-tapping task behavioural conditions and block design.

This task was behaviourally piloted prior to use in the scanner (Table 4.1). Five individuals who were not potential participants for the main study carried out the task on a laptop. The task was presented using Presentation™ software, in the exact same manner as it was to be presented in a scanner environment. Button presses of the scanner triggers were replaced by keyboard presses. Each individual subsequently filled out an evaluation form of the task (Appendix 4.2), which focussed on the clarity of task instructions, ease of carrying out the task and engagement in the task. Individuals were also asked to comment on the sequential and random conditions separately. The majority of individuals rated this task as very simple and very engaging. Four out of five individuals also did not make a differentiation based on easiness between the sequential and random conditions. It was therefore deemed the task was suitable for participants to carry out in an MRI scan.

Table 4.1. Finger-tapping task behavioural pilot data

Individual	Clarity rating (1=confusing, 5=simple)	Engagement rating (1=not engaged, 5=very engaged)
1	4	2
2	2	2
3	5	5
4	5	5
5	5	5

Table 4.1 Finger-tapping task self-reported evaluation form data from behavioural piloting

4.3 fMRI analysis

Statistical analysis on fMRI data was carried out using Statistical Parametric Mapping software (SPM12) (Wellcome Department of Clinical Neurology).

The functional images from all participants were preprocessed according to the following steps: 1) firstly images were realigned, estimated (for optimal transformation from individual images to the reference using SPM12 default quality, separation, smoothing, num passes, interpolation, wrapping and weighting parameters) and resliced 2) images were then slice timed, adjusting for interleaved and bottom up slice order 3) subsequent functional images were coregistered with the source structural image from the T1 MPRAGE anatomical scan 4) coregistered images were segmented into grey matter, white matter and CSF outputs 5) images were normalised to MNI space, and 6) finally the normalised images were smoothed with a 8mm FWHM (full-width at half maximum) Gaussian smoothing kernel.

Movement was controlled for by adding realignment parameters for each participant as a multiple regressor into the first level model. First level analysis was carried out for each participant for each task. For the finger-tapping motor task, the sequential and random conditions were contrasted using a [1 -1] contrast. This type of contrast investigates the linear effect of one condition minus the linear effect of another condition.

For the second level analysis, explicit masking was used to exclude voxel data outwith the brain tissue. This explicit mask was comprised of an average binarised image created from the combined grey matter and white matter segmented images from all participants. Both within and between group analyses were completed. Within group analysis used a one-sample t-test for each task and first level contrasts to look at significant activation for the control and premutation group separately. Within group second level contrasts were defined as either [1] or [-1] to look at linear increase and linear decrease of activation patterns. The between group analyses used a full factorial design to examine the differences between the control and premutation groups. The groups were compared using [1 -1] and the reverse [-1 1] contrasts. An example design matrix is presented in figure 4.2, showing the between group analysis for controls and carriers. In addition, age was added into the full factorial design as a regressor and group x age interactions at a whole brain level were examined in SPM for both the control and the premutation group using [1 -1] and the reverse [-1 1] contrasts. All second level contrasts were calculated using an initial height threshold of $p < 0.005$. Family-wise error correction was then carried out, with significance being indicated by cluster-wise inference ($FWE_{corr}<0.05$).

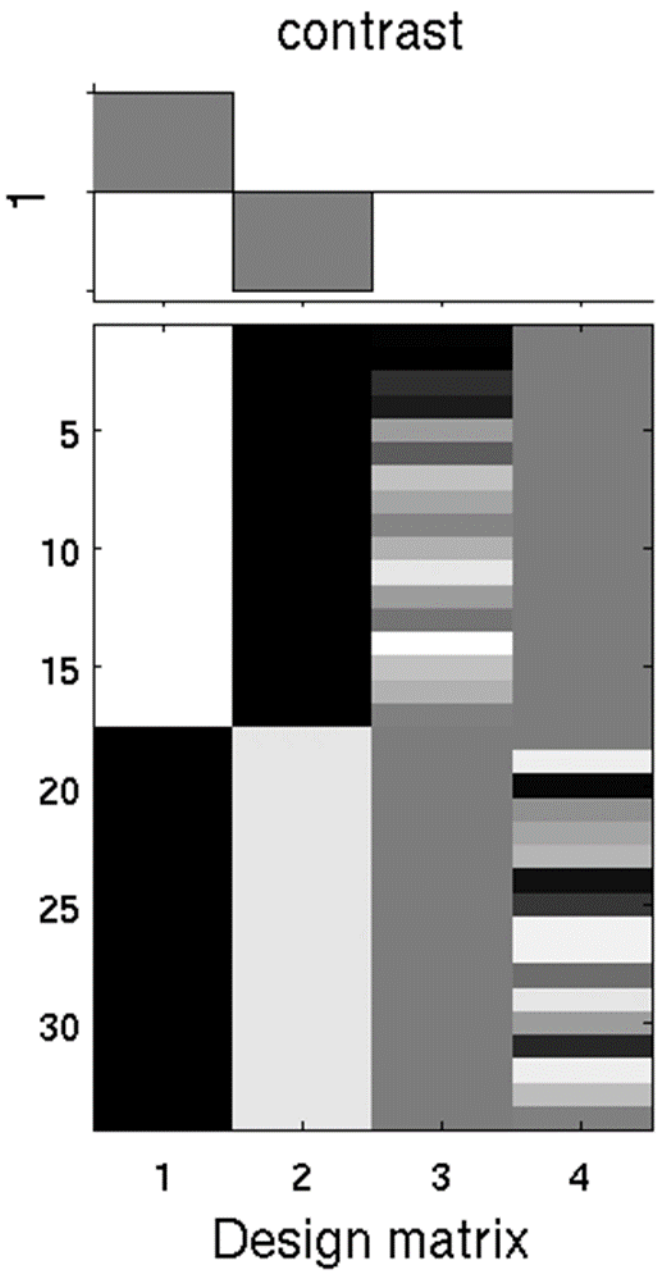

Figure 4.2 Design matrix displaying a control>premutation between group contrast for the finger-tapping second-level analysis. Controls are represented in column 1, premutation carriers are represented in column 2 and age is represented in columns 3 and 4.

4.4 Clinical measurements

The CATSYS-2000 PC-based system was used to assess movement variables in all participants. The CATSYS system groups movement performance into three categories: tremor, balance and co-ordination. For tremor measurements, participants were asked to hold a stylus as they would a pen, vertically in front of their chest with their arm bent. They were then asked to remain as still as possible during the 8 second testing period, where movement parameters were obtained in two dimensions by the stylus accelerometer (m/s^2). Both left and right hands were tested. For balance measurements, each participant was asked to stand on a computerised sway board, without shoes, with feet hip-distance apart, arms straight by their side and head facing forwards. Once standing on the board, participant sway was then measured for 1 minute, using the Pythagorean sum of transversal and sagittal sway (mm). Co-ordination measurements were carried out first using tapping measurements and then reaction time measurements. During tapping assessments, participants were asked to tap their hand on a computerised drum, using a pronation-supination movement to a rhythmic beat that is set by an auditory beep. Measurements were taken for each participant at a slow beat (1 beep per second, 20 second duration), fast beat (2 beeps per second, 10 second duration) and increasing frequency beat (1 beep per second-5 beeps per second, 20 second duration) for both the right and left hands. Participants were also asked to repeat the same measurements on the drum tapping with their index finger, with wrist and thumb resting on the table. Reaction time co-ordination scores were obtained for both the right and left hands for each participant using a hand-held click button. For a duration of 40 seconds, participants were asked to click the button using their thumb as soon as they heard an auditory stimulus. This stimulus was a beep which sounded randomly over the duration of the test. Co-ordination scores were produced from deviation in rhythmic tapping and reaction time with respect to stimulus time (msec).

The CATSYS system then produced performance indices for overall tremor, balance and co-ordination as values between 0 and 2, relating the participant performance to average human performance as determined by the CATSYS normative material (Danish Product Development Ltd.). Indices for performance better than typical human performance are higher than 1.0, indices below typical human performance are less than 1.0. Formulae relating performance indices to average human performance are exponential equations using a Gauss distribution function (Appendix 4.3).

4.5 Molecular measurements

DNA was isolated from blood samples for both control and carrier participants. The assay for CGG repeat length in the *FMR1* gene was carried out using a PCR-only approach based on Triplet Repeat Primed PCR design (AmplideX® PCR/CE *FMR1* reagents).

Whole blood was collected from all participants and processed to isolate total RNA. Total RNA was then reverse transcribed into cDNA, using Real Time (RT) PCR methodology. RT reactions were

performed in 25µl aliquots containing 10µl of patient total RNA sample, 12.5µl 2x RT buffer and RT enzyme mix (Invitrogen Superscript). RT thermal cycling conditions were as follows: 25ºC for 10 minutes, 50ºC for 30 minutes, 85ºC for 5 minutes and 4ºC for 15 minutes. 1µl of RNase H was subsequently added to each aliquot and the samples were incubated at 37ºC for 20 minutes. Each sample was then diluted to a cDNA concentration of 6ng/µl. These dilutions were then used to quantify *FMR1* mRNA using quantitative PCR (qPCR). Once an *FMR1* primer pair was designed and validated (R^2 =-0.998, efficiency = 101.01%), aliquots were prepared in triplicate for each sample, with each aliquot containing 0.6µl 300nM forwards primer, 0.6µl 300nM reverse primer, 10µl SYBR Green (Qiagen), 11.8µl H_2O and 1µl 6ng/µl cDNA sample. An additional control was run in triplicate on each plate with cDNA replaced by H_2O. Thermal cycling conditions for the qPCR were as follows: 95ºC for 15 minutes, (94ºC for 20 seconds, 59ºC for 30 seconds and 32ºC for 30 seconds) x 35 cycles, then 95ºC for 1 minute, 60ºC for 30 seconds and 90ºC for 30 seconds.

All *FMR1* mRNA measurements were averaged per participant and normalized to 18 sRNA measurements from the same samples (primer efficiency = 91.28%, R^2 = -0.994), which were also ran in triplicate on the same qPCR plate as the *FMR1* mRNA probes. All samples underwent qPCR analysis on the same plate as their age-matched counterpart. Carrier *FMR1* mRNA was then additionally normalized to age-matched control. Outlier *FMR1* mRNA or 18 sRNA measurements within the triplicate were discarded and qPCR was repeated for these samples.

4.6 Statistical analysis

Further statistical analyses were carried out in SPSS Statistics 22. Parametric testing of group means was deemed appropriate considering the assumed normal distribution of the data. A two-tailed t-test was used to discern differences between the premutation and control groups for the tremor, balance and coordination measurements, in addition to the *FMR1* mRNA data. Simple linear regressions were also performed on extracted raw voxel values from significant clusters against the movement and molecular variables. All significance levels were assumed at $p<0.05$.

CGG repeat analysis revealed that some individuals in the sample were mosaic or borderline for the full mutation. To ensure this was not causing a bias in the results, mosaic and borderline carriers were separated from the sample, creating three participant groupings: control, premutation and mosaic/borderline. A one-way ANOVA of 3 age-matched groups, followed by a Tukey post-hoc test was performed on extracted voxel data from the maximum voxel of the significantly different between group cluster. An analysis of covariance with age as a covariate, including group, age and group x age interaction in the model was performed on extracted voxel data from the age interaction significant cluster on these 3 age-matched groups using age as an interacting variable.

Chapter 5: Neurodegeneration in the Fragile X premutation: Results

5.1 Participants and recruitment

Male premutation carriers without FXTAS (n=17, mean age 50.4 years, SD=15.1) and a group of age-matched healthy male controls n=17, mean age 47.6 years, SD=12.9) were recruited for this study. A parametric two-sample t-test of age carried out in SPSS revealed participant age in the premutation and control groups not to be significantly different (p=0.570). Level of education was comparable between groups. CGG repeat testing revealed that 12 carriers were within the premutation range, 1 carrier was in the intermediate range, 3 carriers were mosaic for repeat size and one carrier was borderline for the full mutation. All control subjects were within the normal CGG repeat length range. Main CGG repeat length value by group is plotted in figure 5.1. All participants were right handed, apart from one control and two carriers, and all participants had composite IQ >80, as measured by the KBIT Second Edition Intelligence Test (Pearson) (Table 5.1). When compared using a parametric two-sample t-test in SPSS, verbal IQ and composite IQ as measured by the KBIT-2 were not significantly different between the groups (p=0.604, p=0.053), although composite IQ could be seen to exhibit a trend towards being lower in carriers. Non-verbal IQ was identified to be significantly lower in carriers (p=0.015) (Fig. 5.2).

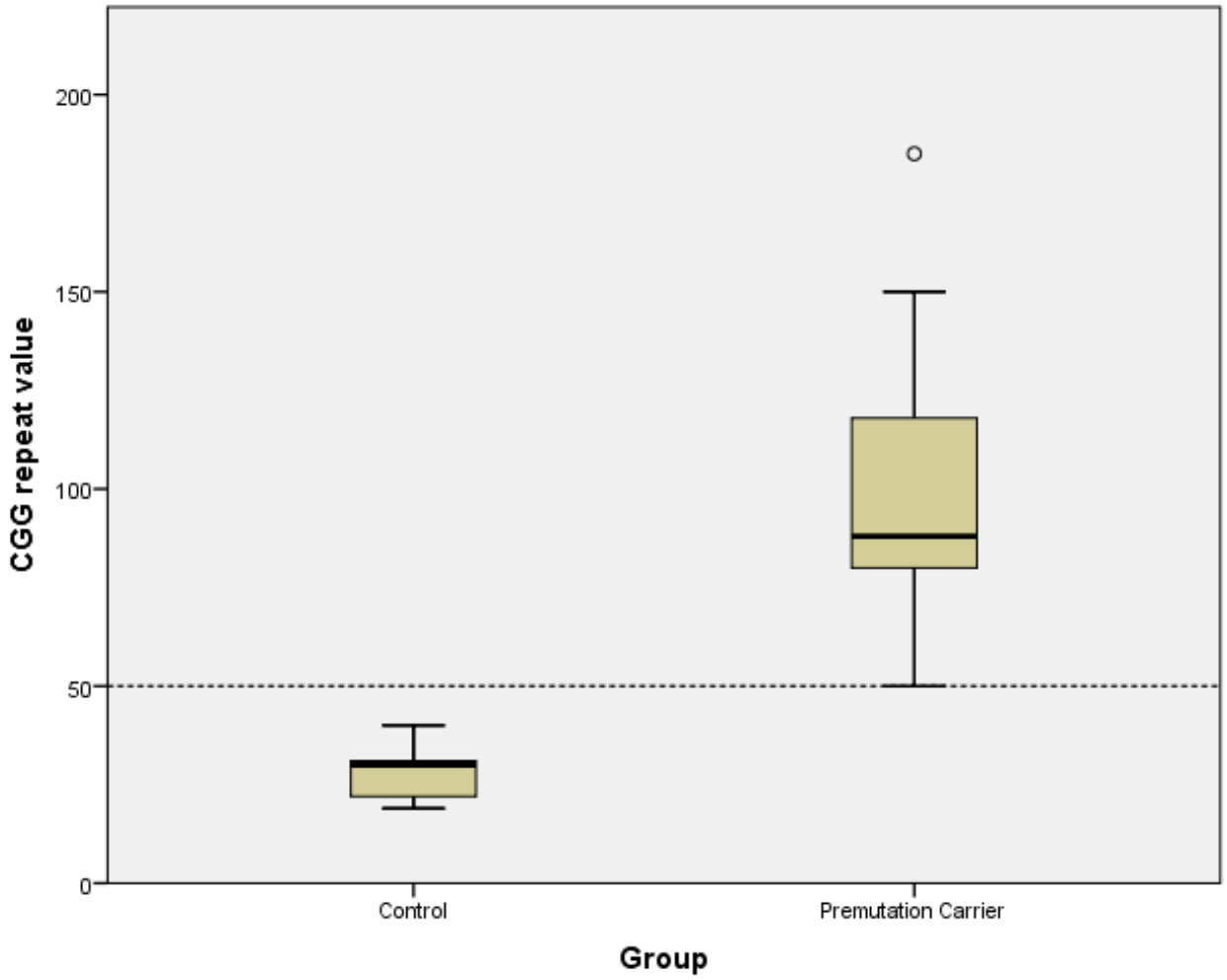

Figure 5.1 Main CGG repeat values by group, excluding secondary mosaic values in carriers. Mean CGG repeat length in the control group was 27.76 repeat units (SD=6.49), and mean for the carrier group was 98.47 repeat units (SD=36.1).

Table 5.1: Participant data

Participant ID	Age	Premutation status	Composite IQ
1	26	**Normal (40 repeats)**	129
2	24	**Normal (20 repeats)**	123
3	33	**Normal (22 repeats)**	110
4	30	**Normal (38 repeats)**	103
5	52	**Normal (19 repeats)**	107
6	41	**Normal (20 repeats)**	128
7	58	**Normal (23 repeats)**	112
8	53	**Normal (30 repeats)**	110
9	48	**Normal (32 repeats)**	110
10	55	**Normal (32 repeats)**	111
11	64	**Normal (31 repeats)**	108
12	52	**Normal (31 repeats)**	105
13	45	**Normal (31 repeats)**	121
14	68	**Normal (23 repeats)**	126
15	58	**Normal (30 repeats)**	127
16	55	**Normal (20 +/-1 repeats)**	122
17	47	**Normal (30 repeats)**	126
18	46	**Premutation (91 +/-3 repeats)**	139
19	67	**Premutation (82 +/- 3 repeats)**	106
20	24	**Premutation (82 +/-2 repeats)**	119
21	50	**Premutation (88 +/- 3 repeats)**	144
22	54	**Premutation (85 +/- 5 repeats)**	108
23	57	**Premutation (185 +/- 10 repeats)**	101
24	26	**Premutation (mosaic 150 +/- 5; ~200 +/- 10 repeats)**	86
25	33	**Premutation (74 +/- 2 repeats)**	111
26	68	**Premutation (118 +/- 8 repeats)**	104
27	68	**Premutation (88 +/- 3 repeats)**	97
28	43	**Premutation (71 +/- 2; 119 +/- 5 repeats)**	107
29	66	**Premutation (mosaic 133, 156; 198 +/- 10 repeats)**	109
30	52	**Premutation (58 repeats)**	94
31	30	**Premutation (mosaic 148 +/- 5; ~200 repeats)**	102
32	67	**Premutation (80 +/- 2 repeats)**	108
33	58	**Premutation (91 +/-3 repeats)**	125
34	47	**Intermediate (50 repeats)**	117

Table 5.1 Details of participant age, CGG repeat length, presence of mosaicism and composite IQ.

a)

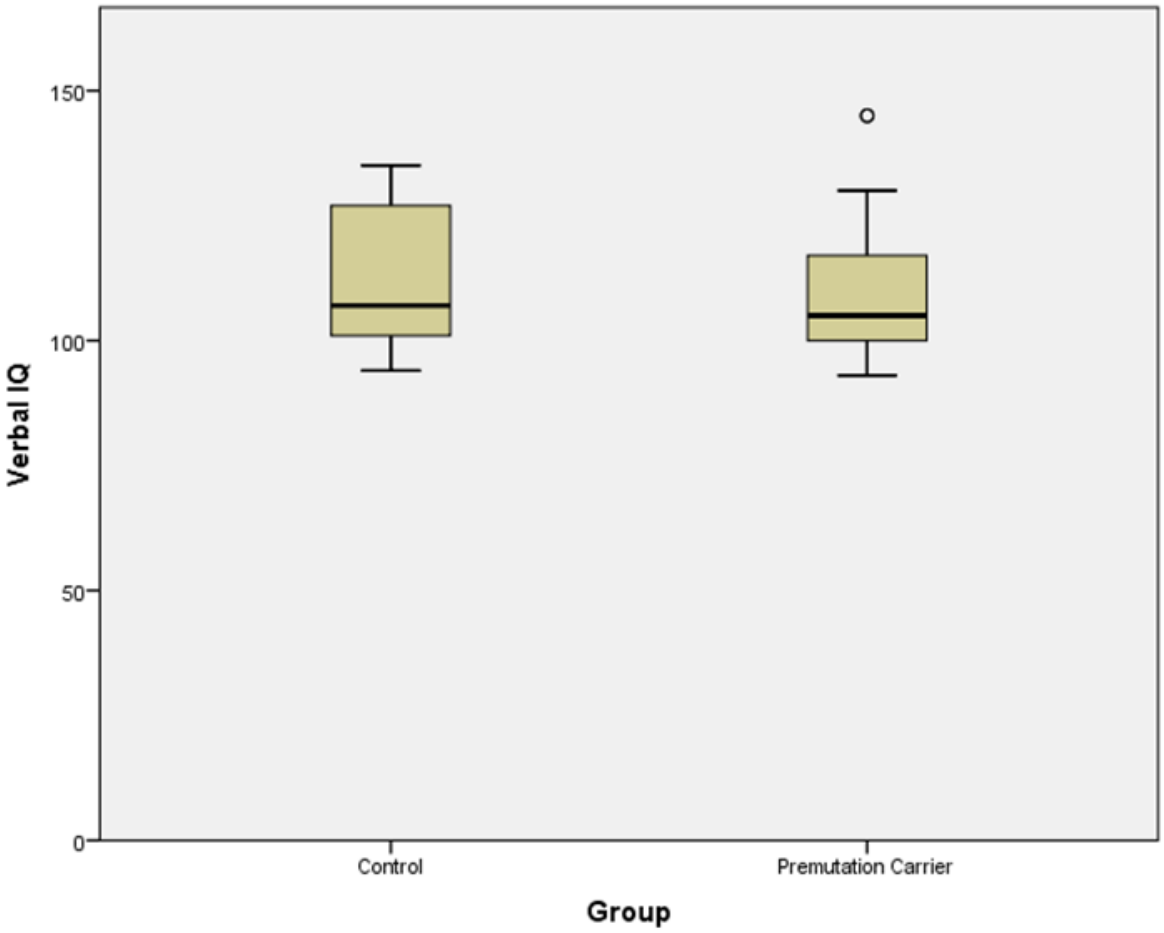

Figure 5.2 IQ scoring by group, analysed statistically using a parametric two-sample t-test in SPSS **a)** Verbal IQ by group. Mean verbal IQ in the premutation group was 111.1 (SD=15.8), mean verbal IQ in the control group was 112.7 (SD=13.5).

b)

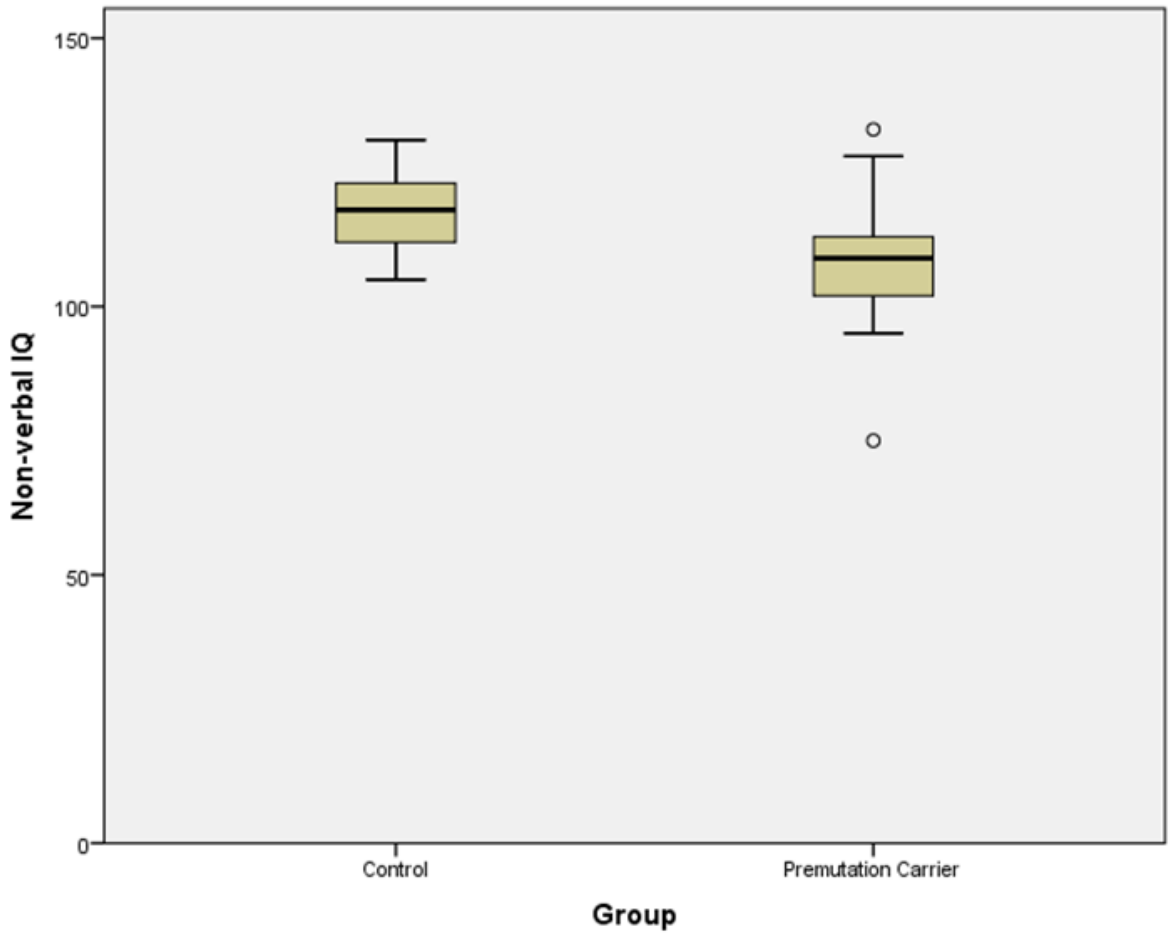

Figure 5.2 IQ scoring by group, analysed statistically using a parametric two-sample t-test in SPSS **b)** Non-verbal IQ by group. Mean non-verbal IQ in the premutation group was 108.1 (SD=13.7), mean non-verbal IQ in the control group was 117.4 (SD=7.7).

c)

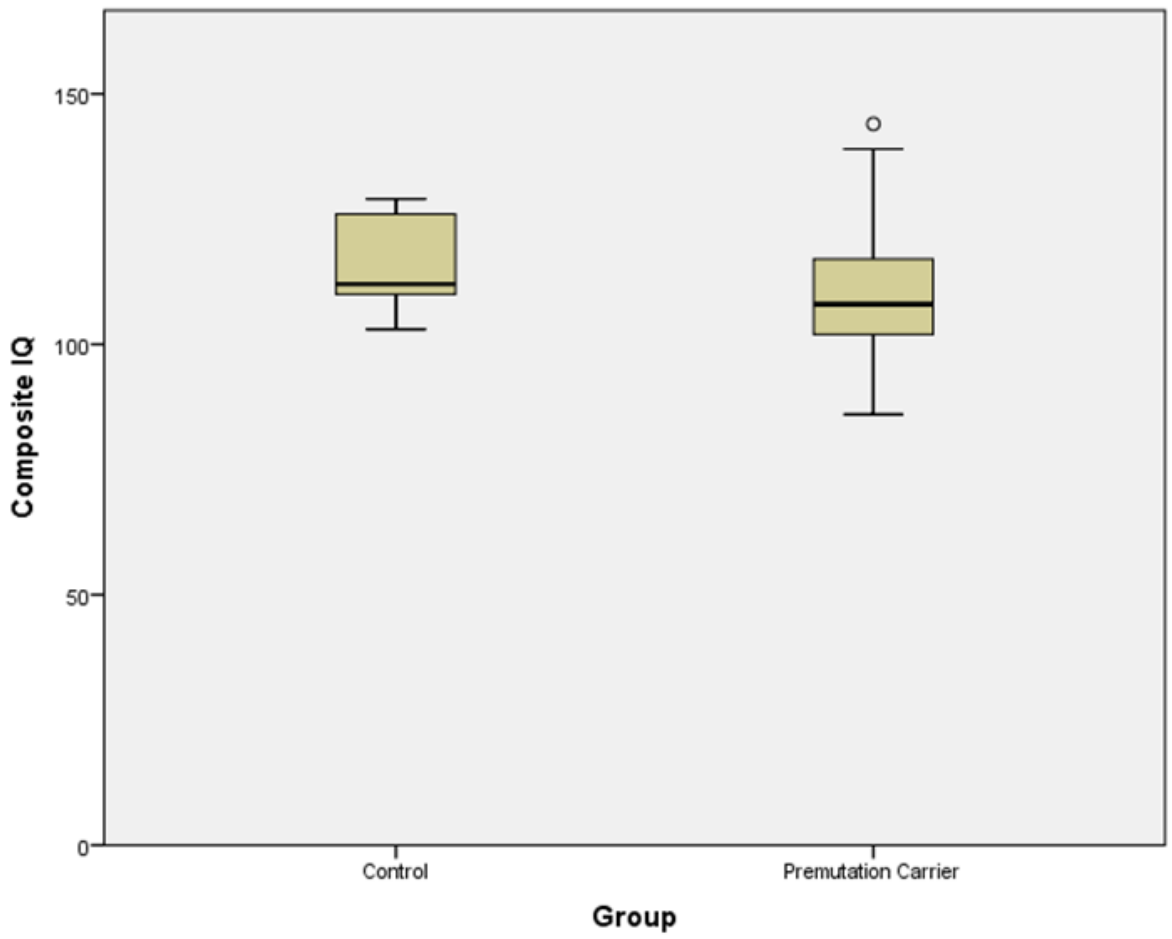

Figure 5.2 IQ scoring by group, analysed statistically using a parametric two-sample t-test in SPSS **c)** Composite IQ by group. Mean composite IQ in the premutation group was 110.4 (SD=14.9), mean composite IQ in the control group was 116.4 (SD=9.1).

5.2 Within group imaging analysis

Within group one sample t-test analysis revealed that when contrasting the sequential tapping and the random tapping conditions, controls exhibited a large cluster of activation (FWE_{corr}<0.001, T=8.62) at the bilateral lobules VI of the cerebellum, right Brodmann Area (BA) 17 of the primary visual cortex and right lobule V of the cerebellum. The maximum of the cluster was located at [14,-48,-16] (Fig. 5.3a). The premutation group exhibited a similar, smaller cluster of BOLD response at the right lobules VI and V of the cerebellum, although this did not reach significance (FWE_{corr}=0.491, T=6.05). The maximum of this cluster was located close to the control significant cluster, at [20,-58,-22] (Fig. 5.3b).

a)

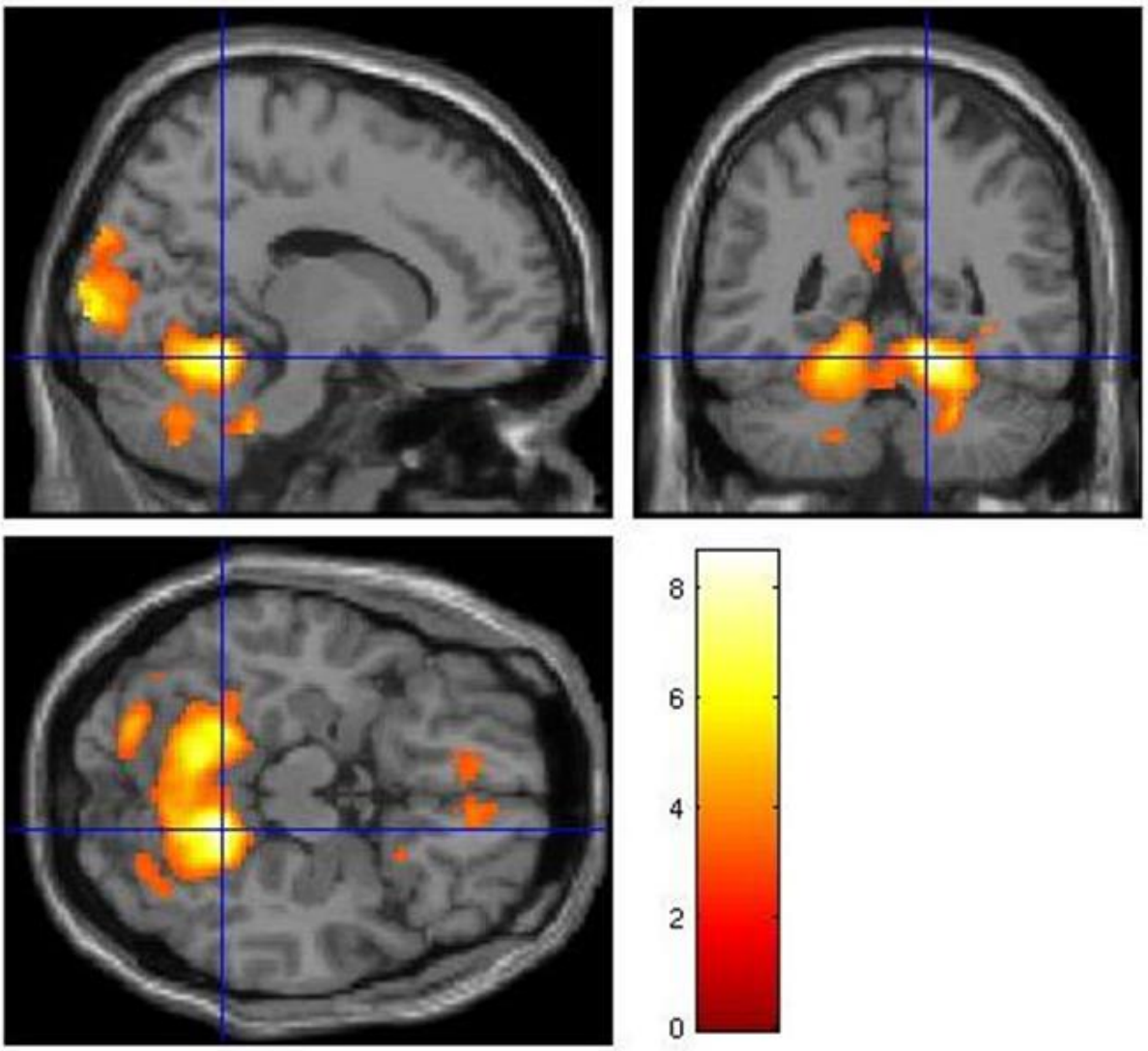

Figure 5.3 Within group functional brain imaging analysis carried out in SPM12 **a)** Within group analysis of the control group. Significant cluster of activation (FWE_{corr} <0.001, *T*=8.62) at the bilateral lobules VI of the cerebellum, right BA17 of the primary visual cortex and right lobule V of the cerebellum in the sequential>random condition contrast. Cluster co-ordinate of maximum voxel: 14,-48,-16, *k*=8039, normalised voxel size: $2mm^3$.

b)

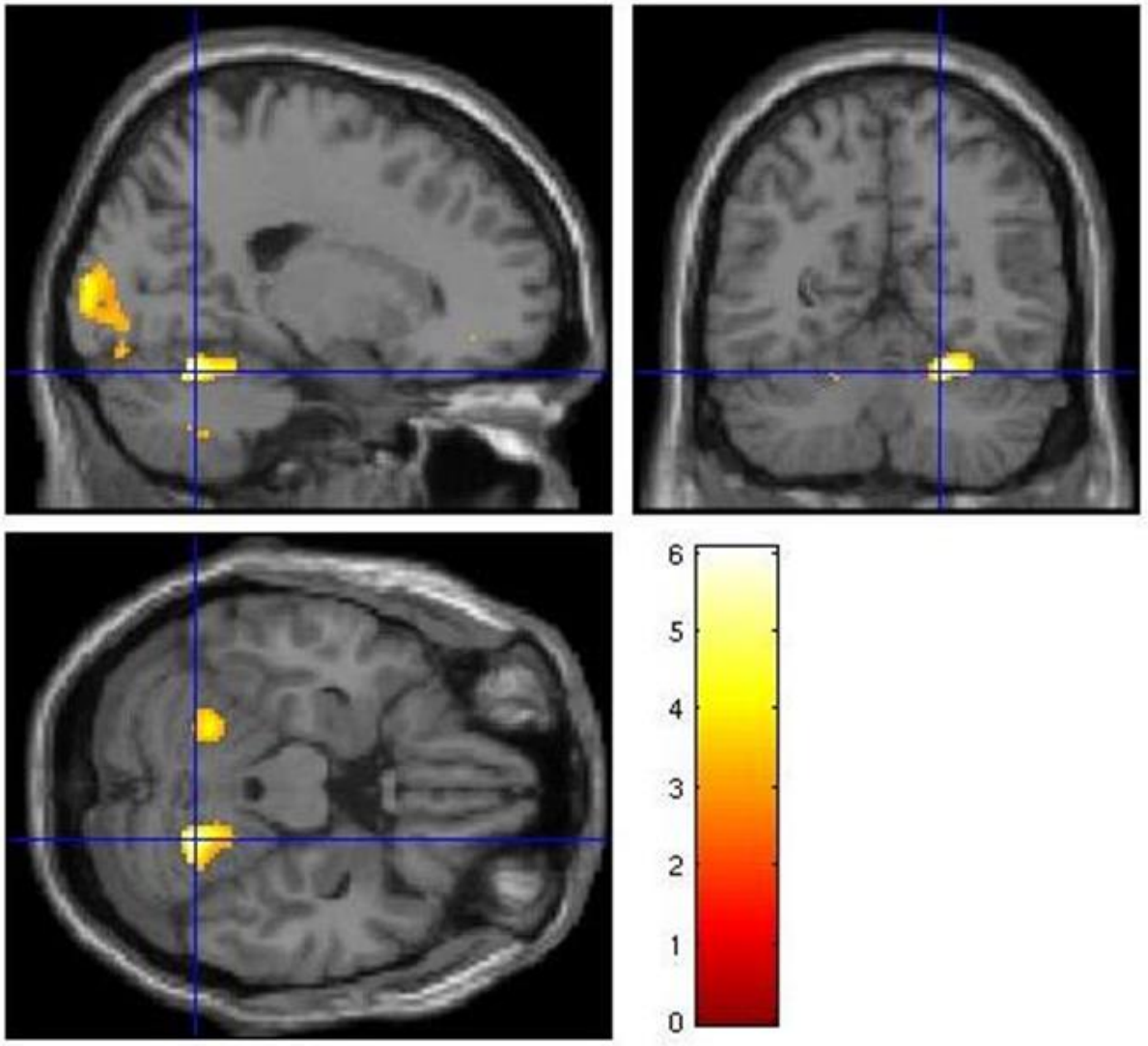

Figure 5.3 Within group functional brain imaging analysis carried out in SPM12 **b)** Within group analysis of the premutation carrier group. Cluster of BOLD activation, not reaching significance (FWE_{corr} <0.491, *T*=6.05) at the right lobules VI and V of the cerebellum in the sequential>random condition contrast. Cluster co-ordinate of maximum voxel: 20,-58,-22, *k*=198, normalised voxel size: $2mm^3$.

5.3 Between group imaging

Between group full factorial analysis carried out in SPM12 revealed that the premutation group had a significantly lower cluster of BOLD response (FWE_{corr}<0.001, T=5.59) at the bilateral lobules VI of the cerebellum, left lobule V and the left hippocampus (subiculum) compared to controls. The maximum of the cluster was located at [-12,-36,-12] (Fig. 5.4a).

As analysis of *FMR1* CGG repeat length revealed a number of carriers in the sample to be mosaic or borderline for the full mutation, a third group was created of mosaic and borderline carriers to ensure that anomalies in CGG repeat length were not skewing the imaging results, and that these individuals were not driving the between group differences. The ANOVA analysis was carried out in SPSS and the groups were defined as the following: control (n=17), premutation (n=13) and mosaic/borderline carriers (n=4). A statistically significant between group difference in BOLD response at the significant cluster maximum voxel [-12,-36,-12] was identified by one-way ANOVA (F(2,31)=14.249, p<0.001). A Tukey post-hoc test revealed that BOLD response for this cluster was significantly different in controls compared to carriers (p<0.001) and controls compared to mosaic/borderline carriers (p=0.026), but not significantly different between carriers and mosaic/borderline carriers (p=0.784). Representative group means are presented in figure 5.4b.

a)

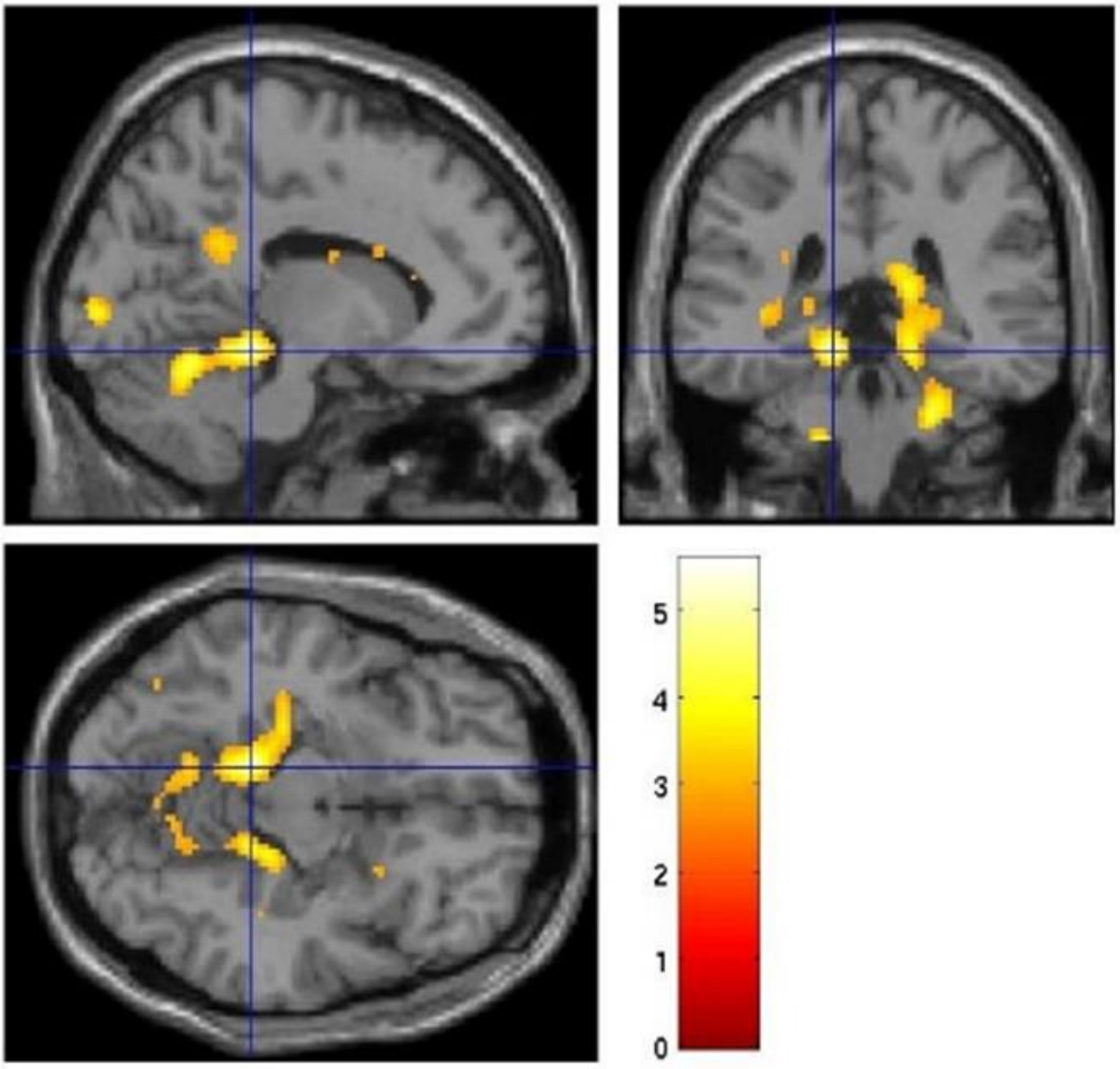

Fig. 5.4 Between group functional brain imaging analysis carried out in SPM12 **a)** Premutation group significantly less activated (FWE_{corr} <0.001, *T*=5.59) at the bilateral lobules VI of the cerebellum, left lobule V and the left hippocampus (subiculum) in the sequential>random condition contrast. Cluster co-ordinate of maximum voxel: -12,-36,-12, *k*=2040, normalised voxel size: $2mm^3$.

b)

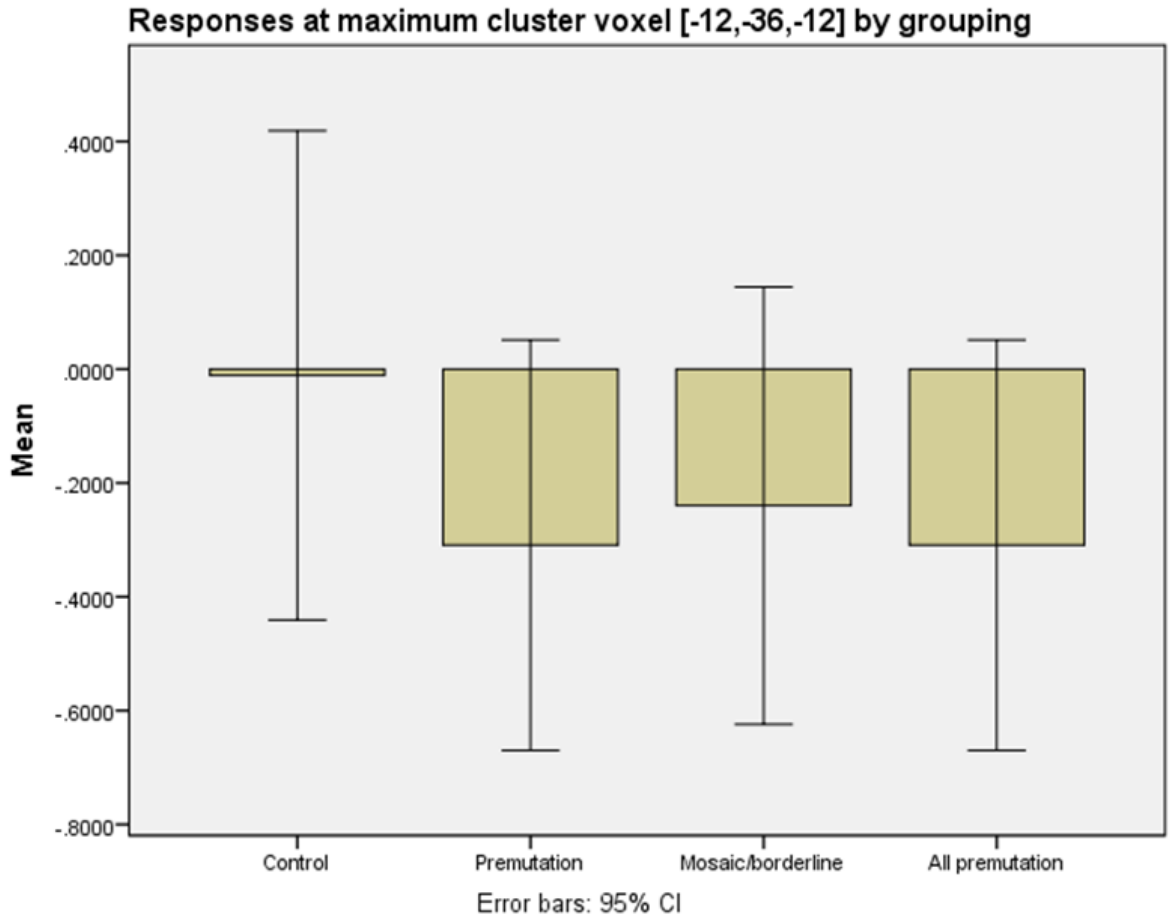

Fig. 5.4 Between group functional brain imaging analysis carried out in SPM12 and subsequently plotted using SPSS **b)** Mean extracted voxel response by grouping at the bilateral lobules VI of the cerebellum, left lobule V and the left hippocampus (subiculum), cluster co-ordinate of maximum voxel: -12,-36,-12.

5.4 Group x age interaction

In the analysis of age related differences, carried out at a whole brain level in SPM12, a significant group x age interaction was seen in a cluster that included the left inferior parietal cortex, the left Brodmann Area (BA) 17 in the primary visual cortex, the left hippocampus (cornu ammonis) and the left temporal lobe (FWE_{corr}<0.001, *T*=5.22). The maximum of the cluster is located at [-26,2,36] (Fig. 5.5a). Subsequently plotting extracted values from this cluster using SPSS indicated there was a negative relationship between age and activation in this cluster in the premutation group, while the relationship was positive in the control group. Within group regression analysis revealed both of these relationships to be significant (Table 5.2).

A univariate analysis of variance was also carried out on this significant cluster in SPSS to ensure anomalous CGG repeat lengths were not causing a bias in the imaging results. The groups for the univariate analysis of variance analysis were defined as the following: control (n=17), premutation (n=13) and mosaic/borderline carriers (n=4). A statistically significant group x age interaction was identified in BOLD response at the significant cluster maximum voxel [-26,2,36] ($p<0.001$), and plotting of group x age extracted voxel data demonstrates that both the premutation and the mosaic/borderline group differ significantly to controls but not to each other (Fig. 5.5b).

Table 5.2: Within group age/BOLD activation regression analyses

Group	DV	IV	β	Standard error	Adjusted R^2	P value
Control	Age	BOLD response at [-26,2,36]	0.763	0.001	0.554	<0.001
Premutation	Age	BOLD response at [-26,2,36]	-0.595	0.001	0.312	0.012

Table 5.2. Statistical results of within group regression analyses between participant age and BOLD activation at the left inferior parietal cortex, the left Brodmann Area (BA) 17 in the primary visual cortex, the left hippocampus (cornu ammonis) and the left temporal lobe, cluster maximum co-ordinate [-26,2,36].

a)

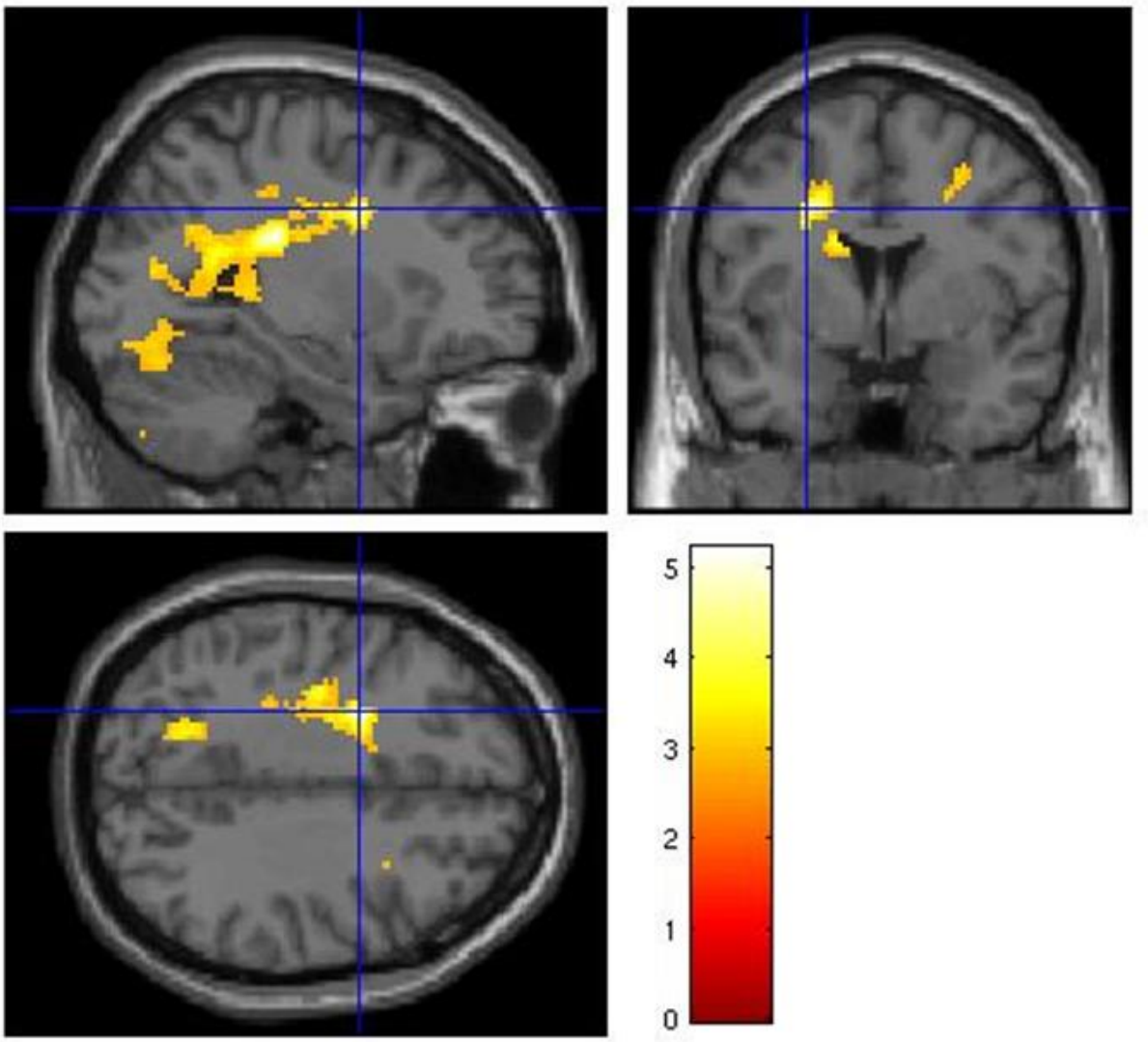

Fig. 5.5 Group x age interaction analysis carried out at a whole brain level in SPM12 **a)** Significant group x age interaction (FWE_{corr} <0.001, *T*=5.22) at the left BA17, left hippocampus (CA), left inferior parietal cortex and left temporal lobe in the sequential>random condition contrast. Cluster co-ordinate of maximum voxel: -26,2,36, *k*=2105, normalised voxel size: $2mm^3$.

b)

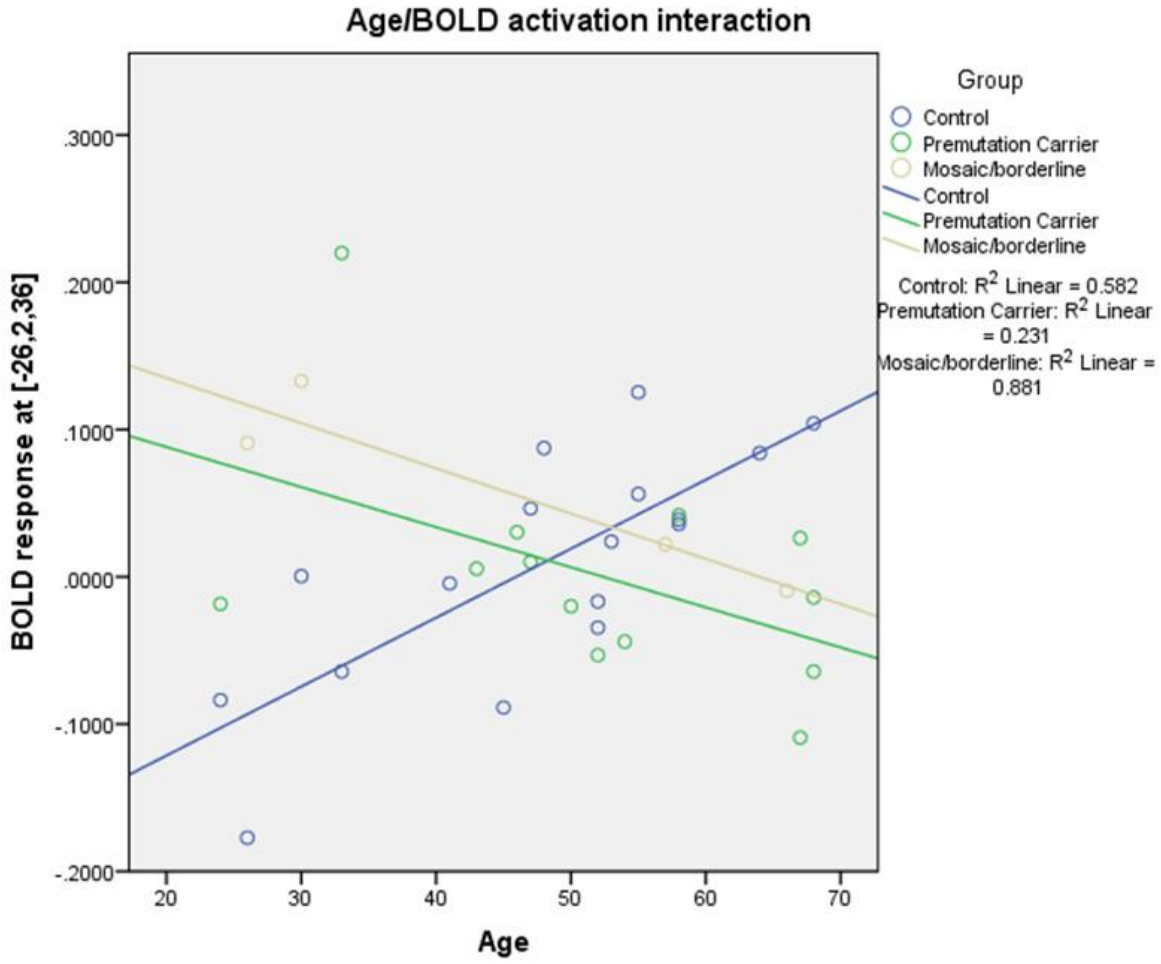

Fig. 5.5 Group x age interaction analysis carried out at a whole brain level in SPM12 and voxel data subsequently analysed and plotted in SPSS **b)** Fit linear regression lines comparing positive control BOLD response and age relationship compared to negative premutation carrier BOLD response and age relationship at maximum cluster voxel [-26,2,36], located at the left BA17, left hippocampus (CA), left inferior parietal cortex and left temporal lobe.

5.5 Clinical measurements

Although none of this population of carriers had been diagnosed with FXTAS, using parametric two-sample t-testing in SPSS, the CATSYS-2000 system identified carriers to have significantly worse tremor and co-ordination ($p=0.002$, $p=0.001$), although not balance ($p=0.931$) compared to controls (Fig. 5.6). Both populations had mean performance indices of better than normal human performance on the co-ordination and balance measurements and below normal human performance on the tremor measurement (Table 5.3).

a)

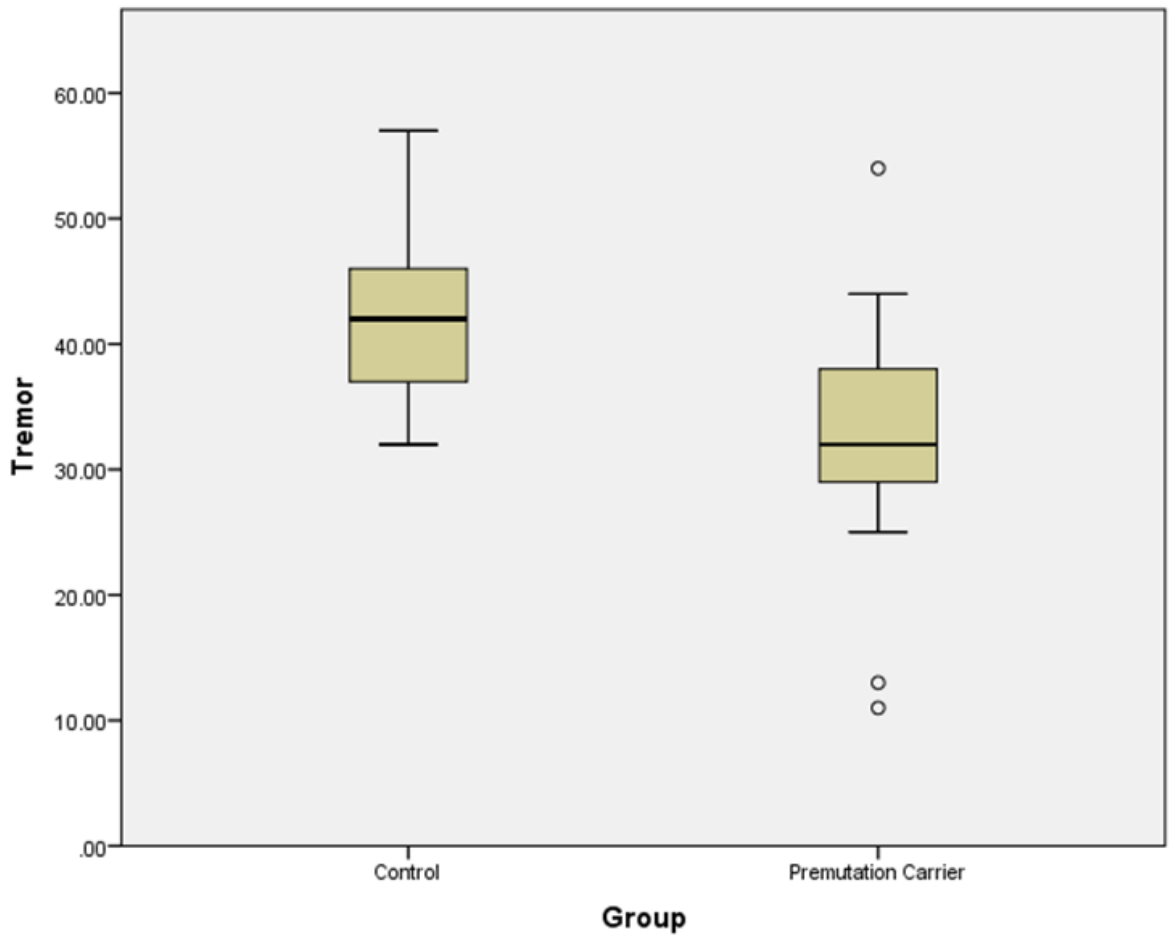

Figure 5.6 CATSYS-2000 movement data analysed using parametric two-sample t-testing in SPSS **a)** Participant tremor score by group. Mean tremor score for the premutation carrier group was 0.325 (SD=0.106) and mean tremor score for the control group was 0.431 (SD=0.72).

b)

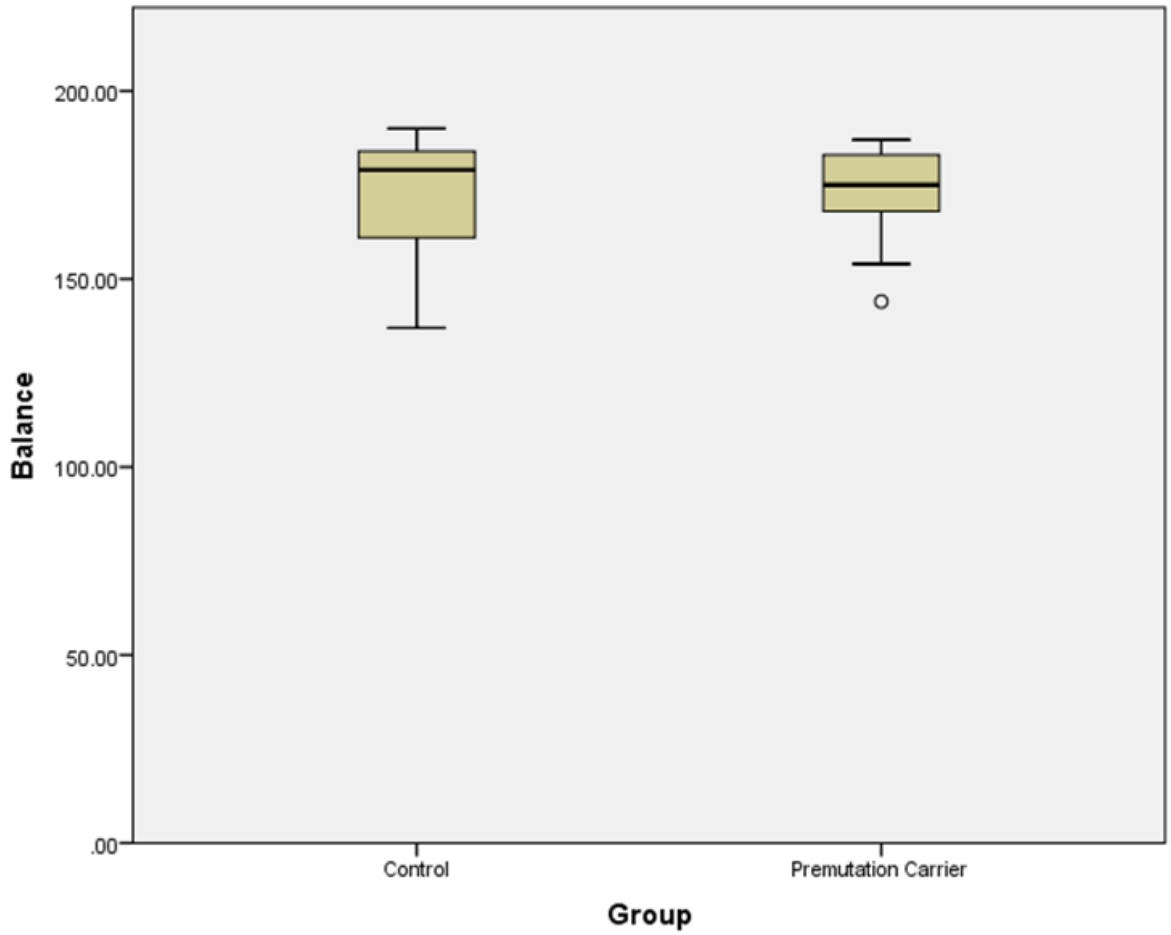

Figure 5.6 CATSYS-2000 movement data analysed using parametric two-sample t-testing in SPSS **b)** Participant balance score by group. Mean balance score for the premutation carrier group was 1.73 (SD=0.13) and mean balance score for the control group was 1.719 (SD=0.156).

c)

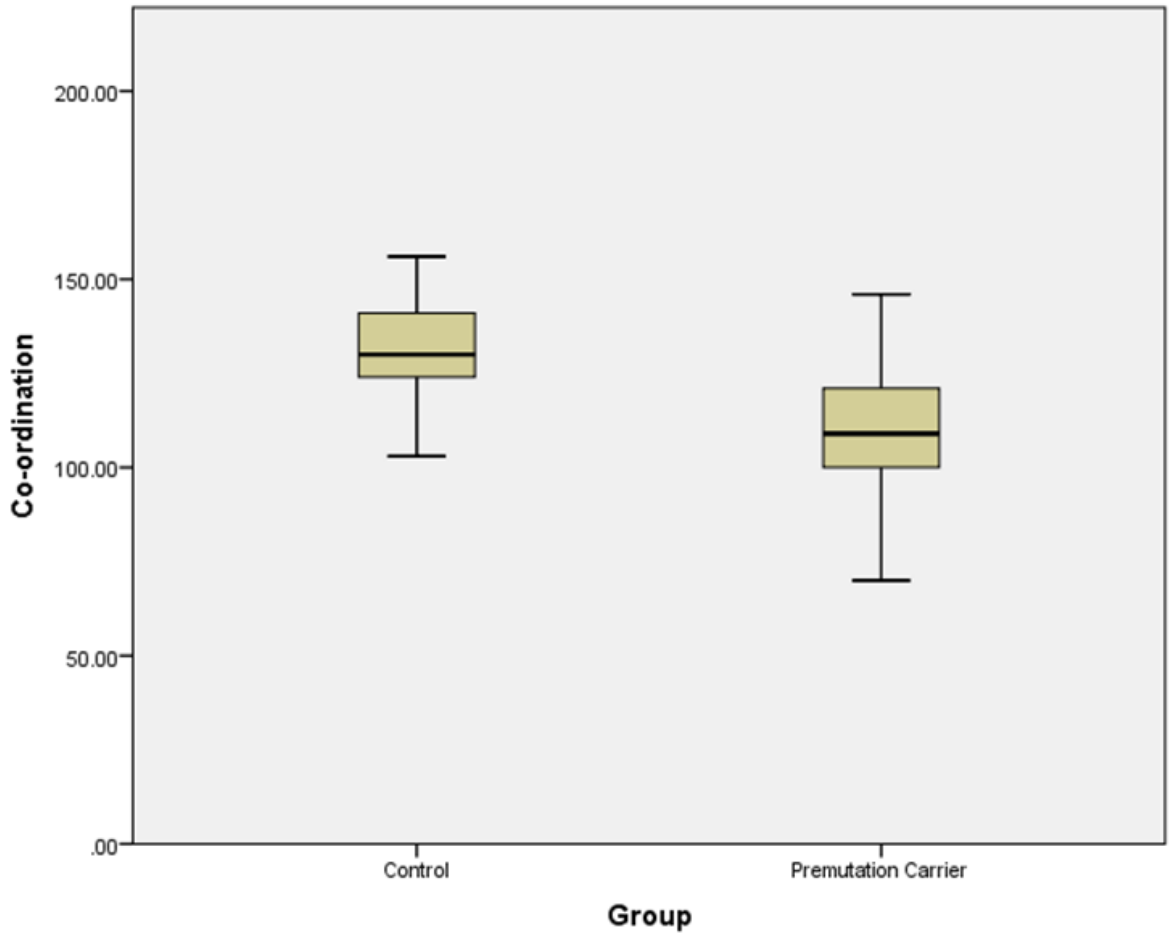

Figure 5.6 CATSYS-2000 movement data analysed using parametric two-sample t-testing in SPSS **c)** Participant co-ordination score by group. Mean co-ordination score for the premutation carrier group was 1.089 (SD=0.191) and mean co-ordination score for the control group was 1.312 (SD=0.154).

Table 5.3: CATSYS-2000 movement data

Group	Mean tremor score	Tremor SD	Mean balance score	Balance SD	Mean co-ordination score	Co-ordination SD
Control	0.43	0.72	1.719	0.156	1.311	0.154
Premutation	0.325	0.106	1.730	0.130	1.088	0.191

Table 5.3 Comparison of mean tremor, balance and co-ordination measurements obtained from the CATSYS-2000.

5.6 Molecular measurements

Quantative PCR analysis revealed that this population of asymptomatic premutation carriers do not have significantly higher levels of *FMR1* mRNA relative to 18 sRNA when measured from peripheral blood samples (p=0.3223). However, normalization of carrier *FMR1* mRNA relative to 18 sRNA to age-matched control data suggests there is a higher mean level than controls and some carriers have up to a 7-fold increase in *FMR1* mRNA when compared directly to an age-matched control (Fig 5.7a). To examine again whether the borderline or mosaic carriers were causing anomalies in the data, these individuals were separated from the analysis. One-way ANOVA analysis revealed no significant difference in borderline or mosaic carrier *FMR1* mRNA level relative to 18 sRNA compared to controls or premutation carriers (Fig. 5.7b).

a)

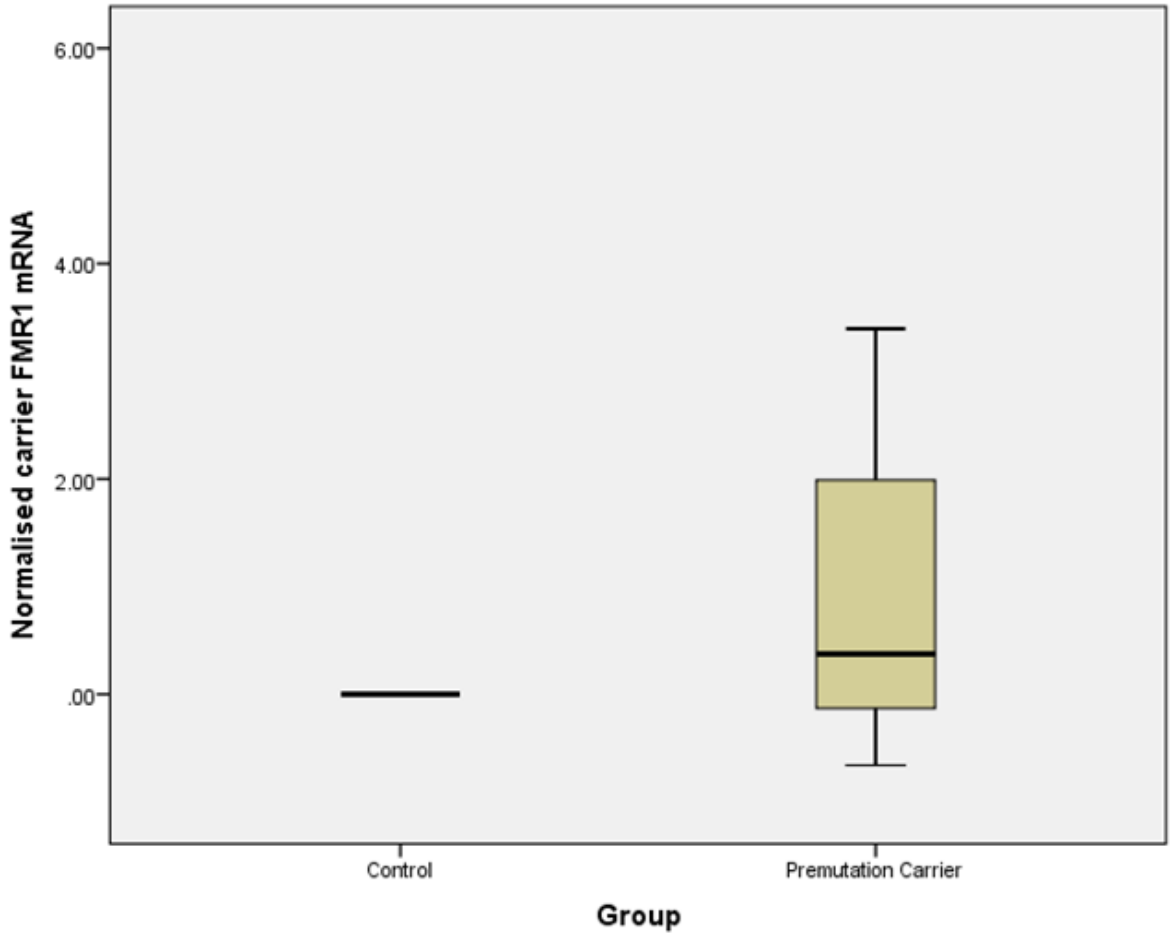

Fig. 5.7 *FMR1* mRNA quantification data analysed using parametric two-sample t-testing in SPSS **a)** Carrier *FMR1* mRNA amount relative to 18 sRNA normalised to age-matched control levels.

b)

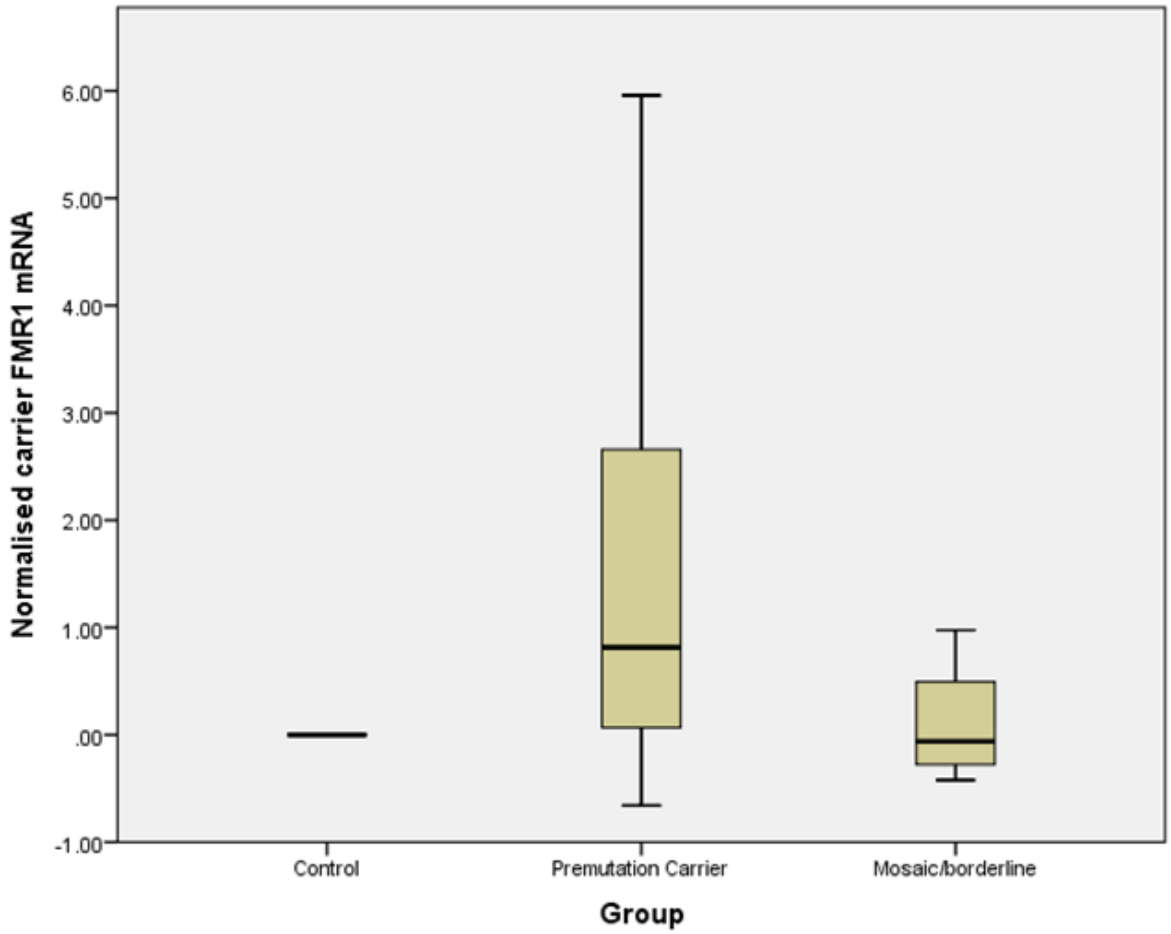

Fig. 5.7 *FMR1* mRNA quantification data analysed using parametric one-way ANOVA testing in SPSS **b)** Carrier and mosaic or borderline carrier *FMR1* mRNA amount relative to 18 sRNA normalised to age-matched control.

5.7 Linear regression analyses

Simple linear regression analyses were carried out in SPSS on the imaging and clinical variables (Table 5.4). Extracted raw voxel data from the cluster global maxima originating from the between group analysis, located at the bilateral lobules VI of the cerebellum, left lobule V and the left hippocampus (subiculum) was regressed against measures of tremor, co-ordination and balance. No significant association was found between these variables and the between group significant cluster in either carriers or controls. Extracted raw voxel data from the global maxima of the significant cluster from the age interaction analysis, located at the left BA17, left hippocampus (cornu ammonis), left inferior parietal cortex and left temporal lobe, was also regressed against participant tremor, co-ordination and balance data. None of the linear regression analyses showed an association between age-related functional brain changes and these variables in either carriers or controls.

Simple linear regression analyses were also carried out on the imaging data and measurements of *FMR1* mRNA (Table 5.4). Neither the between group imaging significant cluster or the significant group x age cluster revealed a significant relationship with *FMR1* mRNA.

Table 5.4: Within group regression analysis

Group	DV	IV	β	Standard error	Adjusted R^2	P value
Control	BOLD response at [-12,-36,-12]	Tremor	-0.196	0.009	-0.026	0.452
		Balance	-0.027	0.004	-0.066	0.917
		Co-ordination	-0.053	0.004	-0.064	0.839
		FMR1 mRNA	0.105	34399.317	-0.055	0.689
Premutation	BOLD response at [-12,-36,-12]	Tremor	-0.054	0.006	-0.064	0.838
		Balance	-0.311	0.005	0.036	0.225
		Co-ordination	0.322	0.003	0.044	0.207
		FMR1 mRNA	-0.024	19615.590	0.066	0.926
Control	BOLD response at [-26,2,36]	Tremor	-0.100	0.003	-0.056	0.702
		Balance	-0.177	0.001	-0.033	0.479

		Co-ordination	-0.010	0.001	-0.067	0.970
		FMR1 mRNA	0.359	9677.064	0.071	0.157
Premutation	BOLD response at [-26,2,36]	Tremor	-0.202	0.002	-0.023	0.438
		Balance	-0.007	0.002	-0.067	0.978
		Co-ordination	0.217	0.001	-0.017	0.403
		FMR1 mRNA	0.048	6058.494	-0.064	0.354

Table 5.4 Statistical results of within group regression analyses between extracted BOLD activation data from the significant cluster, located at the bilateral lobules VI of the cerebellum, left lobule V and the left hippocampus (subiculum) in the classic between group analysis, cluster maximum co-ordinate [-12,36,-12], and the significant cluster in the group x age interaction analysis, located at the left BA17, left hippocampus (CA), left inferior parietal cortex and left temporal lobe, cluster maximum co-ordinate [-26,2,36], with clinical and molecular variables.

Chapter 6: Neurodegeneration in the Fragile X premutation: Discussion

6.1 Within group imaging

Within group one sample t-test analysis revealed a large significant cluster of BOLD activation in the control group, centred at the lobules VI and V of the cerebellum and extending into BA17 of the primary visual cortex, when contrasting the sequential and random finger-tapping conditions. A smaller cluster centred in the same region, but not reaching statistical significance, was evident in the premutation group within group analysis. These BOLD responses in the anterior lobe of the cerebellum (lobules I-VI) is consistent with both the cerebellar homunculus and previous reported findings (O'Reilly et al. 2010a). In a similar manner to the present study, an fMRI investigation into patients with essential tremor revealed within group activation during blocks of upper limb movement of cerebellar lobule V in both controls and patients (Broersma et al. 2016). Functional topography studies report cerebellar lobule V in particular as being activated in response to finger-tapping, and lobule VI is reported as being involved during more cognitively demanding tasks (Stoodley et al. 2012). The involvement of both lobules V and VI in the present within group analysis is in line with these previous reports of differential activation and demand responses, as contrasting two finger-tapping conditions here was hypothesised to provide activation patterns consistent with a change in task demand, given that choice-driven, random tapping is known to elicit higher peak and more diffuse activation patterns than sequential tapping (Gountouna et al. 2010).

Although both the control and premutation group separately exhibited a cluster of activation centred at the anterior lobe of the cerebellum, the cluster was significant in the control group but not in the carrier group. It is possible that an increased heterogeneity of activation patterns in the carrier group may have contributed to no significant clusters being identified, given that it is a high-risk group for neurological disease. However, the within group analyses robustly indicate an overall reduction in BOLD response in the carrier group when contrasting sequential and random finger-tapping conditions. The regional activation specificity of this finger-tapping task is also reflective of previous findings into fMRI motor-based tasks and the cerebellar topography.

6.2 Between group imaging

Consistent with the primary hypothesis, differences between carriers and controls were identified when contrasting random and sequential finger-tapping conditions in this fMRI task in the bilateral lobules VI of the cerebellum, left lobule V and the left hippocampus (subiculum), reflective of the within group analysis.

The cerebellum is a brain region which is strongly associated with movement initiation and processing, as well as being a site of degeneration in FXTAS (Berry-Kravis, Abrams, et al. 2007). Cerebellar involvement is a key part of FXTAS, with generalised loss of cerebellar volume

disproportionate for age being commonly reported in patients and hyperintensity at the middle cerebellar peduncles seen in T2 and FLAIR acquisitions, known as the MCP sign, forming part of the primary diagnostic criteria for FXTAS (Capelli et al. 2010). The MCP sign is reported in approximately 60% of FXTAS patients, and diffusion tensor tractography has revealed that the middle cerebellar peduncles exhibit weaker structural connectivity compared to controls (Wang, Hessl, et al. 2013; Apartis et al. 2012). In addition, other cerebellar tracts, such as the superior cerebellar peduncles, showed weaker structural connectivity than normal in FXTAS, and these measurements exhibited a correlation with motor functioning across the control, FXTAS and asymptomatic carrier groups (Wang, Hessl, et al. 2013). It is therefore not unexpected that a between group difference has been identified at the cerebellum, extending into the hippocampus, during a finger-tapping task in a premutation population. Sensorimotor mapping of the cerebellum labels lobule V as primarily related to movements of the hand, and finger-tapping tasks have previously been found to reliably activate cerebellar lobule V, with more cognitively demanding tasks also recruiting lobule VI (Stoodley et al. 2012; Grodd et al. 2001). Our finding of significantly lower activation at lobule VI of the cerebellum may well reflect deficits in recruitment during higher levels of demand during the task, in addition to a lower level of basic sensorimotor processing at lobule V. The hippocampus is not routinely cited as being significantly activated during within group analyses of fMRI motor tasks, however the extension of the significant between group cluster to the hippocampal subiculum may also indicate a deficit in more diffuse recruitment in response to a change in task demand (De Guio et al. 2012; Berns et al. 1999). This type of evidence of significant differences between carriers without FXTAS and controls during a motor task is suggestive of neurological vulnerability to disease prior to onset.

Our results also indicate parallels with other neurodegenerative diseases. Interestingly, cerebellar lobule VI has previously been highlighted as an area of significantly different BOLD response during self-cued finger-tapping in Parkinson's patients when compared to healthy controls (Mak et al. 2016). Lobule V of the cerebellum has also been indicated in functional connectivity analysis to be associated with tremor variation in both its intrinsic activity and extrinsic connectivity to the thalamus in patients with an essential tremor (Buijink et al. 2015). These links to functional changes at cerebellar lobules V and VI with other neurodegenerative diseases or movement disorders tie to FXTAS symptomology, given the presence of both tremor and Parkinsonism in most FXTAS patients, and here we demonstrate for the first time functional imaging evidence of similar motor processing differences in premutation carriers.

6.3 Group x age interaction

A significant group x age interaction was also identified that revealed that, compared to controls, carriers showed a significantly more negative association between age and activation in the left BA17, left hippocampus (cornu ammonis), left inferior parietal cortex and left temporal lobe. Involvement of

the cerebrum is a major part of FXTAS development, with generalised cerebral atrophy being reported in virtually all FXTAS patients studied (Brunberg et al. 2002; Jacquemont et al. 2003b; Greco et al. 2002; Leehey et al. 2003). Volumetric studies revealed significant loss of volume in the thalamus, amygdalo-hippocampal complex and cerebral cortex in patients with FXTAS, and in particular, reduction in hippocampal volume was correlated with more advanced clinical staging of FXTAS (Adams et al. 2007; Loesch et al. 2005; Moore et al. 2004). Given that the cerebrum has been globally implicated in FXTAS pathology, moreover in a progressive manner, it is pertinent that imaging results of this group x age interaction analysis reveal a cluster that involves the hippocampal formation, visual cortex and other areas of the cerebrum.

Within group regression analysis of the voxel data from this significant cluster revealed that both the positive age-related correlation in the control group and the negative age-related correlation in the premutation group were significant. In normal elderly populations, finger-tapping has been seen to elicit over-recruitment of the occipito-temporo-parietal regions, suggesting an increased level of visual or mental strategizing (Zapparoli et al. 2013). This idea of compensatory activity is reflected in our regression analysis, with activation in the temporo-parietal cluster identified in this analysis showing a positive linear relationship with increasing age in the control population. However, this cluster shows significant deactivation in relation to age in the premutation group, suggesting that there is degeneration affecting the functional compensatory response to changes in movement demands.

Additionally, links to other types of neurodegeneration can me made here, as the hippocampus and medial temporal lobe, areas identified as significantly different between groups in their interaction with aging, have long been known to be areas of early neurodegeneration, being particularly vulnerable to the development of molecular and cellular pathology (Braak & Braak 1991; Serrano-Pozo et al. 2011; Hochgräfe et al. 2013). The parietal lobe has also exhibited significant grey matter reduction in Spinocerebellar Ataxia Type 3 patients, a disease often likened to FXTAS in its molecular and radiological development (Duarte et al. 2016). In Huntington pre-symptomatic carriers, another useful disease parallel for FXTAS and premutation carriers, a fMRI finger-tapping task revealed an inhibitory effect on the connection from the parietal cortex to premotor areas during dynamic causal modelling analysis (Minkova et al. 2015). In addition, cognitive decline in FXTAS is of a mixed subcortical pattern, much like other neurodegenerative diseases that implicate the hippocampal formation as an area of early pathology (Seritan et al. 2008; Berry-Kravis, Goetz, et al. 2007; Brega et al. 2008). These parallels of neurodegeneration may be useful in further characterising the nature and progression of FXTAS.

6.4 Clinical measurements

In addition to imaging data, the present study utilised clinical measurements of tremor, co-ordination, balance using the CATSYS-2000 computerised system to further characterise the participant sample.

Independent two-sample T-tests revealed that performance on the tremor and co-ordination measurements were significantly worse in carriers, suggesting subtle motor symptoms in the absence of a diagnosis of FXTAS. CATSYS measurements in female carrier populations both with and without FXTAS also exhibited significantly worse tremor and co-ordination, and a study of high CGG repeat size and low CGG repeat size asymptomatic carriers identified tremor in 23% of men who did not self-report tremor symptoms, and ataxia in 30% of men who did not report ataxic symptoms (Allen et al. 2008b; Narcisa et al. 2011). Interestingly however, in the present study, both the control and carrier groups performed worse than normal human performance on average on the tremor measurements, but better than normal human performance on average on the co-ordination measurements. Other studies utilizing CATSYS measurements in carriers have not reported indices relating to normal human performance, and therefore there are difficulties in reconciling these results with other findings. One possible explanation however may be that other CATSYS studies in premutation carriers have described the exclusion of outlying data due to concerns about instrument malfunction, which was not replicated in this study (Allen et al. 2008b; Narcisa et al. 2011). In addition, age may be a confounding factor here, given the cross-sectional nature of this study and unknown concordance of subject age with the original CATSYS normal material (Danish Product Development Ltd.). Independent T-test analyses did not reveal balance to be significantly different in carriers than in controls, and this may be explained by balance being affected later on during FXTAS progression, as falls are not often reported in early disease stages, meaning that balance symptomatology is not present in this asymptomatic or pre-clinical sample. Again, balance indices on average were higher than normal human performance in both the control and carrier groups, which may possibly be explained by the same confounds as described for the tremor and co-ordination CATSYS measurements.

6.5 Molecular measurements

FMR1 mRNA has frequently been reported as higher in premutation carriers and is theorised to be one of the primary molecular driving forces behind the development and progression of FXTAS. However, results have been inconsistent as to whether these differences reach statistical significance (Hagerman & Hagerman 2013; Garcia-Arocena & Hagerman 2010; Jacquemont et al. 2003a). Independent two-sample T-test analysis of the *FMR1* mRNA amount relative to control 18 sRNA amount does not reveal levels of *FMR1* mRNA to be significantly higher in carriers compared to controls. Nevertheless, when each carrier *FMR1* mRNA amount relative to 18 sRNA was normalised to counterpart age-matched control data, carrier levels were often higher, with some carriers exhibiting up to 7-fold increases compared to age-matched control. These results are in line with previous data, with evidence of higher *FMR1* mRNA in carriers when normalised to control data and the fold increase of RNA being comparable to previous findings (Kenneson et al. 2001; Tassone, Hagerman, Taylor, Gane, et al. 2000).

6.6 Linear regression analyses

None of the tremor, balance or co-ordination index variables exhibited an association with the raw voxel data extracted from the between group analysis at the cluster at the bilateral lobules VI of the cerebellum, left lobule V and the left hippocampus (subiculum). It is possible in this case that a relatively small sample size for this study may have led to these results not reaching significance. Additionally, in the absence of overt FXTAS, it may be that symptomatology and functional brain changes are not yet developed enough to display a significant relationship. Tremor, co-ordination and balance as measured by the CATSYS-2000 system also did not prove to be significantly associated with raw voxel data extracted from the age-related significant cluster at the left BA17, left hippocampus (cornu ammonis), left inferior parietal cortex and left temporal lobe. This may be due to the likelihood of this predominantly limbic cluster being more relevant to compensatory activity and motor imagery, instead of overt motor processing and associated deficits, in addition to the aforementioned limitations regarding power to detect a small effect size and the present study's cross-sectional design.

Measurements of *FMR1* mRNA from peripheral blood samples did not show any relationship with significant differences in BOLD response, in either the between group or age-related analysis. *FMR1* mRNA levels are thought to be one of the main molecular causes of neurodegenerative processes in FXTAS, and it is therefore somewhat surprising that *FMR1* mRNA amount is not related to these functional imaging changes. Previous studies have found hippocampal volume to be correlated with *FMR1* mRNA and IQ scores in premutation carriers, which is supportive of the hypothesis that brain changes that are most likely early signs of FXTAS should be associated with changes in mRNA levels or metabolism (Cohen et al. 2006; Adams et al. 2007). It can be theorised from the findings of the present study, in addition to some inconsistent findings in the literature pertaining to *FMR1* mRNA levels and associated variables in carriers, that using peripheral blood samples to ascertain RNA measurements may be only a loose estimate and reflection of brain expression profiles (Tassone, Adams, Elizabeth M Berry-Kravis, et al. 2007; Cohen et al. 2006; Leehey et al. 2008). It is possible however that statistical power may be a contributing factor to the discrepancies in the findings into *FMR1* mRNA levels in carriers, in addition to variation in asymptomatic premutation carrier populations in terms of future FXTAS penetrance. To elucidate this further, work in the field should attempt to strive towards methodology that can more directly identify molecular changes in the brain *in vivo* or post mortem.

6.7 Limitations and conclusions

Here, we report neuroimaging and clinical evidence of possible early, pre-FXTAS neurodegeneration, however, limitations of the present study should be considered. The future FXTAS penetrance of the sample may be a confounding factor of the study. As previously mentioned, 40-60% of males with the

premutation will go on to develop FXTAS later in life (Sébastien Jacquemont et al. 2004). Firstly, when using a sample of *FMR1* carriers without FXTAS, the reality of this penetrance within the sample is unknown. Additionally, the study utilised a cross-sectional design to allow the investigation of age as a regressor. A cross-section of participants aged between 20-70 years without FXTAS may introduce a bias in the sample therefore towards older carriers who are less at risk or will not develop FXTAS. Unfortunately, without longitudinal data, the impact of FXTAS penetrance on this sample cannot be established, although this is something possible to achieve in future follow-up investigations.

Another notable limitation in the methodology of the present study is using peripheral blood measurements of *FMR1* mRNA with the aim of reflecting brain expression levels. Firstly, it is known that expression profiles of *FMR1* mRNA are variable across regions of the brain, with relative isoform transcripts varying by as much as two orders of magnitude. Different biochemical properties are inferred by different isoforms, and isoform expression patterns in the hippocampus and olfactory bulb are reported to differ from patterns of dominant isoform types elsewhere in the brain (Brackett et al. 2013). Region specific expression patterns in the brain therefore are unlikely to be reflected in a relative *FMR1* mRNA average measurement derived from peripheral blood mononuclear cells. Additionally, studies into *FMR1* mRNA isoforms have revealed differential expression between human carriers and controls, which do not remain statistically consistent between brain tissue and peripheral blood mononuclear cells (Pretto et al. 2015). However, blood sample derived molecular measurements remain the safest, least invasive and most ethically sound methodology to use in a clinical research setting. In addition, blood-based molecular analyses promise the potential scope for easily accessible future biomarkers.

Here we show for the first time in asymptomatic *FMR1* premutation carriers evidence of significantly lower cerebellar activity during an fMRI motor task. The neuroimaging analyses also revealed a cerebral and limbic cluster where the group x age interaction differed significantly between carriers and controls. These findings of deviation from normal BOLD activation patterns during a movement-orientated task and activation changes differing significantly from normal aging are likely to be indicative of a functional vulnerability to FXTAS in the anterior lobe of the cerebellum and hippocampal formation. Longitudinal follow-up investigations into this cohort may confirm a susceptibility to FXTAS and indeed progression of symptomatology in some individuals.

Additionally, we also identify in this sample premutation carriers without FXTAS demonstrating significantly worse measurements of sub-clinical tremor and co-ordination. These subtle movement phenotypes in carriers indicate that motor problems are present before the onset of diagnosable FXTAS, and may even be present from a young age. Again, longitudinal study of this sample may

allow formation of a third FXTAS group, which can then be compared against non-FXTAS carriers and the stability of movement symptoms over long periods of time may be mapped.

Consistent with previous reports, we also find that relative *FMR1* mRNA levels in carriers are increased, although this does not reach statistical significance. Further insights into the molecular pathology of FXTAS may be gained through using existing RNA aliquots to probe specific *FMR1* isoforms, with the aim of replicating isoform abundance levels as previously reported in carrier populations, and building on clinical understanding by using regression analyses to establish any possible relationships between isoform expression profiles and movement symptomatology or functional brain responses.

Regression analyses carried out within this study revealed no association of clinical or molecular variables to significant second level clusters of brain activation. Given the strong hypothetical links between a functional MRI motor task, movement symptoms, the *FMR1* mRNA gain-of-function toxicity model and FXTAS phenotypes, we may have expected to see a significant relationship between some of these measurements. However, a higher level of power may allow for such relationships to reach significance in future studies, or indeed, establish that such associations do not exist in carriers without FXTAS.

Overall, these novel neuroimaging findings, replication of previous molecular findings and insights into sub-clinical movement problems in asymptomatic premutation carriers provide new understanding of the development of FXTAS-related neurodegeneration.

Chapter 7: Neurodevelopment in the Fragile X premutation: Methods

7.1 Participants and recruitment

The same 34 individuals who took part in the investigation into neurodegeneration in the premutation, also took part in this neurodevelopmental part of the study. The recruitment process, inclusion and exclusion criteria are described in Chapter 4.1.

7.2 Imaging methods

All MRI data was acquired in the same scanning session and image acquisition is described in Chapter 4.2.

The emotional processing task used in the scanning protocol was designed and ran on Presentation™ software. The task utilised 120 pictures sourced from the International Affective Picture System (IAPS), which differentiates images based on arousal and valence (pleasure) ratings, as defined by IAPS normative data. Arousal and valence are rated on a scale of 1-10, with higher scores indicating higher levels of arousal or pleasure. Normative affective ratings were obtained to form this material from approximately 50 male college students (Lang et al. 2005). In the present task, 20 pictures for each of the following conditions were used: high pleasure/low arousal, high pleasure/high arousal, low pleasure/low arousal, low pleasure/high arousal, neutral pleasure/high arousal and neutral pleasure/low arousal. Pictures that were judged to be too distressing, disturbing or graphic were removed from the task, meaning that arousal rating of the pictures was not above 7.02. Neutral images were chosen based on a median valence range of 4.5-5.5. Selected IAPS images for this study are plotted according to valence and arousal ratings in figure 7.1 and image details are listed in Appendix 7.1. The task utilised an event-related design, with each trail duration comprising of stimulus presentation and an inter-stimulus interval. Order of the presentation of stimulus condition was randomised, without variation between participants. Jittering of the stimuli relative to the TR was achieved by varying inter-stimulus interval length at upper and lower truncation points of 1.5 and 2.5 seconds. Mean inter-stimulus interval for each condition was 2 seconds. All stimuli presentation durations were 1.5 seconds, and mean trial duration was 3.5 seconds for each condition. A 2 second fixation period was presented every 10 trials. Each total condition duration was 1 minute 10 seconds. Participants were asked to indicate using left and right trigger buttons in the scanner whether or not there was a face in each of the pictures – i.e. “Face” or “No face” – as a measure of engagement with the task. Participants were given written instructions for all of the tasks before entering the MRI scanner (Appendix 4.1), shown an example of each task on a laptop screen and given the chance to ask any questions they may have had. The tasks were visually presented to participants using goggles that fit onto the scanner head coil.

The IAPS emotional processing task used here was designed specifically for this study and was behaviourally tested on 5 individuals who were not prospective participants for the main study (Table 7.1). The task was presented exactly as it would be in the scanner on a laptop using Presentation™ software, using keyboard buttons in the place of trigger buttons. Each individual taking part in the behavioural testing filled out an evaluation form of the task (Appendix 7.2) which focussed on clarity of the task instructions and engagement in the task. Subjects were also asked whether choosing "Face" or "No Face" for each picture during the task distracted them from the picture content, and whether they found the images emotional. The majority of individuals rated the task as simple and engaging. None of the individuals behaviourally testing this task rated that choosing "Face" or "No Face" for each picture as distracting from the picture content, and the majority found that indicating "Face" or "No Face" was not confusing or difficult. It was therefore deemed that the task was suitable for participants to undergo in a functional MRI scan.

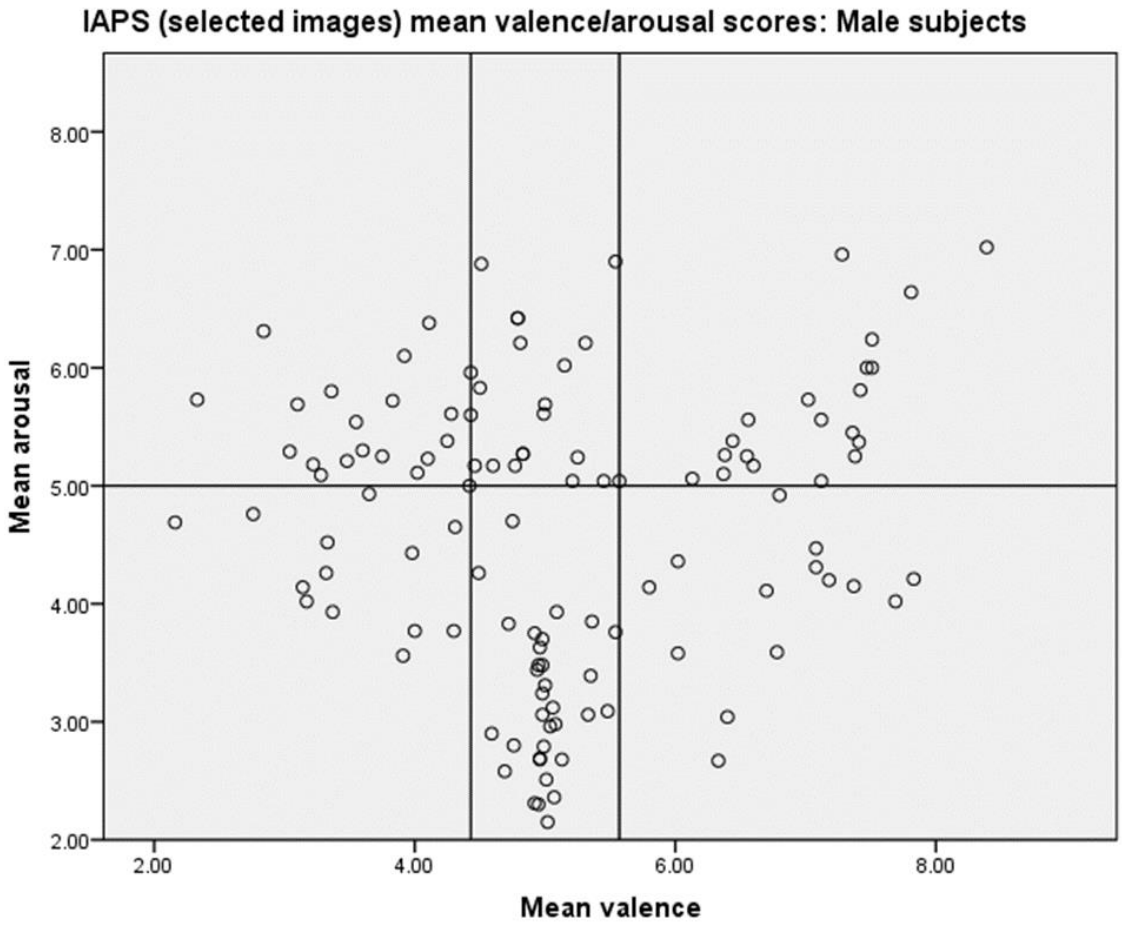

Figure 7.1 Selected images from the IAPS that form the fMRI emotional processing task: Mean valence and arousal scores for male subjects from the IAPS normative data set. Reference line for arousal indicates differentiation between 'high' and 'low' arousal images and reference lines for valence indicate differentiation between 'high', 'neutral' and 'low' valence images.

Table 7.1 IAPS task behavioural test data

Individual	Clarity rating	Engagement rating	"Face"/"No Face" distraction rating	"Face"/"No Face" confusion/difficulty rating	Picture emotionality rating
1	4	5	3	4	5
2	1	5	3	2	4
3	4	4	3	2	5
4	5	5	3	3	4
5	5	5	2	1	4

Table 7.1. IAPS task self-reported evaluation form data from behavioural testing. Clarity rating (1=confusing, 5=simple), engagement rating (1=not engaged, 5=very engaged), "Face"/"No Face" distraction rating (1=not distracting, 5=very distracting), "Face"/"No Face" confusion/difficulty rating (5=not confusing or difficult, 1=very confusing or difficult) and picture emotionality rating (1=not emotional, 5=very emotional)

7.3 fMRI analysis

Statistical analysis on fMRI data was carried out using Statistical Parametric Mapping software (SPM12) (Wellcome Department of Clinical Neurology).

The functional images from all participants were preprocessed according to the following steps: 1) firstly images were realigned, estimated and resliced 2) images were then slice timed, adjusting for interleaved and bottom up slice order 3) subsequent functional images were coregistered with the source structural image from the T1 MP RAGE anatomical scan 4) coregistered images were segmented into grey matter, white matter and CSF outputs 5) images were normalised to MNI space, and 6) finally the normalised images were smoothed with a 8mm FWHM (full-width at half maximum) Gaussian smoothing kernel.

For first-level analysis of the IAPS emotional processing task, the images were split into high/low arousal combined conditions. The high and low arousal conditions across the whole task where then compared using a [1 -1 1 -1 1 -1] contrast, and the reverse [-1 1 -1 1 -1 1] contrast. This type of contrast investigates the combined brain activation effects of high arousal versus low arousal conditions, irrespective of valence.

For the second level analysis, explicit masking was used to exclude voxel data outwith the brain tissue. This explicit mask was comprised of an average binarised image created from the combined grey matter and white matter segmented images from all participants. Both within and between group analyses were completed. Within group analysis used a one-sample t-test for each task and first level contrasts to look at significant activation for the control and premutation group separately. Within group second level contrasts were defined as either [1] or [-1] to look at positive and negative activation patterns in the high/low arousal contrast. The between group analyses used a full factorial design to examine the differences between the control and premutation groups. The groups were compared using [1 -1] and the reverse [-1 1] contrasts. In addition, age was added into the full factorial design as a regressor and group x age interactions were examined for both the control and the premutation group using [1 -1] and the reverse [-1 1] contrasts between age data and group BOLD response. The design matrix for this task is presented in figure 7.2. All second level contrasts were calculated using a height threshold value of p=0.005 and a voxel threshold of 0 to allow for the detection of spike activations. Family-wise error correction was then carried out, with significance being indicated by cluster-wise inference (FWE_{corr}<0.05).

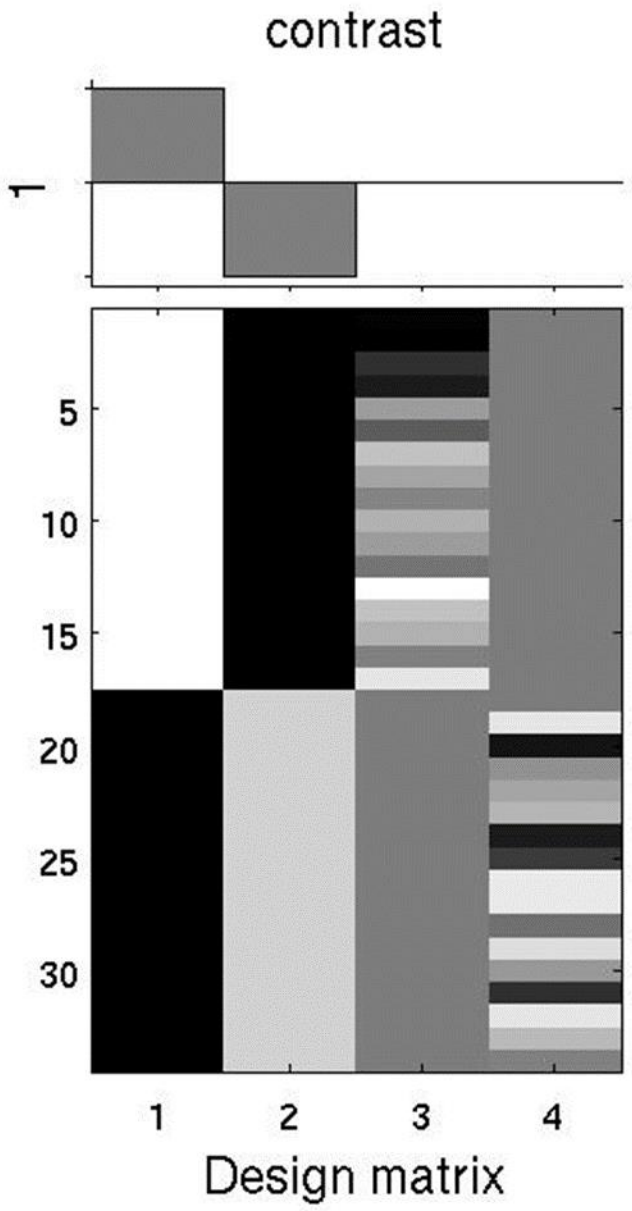

Figure 7.2 Design matrix displaying a control>premutation between group contrast for the emotional processing second-level analysis. Controls are represented in column 1, premutation carriers are represented in column 2 and age is represented in columns 3 and 4

7.4 Clinical measurements

Each participant completed several clinical and neuropsychological measurements outside of the scanner linking to neurodevelopmental and psychiatric symptoms. The Symptom Checklist 90 Revised (SCL-90-R®) (Pearson) was used to evaluate participant psychiatric symptomatology. The SCL-90-R is a self-report questionnaire comprising of 90 questions asking participants to rate how much they were distressed by various psychiatric symptom manifestations on a scale of 0-4, 0 being not at all distressed and 4 being extremely distressed. The SCL-90-R is a measure of current psychiatric symptomatology, and so participants are asked to rate their distress in response to certain problems within the context of the last 7 days, including the day of testing. Symptoms measured in the SCL-90-R are somatization, obsessive-compulsiveness, interpersonal sensitivity, depression, anxiety, hostility, phobic anxiety, paranoid ideation and psychoticism. These symptoms are scaled by dividing total additive score by number of question responses and adding 0.005 to the result. Combined scores also produce measurements of global severity index, which is the severity of all symptoms combined, positive symptom total, which is the total number of questions responded to above a 0, and positive symptom distress index, which is a measure of how severe symptoms were when reported as positive. Normative sample data for the SCL-90-R is comprised of 3 major cohorts applicable to this research: 1,002 heterogeneous psychiatric outpatients, 947 non-patients and 423 psychiatric inpatients. Raw score means and standard deviations for the nine primary symptom dimensions and three combinative indices for males, as is applicable to the present study, in these three normative cohorts are summarised in Table 7.2.

The Ekman 60 Faces Test (Version 1.0, Thames Valley Test Company) was carried out by all participants on a laptop (Young et al. 2002). The Ekman 60 Faces Test asked participants to correctly identify the facial emotion in 60 pictures of males and females, which were presented for a duration of 5 seconds each in a random order. The facial emotions used in the test are anger, disgust, fear, happiness, sadness and surprise and 10 of each were presented during the test. Scores are reported as number of correctly identified images out of 10 per emotion, and a total of correctly identified images out of 60. Each participant was given verbal instructions and given a short practice run of the test. Normative material based on a cohort of 227 individuals aged between 20-70 years old with IQ scores above 90 is summarised in Table 7.3.

A neuropsychological, laptop based test of social judgement was also carried out by all participants, known as the Social Judgement Test (Hall et al. 2004). Here, participants were asked to identify pictures of faces based on a series of variables, which were age, approachability, attractiveness, distinctiveness, intelligence and trustworthiness. In each of the 6 test conditions, the pictures were designed to exhibit an overt socially recognisable trait in a binary manner, for instance, in the age variable individuals in the image stimuli were either young or old, and in the trustworthy variable

individuals in the image stimuli stereotypically appeared to be either trustworthy or not trustworthy. For each variable, 32 images were presented for a duration of 5 seconds each. Scores for each social variable are therefore number of images correctly identified out of a maximum of 32.

All participants also completed the Autism Quotient (AQ) and Empathy Quotient (EQ) self-report questionnaires, which report levels of autistic traits (Baron-Cohen et al. 2001). Scores over 26 in the AQ correctly identify autism spectrum disorder in 83% of cases, and scores below 30 in the EQ correctly report autism spectrum disorder in 81% of cases (Woodbury-Smith et al. 2005; Baron-Cohen & Wheelwright 2004). A maximum score in the AQ is 50, indicating high levels of ASD symptoms (difficulty with social skill, attention switching, attention to detail, communication and imagination) and a minimum score is 0, indicating absence of autistic traits. A maximum score in the EQ is 80, indicating a very high level of empathy and low level of autistic traits, and a minimum score is 0, indicating a very low level of empathy and high level of autistic symptomatology. The scores of the AQ and the EQ are also highly correlative (Wheelwright et al. 2006).

Table 7.2. SCL-90-R normative sample raw score means and standard deviations (males only)

	Psychiatric outpatient cohort		Non-patient cohort		Psychiatric inpatient cohort	
Dimension	**Mean**	**SD**	**Mean**	**SD**	**Mean**	**SD**
Somatization	.70	0.67	0.29	0.33	0.82	0.78
Obsessive-compulsive	1.41	0.89	0.34	0.39	1.22	0.96
Interpersonal sensitivity	1.36	0.90	0.25	0.32	1.03	0.87
Depression	1.59	0.92	0.28	0.32	1.41	1.02
Anxiety	1.30	0.83	0.22	0.27	1.22	0.95
Hostility	1.00	0.89	0.29	0.37	0.73	0.76
Phobic anxiety	0.65	0.74	0.08	0.19	0.71	0.88
Paranoid ideation	1.07	0.90	0.34	0.40	1.08	0.84
Psychoticism	0.90	0.65	0.13	0.22	0.91	0.78
Global severity index	1.14	0.64	0.25	0.24	1.06	0.74
Positive symptom distress index	2.04	0.58	1.31	0.37	1.99	0.72

Positive symptom total	47.64	19.22	16.37	13.85	43.90	22.95

Table 7.2. Raw score means and standard deviations for the SCL-90-R primary symptom dimensions and global indices for males in three normative sample groups

Table 7.3. Ekman 60 Faces Test normative sample means and cut-offs for impairment

		Total Score	Anger	Disgust	Fear	Happiness	Sadness	Surprise
Whole sample	Mean	50.64	7.86	8.59	7.19	9.87	8.33	8.55
	Cut-off	42	5	6	4	9	6	6
Age 20-40	Mean	51.43	8.21	8.38	7.82	9.90	8.59	8.54
	Cut-off	45	5	6	4	9	6	6
Age 41-60	Mean	51.20	8.17	8.77	7.23	9.84	8.53	8.61
	Cut-off	43	5	6	4	9	6	6
Age 61-70	Mean	49.41	7.33	9.00	6.47	9.93	8.03	8.66
	Cut-off	41	4	6	3	9	5	6

Table 7.3. Raw score means and cut-off scores indicating the boundary between normal range and impaired scores for the Ekman 60 Faces Test. All total scores are out of 60, all individual emotion scores are out of 10

7.5 Molecular measurements

Protein quantification was carried out by Western blotting analysis. All participants provided a blood sample, part of which was purified to peripheral blood mononuclear cells using Histopaque layering.

Protein was then extracted from the samples by firstly quickly thawing the peripheral blood mononuclear cell samples at 37˚C and spinning them at 5000 rpm for 5 minutes at 4˚C. The supernatant was then carefully removed and discarded. Pellets were then re-suspended in 100µl lysis buffer (RIPA buffer: 50mM Tris-HCl, 150mM NaCl, 1% Triton X-100, 0.5% sodium deoxycholate, 0.1% SDS and 1mM EDTA made up with ddH_2O with an additional protease inhibitor tablet) and lysed on ice for 30 minutes. The samples were then centrifuged again at 11,000 rpm for 15 minutes at 4˚C, and the supernatant was aliquoted 1:1 with 95:5 laemmli sample buffer:2-mercaptoethanol. An aliquot without sample buffer per sample was retained for protein quantification analysis. The protein aliquots with added sample buffer were then boiled for 5 minutes at 100˚C to kill the proteases, vortexed and centrifuged for ten seconds. Samples were stored at -80˚C before use for protein quantification or Western blotting.

Total protein concentration for each sample using the RC/DC Protein Assay (BioRad, United States). SDS-PAGE electrophesis was then used to separate 25µg of sample loaded into each well of Mini-PROTEAN® TGX™ Precast Gels, 4-20% polyacrylamide. The gels were run in 1 x running buffer (0.1% SDS, 25mM Tris base and 190mM glycine made up with ddH_2O) for 25 minutes at a constant of 100V, and then 30 minutes at a constant of 200V. Each sample was ran three times in total, on the same gel as counterpart age-matched control. Protein was then transferred from the gel to a nitrocellulose membrane in 1 x transfer buffer (25mM Tris base, 190mM glycine and 20% methanol made up with ddH_2O) on ice for 2 hours at a constant of 85V. The membranes were then blocked using a 1:1 blocking buffer and PBS-T solution for one hour at room temperature and then probed with Ab17722 rabbit anti-FMRP polyclonal antibody (ABCAM, Cambridge, UK) at a dilution of 1:1000 and ab6276 mouse anti-beta actin (ABCAM, Cambridge, UK) at a dilution of 1:5000, overnight at 4˚C. The membranes were then washed once in ddH_2O and then three times for 5 minutes in PBS-T. An IRDye goat anti-rabbit 800CW secondary antibody at a dilution of 1:5000 and an IRDye goat anti-mouse 680CW secondary antibody at a dilution of 1:5000 were then incubated with the membranes at room temperature for 1 hour. The membranes were subsequently washed again once with water and three times for 5 minutes in PBS-T. Beta actin bands were then imaged at 169µm resolution in the 700 channel and FMRP bands were imaged at 169µm resolution in the 800 channel using the Odyssey infrared scanner following manufacture recommendations. Analysis was performed using densitometry methodology using Image Studio version 2.0.

7.6 Statistical analysis

Further statistical analyses were carried out in SPSS Statistics 22. Independent two-tailed t-tests were used to discern differences between the premutation and control groups for the clinical, neuropsychological and molecular data. For the Ekman 60 faces test, data was statistically analysed using an (M)ANOVA to investigate group by emotion interactions. Simple linear regressions were also performed on extracted raw voxel values from significant neuroimaging clusters against the psychiatric, neuropsychological and molecular variables. All significance levels were assumed at $p<0.05$.

CGG repeat analysis revealed that some individuals in the sample were mosaic or borderline for the full mutation. To ensure this was not causing a bias in the results, mosaic and borderline carriers were separated from the sample, creating three participant groupings: control, premutation and mosaic/borderline. A one-way ANOVA of 3 groups, followed by a Tukey post-hoc test was performed on extracted voxel data from the maximum voxel of the significantly different between group cluster.

Chapter 8: Neurodevelopment in the Fragile X premutation: Results

8.1 Participants and recruitment

The same participant group who took part in the neurodegenerative section of the study took part in the neurodevelopmental section of the study. As described in Chapter 5, section 5.1, the group of male premutation carriers (n=17) had a mean age of 50.4 years old (SD=15.1), and the age-matched male control group had a mean age of 47.6 years old (SD=12.9). Independent two-sample t-testing revealed that age did not differ significantly between the groups (p=0.507). CGG repeat length testing indicated that 12 carriers were in the premutation range, 1 carrier was in the intermediate range, 3 carriers were mosaic for repeat size and one carrier was borderline for the full mutation. It was confirmed that all control subjects were within the normal CGG repeat length range. Main CGG repeat value by group is plotted in figure 5.1. All participants were right handed, excepting one control subject and two carrier subjects, who were left handed. All participants had a composite IQ >80, as measured by the KBIT Second Edition Intelligence Test (Pearson) (Table 5.1). Two-sample t-testing of IQ data revealed that composite and verbal IQ as measured by the KBIT-2 were not significantly different between the groups (p=0.053, p=0.604), although composite IQ exhibits a trend towards being lower in carriers. Non-verbal IQ as measured by the KBIT-2 was significantly lower in carriers (p=0.015) (Fig. 5.2).

8.2 Within group imaging

One sample t-test within group analysis revealed that when contrasting the combined low arousal and high arousal conditions, controls exhibited four significant clusters of activation. The first and largest significant cluster (FWE_{corr}<0.001, *T*=10.17) incorporated the right intraparietal cortex and the right human intraparietal areas 1 and 3. The maximum of the cluster was located at [48,-48,34]. A second significant cluster (FWE_{corr}<0.001, *T*=7.37) was located at the left cerebellar lobule VIIa Crus I, left cerebellar lobule VI and the right human occipital cortex 3 dorsal (hOC3v) with the co-ordinates of the cluster maximum at [-18,-76,-26]. A third significant cluster (FWE_{corr}<0.001, *T*=6.90) was located at the bilateral superior parietal lobes, with the co-ordinates of the cluster maximum at [12,-62,40] and a final significant cluster (FWE_{corr}=0.001, *T*=6.18) was located at the right middle and superior frontal gyri, with the co-ordinates of the cluster maximum at [22,54,30] (Fig. 8.1a). In contrast, a one sample t-test within group analysis in the carrier group showed no clusters of significant activation (Fig. 8.1b).

a)

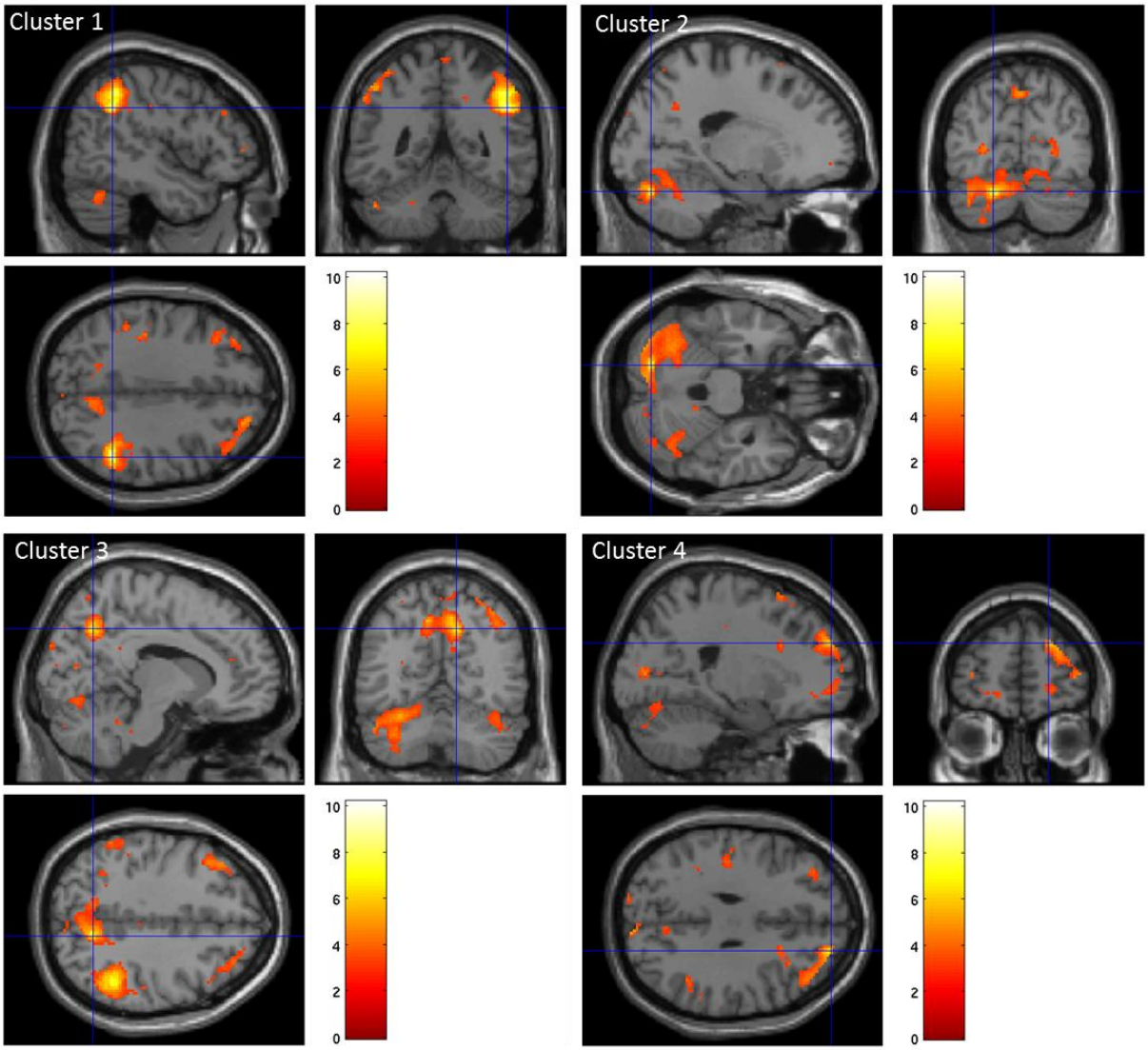

Figure 8.1 Within group functional brain imaging analysis carried out in SPM12 **a)** Within group analysis of the control group for the high arousal-low arousal contrast. Significant cluster 1 (FWE_{corr}<0.001, T=10.17) at the right intraparietal cortex and the right human intraparietal areas 1 and 3. Cluster co-ordinate of maximum voxel: 48,-48,34, k=1321, normalised voxel size: $2mm^3$. Significant cluster 2 (FWE_{corr}<0.001, T=7.37) at the left cerebellar lobule VIIa Crus I, left cerebellar lobule VI and the right human occipital cortex 3 dorsal (hOC3v). Cluster co-ordinate of maximum voxel: -18,-76,-26, k=2102, normalised voxel size: $2mm^3$. Significant cluster 3 (FWE_{corr}<0.001, T=6.90) at the bilateral superior parietal lobes. Cluster co-ordinate of maximum voxel: 12,-62,40, k=1070, normalised voxel size: $2mm^3$. Significant cluster 4 (FWE_{corr}=0.001, T=6.18) at the right middle and superior frontal gyri. Cluster co-ordinate of maximum voxel: 22,54,30, k=754, normalised voxel size: $2mm^3$.

b)

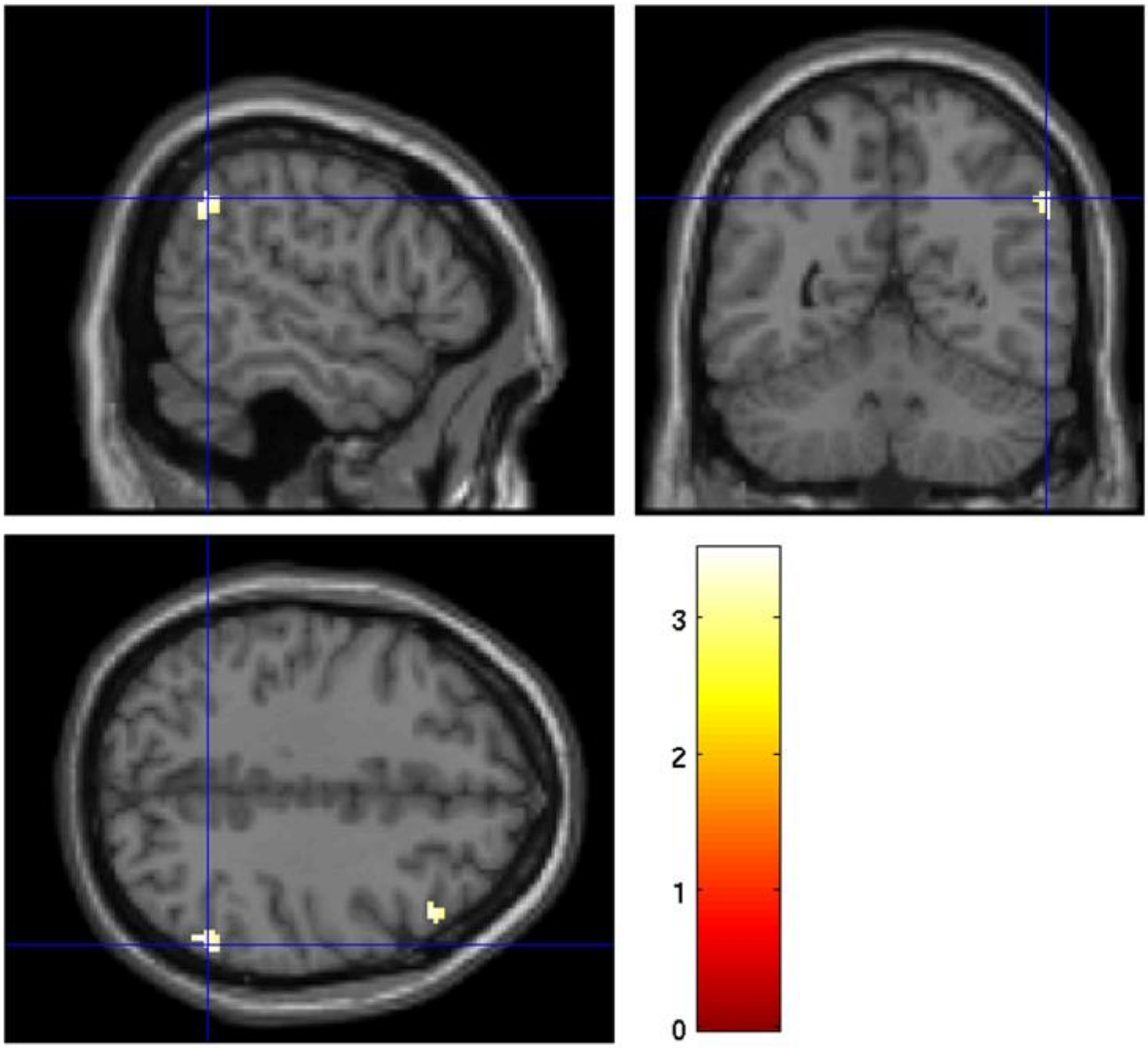

Figure 8.1 Within group functional brain imaging analysis carried out in SPM12 **b)** Within group analysis of the carrier group for the high arousal>low arousal contrast. No significant clusters of activation.

8.3 Between group imaging

Full factorial between group analysis revealed that the premutation group had two clusters of significantly lower BOLD response when compared to the control group. The first, largest cluster of significantly lower activation (FWE_{corr}=0.001, *T*=4.77) was located at bilateral BA17 of the primary visual cortex, right BA18 of the visual association area and the right superior parietal lobe. The maximum of the cluster was located at [16,-88,14]. The second cluster of significantly lower activation in the carrier group (FWE_{corr}=0.021, *T*=4.26) was located at the bilateral superior parietal lobes, right BA2 of the primary somatosensory cortex and right human intraparietal area 1. The maximum of the cluster was located at [34,-40,42] (Fig. 8.2a).

As analysis of the length of the *FMR1* CGG repeat island revealed a number of carrier individuals in the sample to be mosaic or borderline for the full mutation, an additional group was created of these mosaic or borderline carriers to ensure that anomalous CGG repeat length data were not skewing imaging results and that these individuals were not driving significant between group differences. The groups for the ANOVA analysis were defined as the following: control (n=17), premutation (n=13) and mosaic/borderline carriers (n=4). A statistically significant between group difference in BOLD response at significant cluster 1 maximum voxel [16,-88,14] was identified by one-way ANOVA ($F(2,31)=11.737$, $p<0.001$). A Tukey post-hoc test revealed that BOLD response for this cluster was significantly different in controls compared to carriers (p=0.001) and controls compared to mosaic/borderline carriers (p=0.003), but not significantly different between the premutation group and mosaic/borderline carriers (p=0.726). Representative group means are presented in figure 8.2b. A statistically significant between group difference in BOLD response at significant cluster 2 maximum voxel [34,-40,42] was also identified by one-way ANOVA ($F(2,31)=8.459$, p=0.001). Tukey post-hoc showed that BOLD response for this cluster was significantly different in controls compared to carriers (p=0.012) and controls compared to mosaic/borderline carriers (p=0.004), but not significantly different between the premutation group and mosaic/borderline carriers (p=0.345). Representative group means are presented in figure 8.2c.

a)

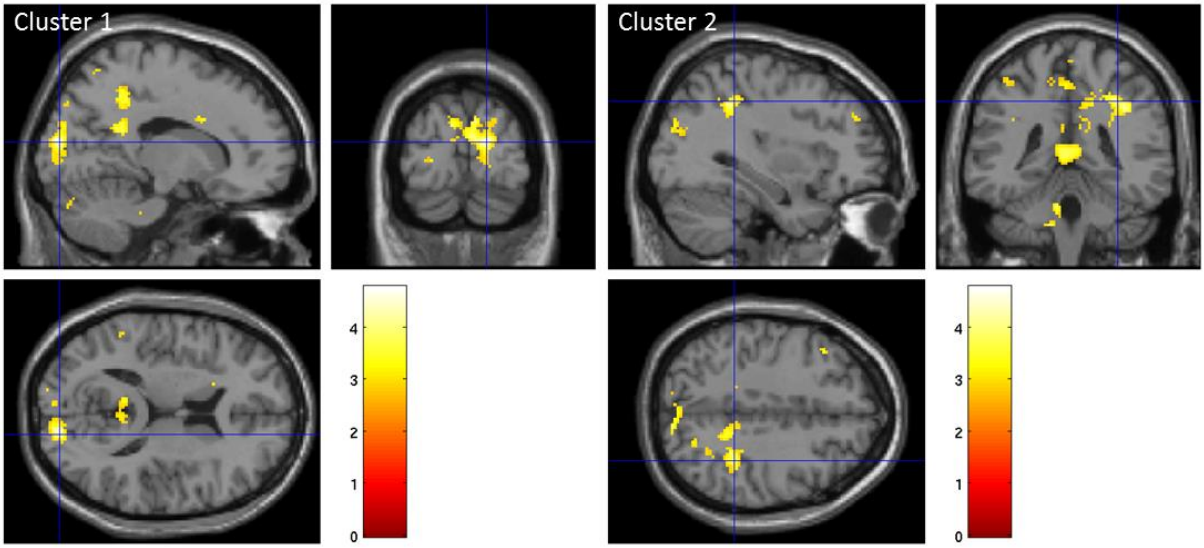

Figure 8.2 Between group functional brain imaging analysis carried out in SPM12 **a)** Cluster 1 of significantly lower BOLD activation in carriers compared to controls (FWE_{corr}=0.001, *T*=4.77) at bilateral BA17 of the primary visual cortex, right BA18 of the visual association area and the right superior parietal lobe. Cluster co-ordinate of maximum voxel: 16,-88,14, *k*=938, normalised voxel size $2mm^3$. Cluster 2 of significantly lower activation in the carrier group compared to controls (FWE_{corr}=0.021, *T*=4.26) at the bilateral superior parietal lobes, right BA2 of the primary somatosensory cortex and right human intraparietal area 1. Cluster co-ordinate of maximum voxel: 34,-40,42, *k*=555, normalised voxel size $2mm^3$.

b)

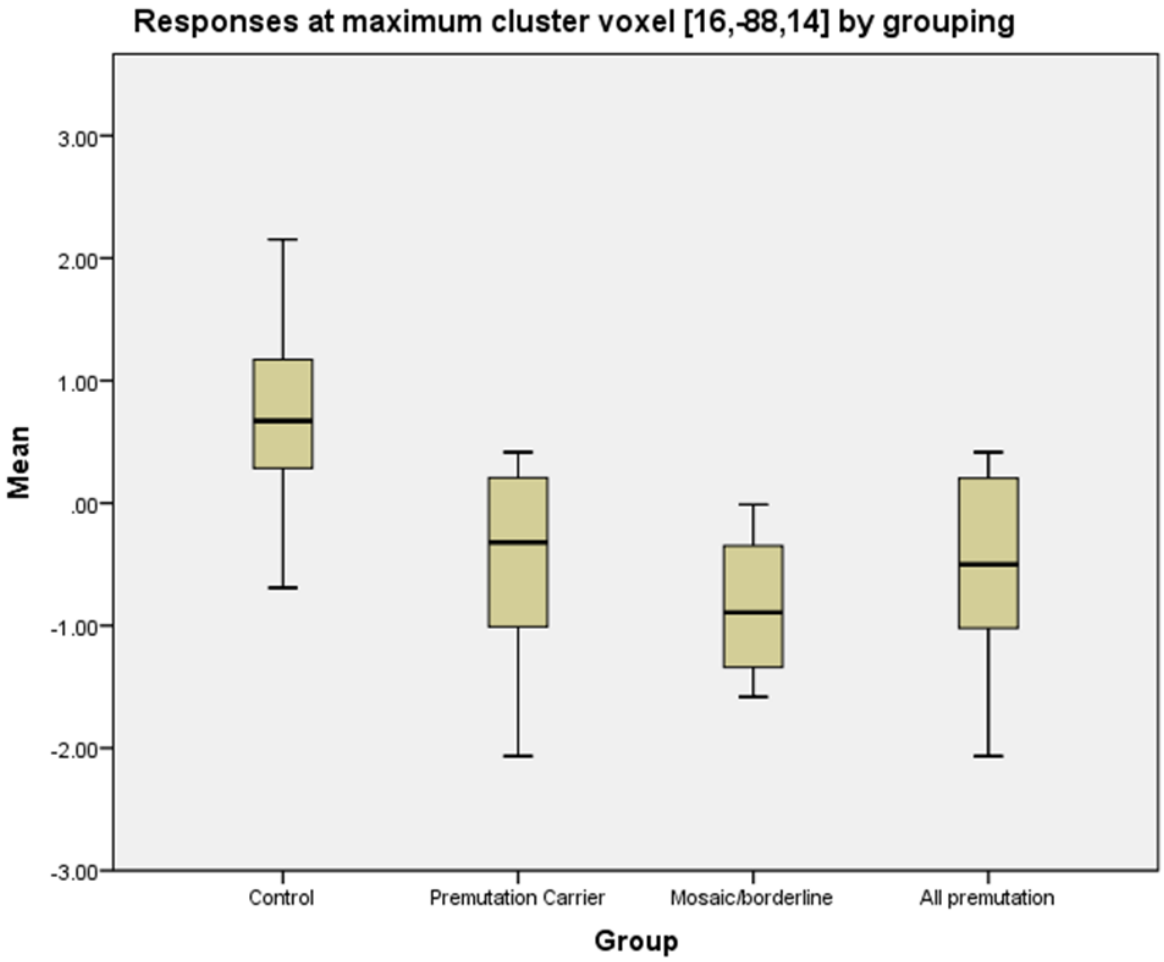

Figure 8.2 Between group functional brain imaging analysis carried out in SPM12 and subsequently plotted using SPSS **b)** Cluster 1, located at bilateral BA17 of the primary visual cortex, right BA18 of the visual association area and the right superior parietal lobe, mean extracted voxel response by grouping at cluster maximum, co-ordinate [16,-88,14].

c)

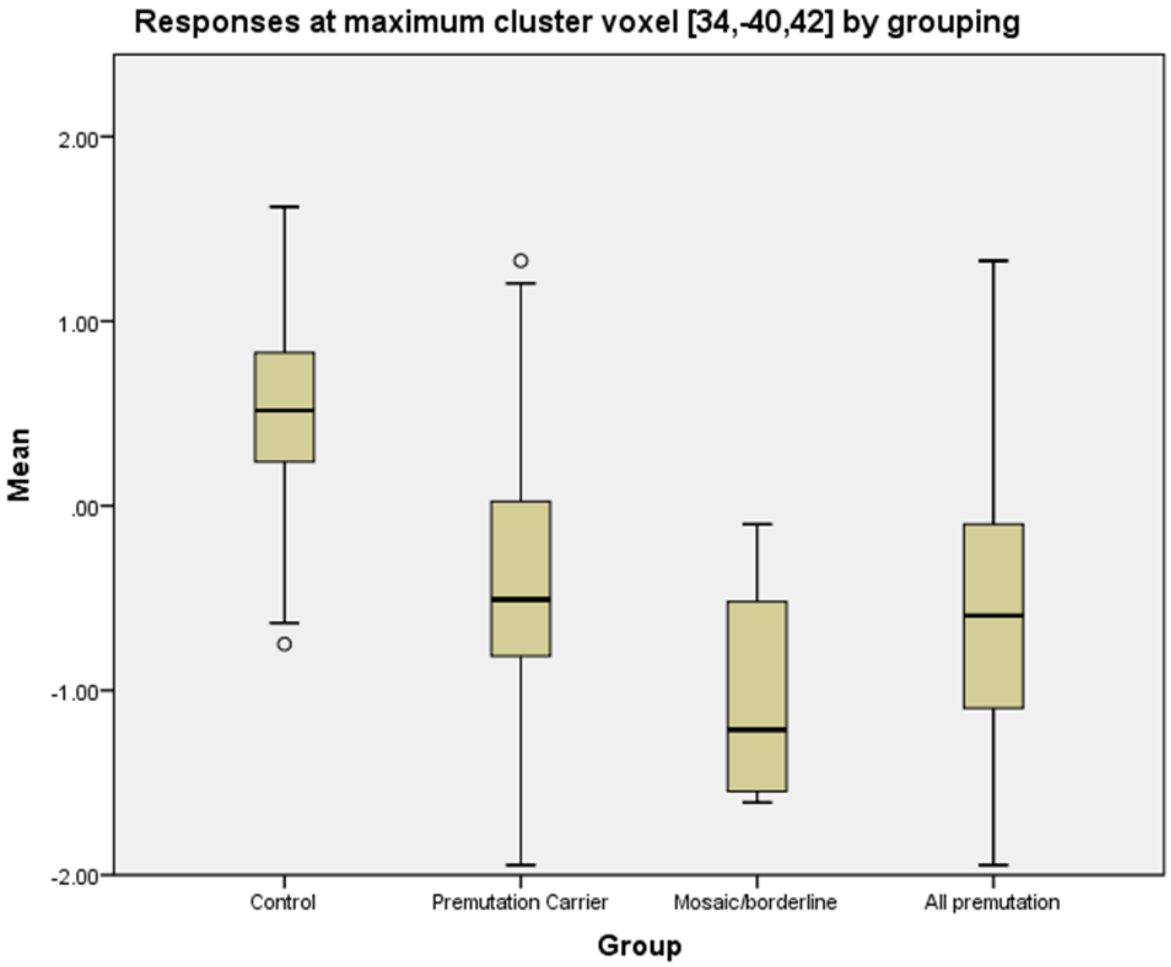

Figure 8.2 Between group functional brain imaging analysis carried out in SPM12 and subsequently plotted using SPSS **c)** Cluster 2, located at bilateral superior parietal lobes, right BA2 of the primary somatosensory cortex and right human intraparietal area 1, mean extracted voxel response by grouping at cluster maximum, co-ordinate [34,-40,42].

8.4 Group x age interaction

In the analysis probing presence of age related group differences, no significant group x age clusters were identified at a whole brain level (Fig. 8.3). Within group regression analyses also confirmed that there was no significant association between age and activation at global maxima in either group.

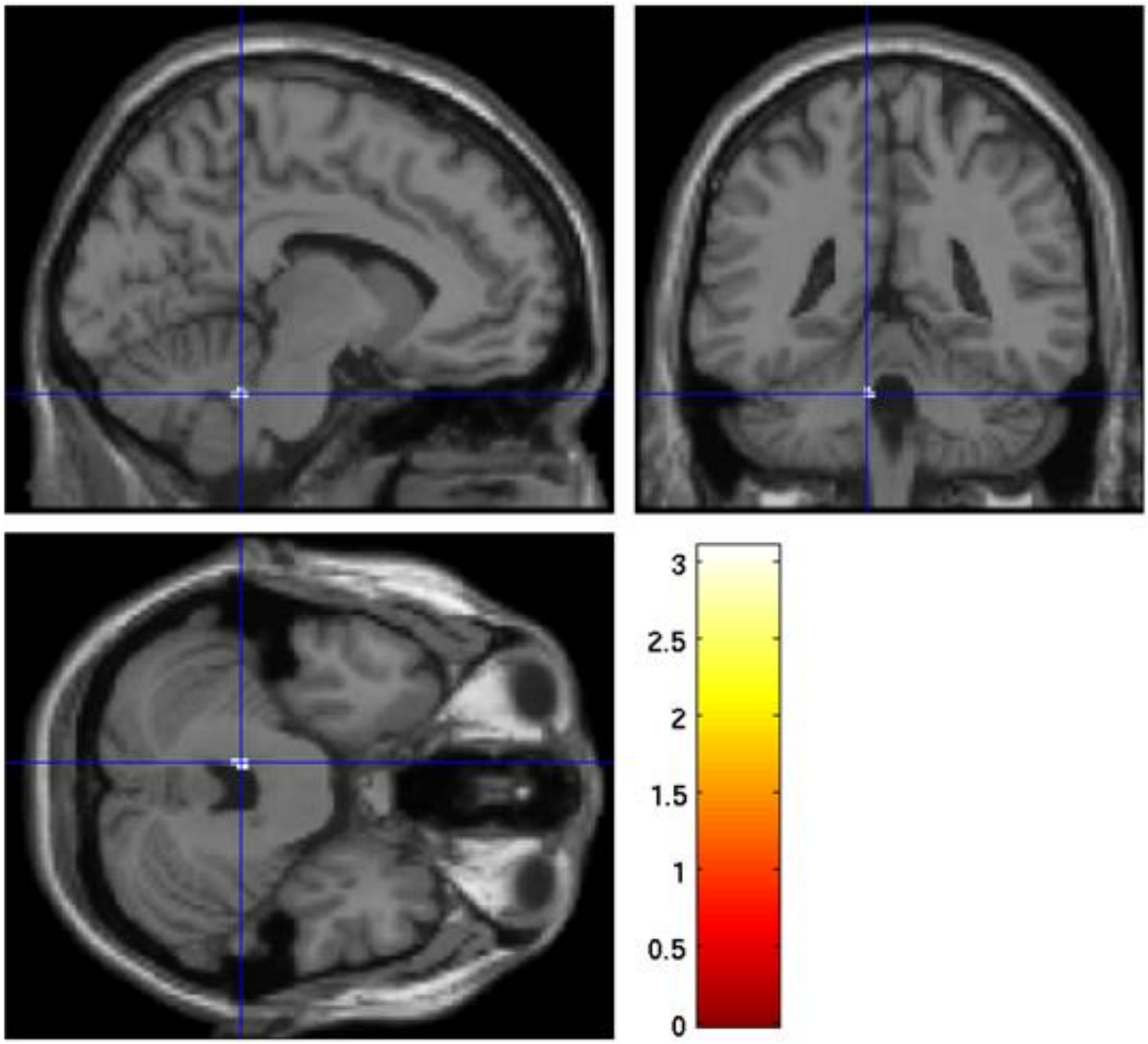

Figure 8.3. No significant group x age clusters of BOLD activation.

8.5 Clinical and neuropsychological measurements

The psychiatric symptomatology checklist, SCL-90-R, revealed that premutation carriers had significantly worse obsessive-compulsiveness (p=0.006), anxiety (p=0.028), global severity index (GSI) (p=0.033) and positive symptom distress index (PSDI) (p=0.002) scores compared to controls. Somatisation, interpersonal sensitivity, depression, hostility, phobic anxiety, paranoid ideation, psychoticism and positive symptom total (PST) were not significantly different between the groups (p=0.212, 0.389, 0.135, 0.187, 0.171, 0.161, 0.122, 0.202 respectively). Mean carrier and control scores of the SCL-90-R are plotted with normative mean material of non-patients in figure 8.4 and summarised in table 8.2.

a)

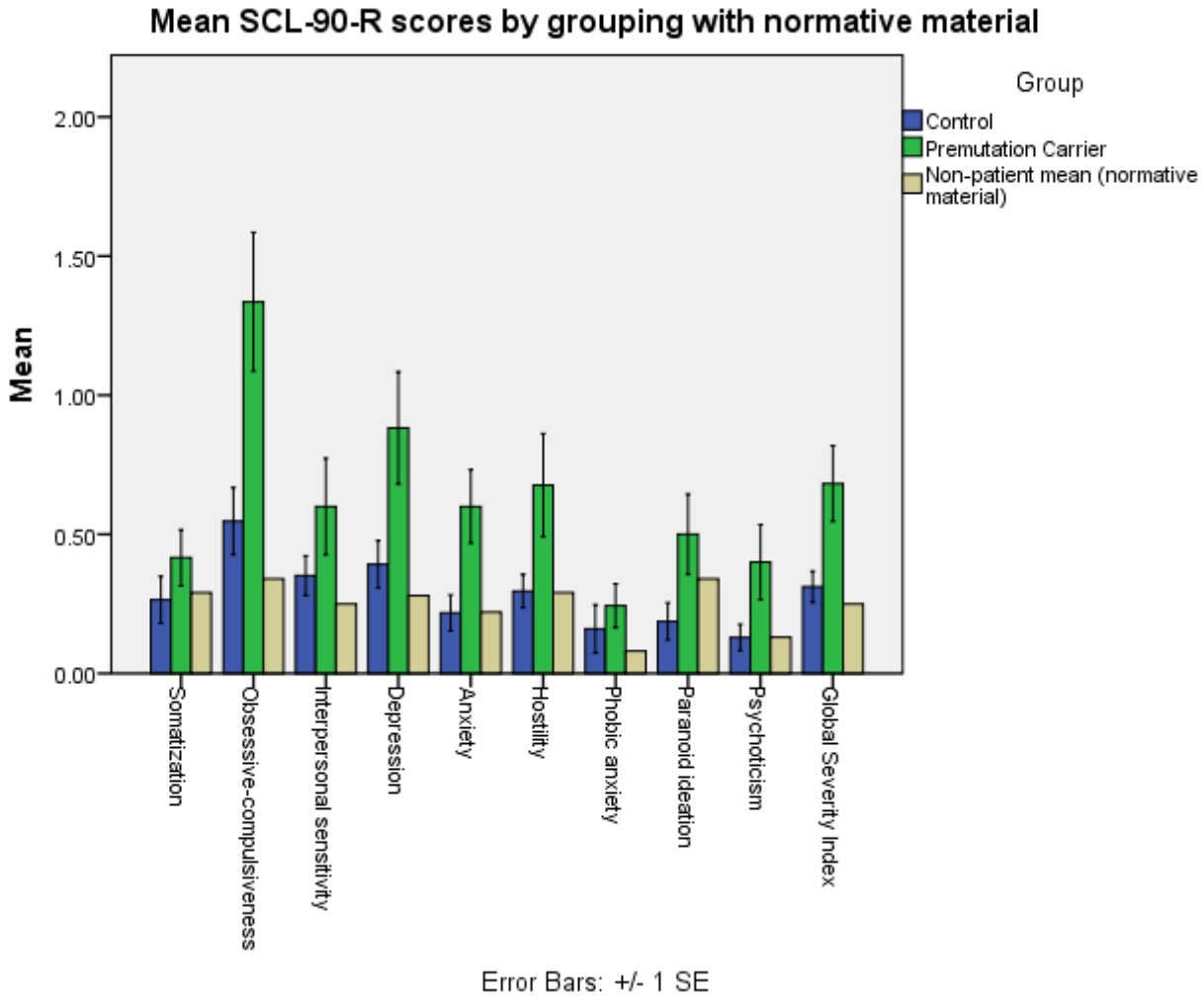

Figure 8.4 SCL-90-R psychiatric data analysed using parametric two-sample t-testing in SPSS **a)** Mean scores of somatization, obsessive-compulsiveness, interpersonal sensitivity, depression, anxiety, hostility, phobic anxiety, paranoid ideation, psychoticism and global severity index as measured by the SCL-90-R for the control group and premutation group with mean scores from SCL-90-R normative non-patient data.

b)

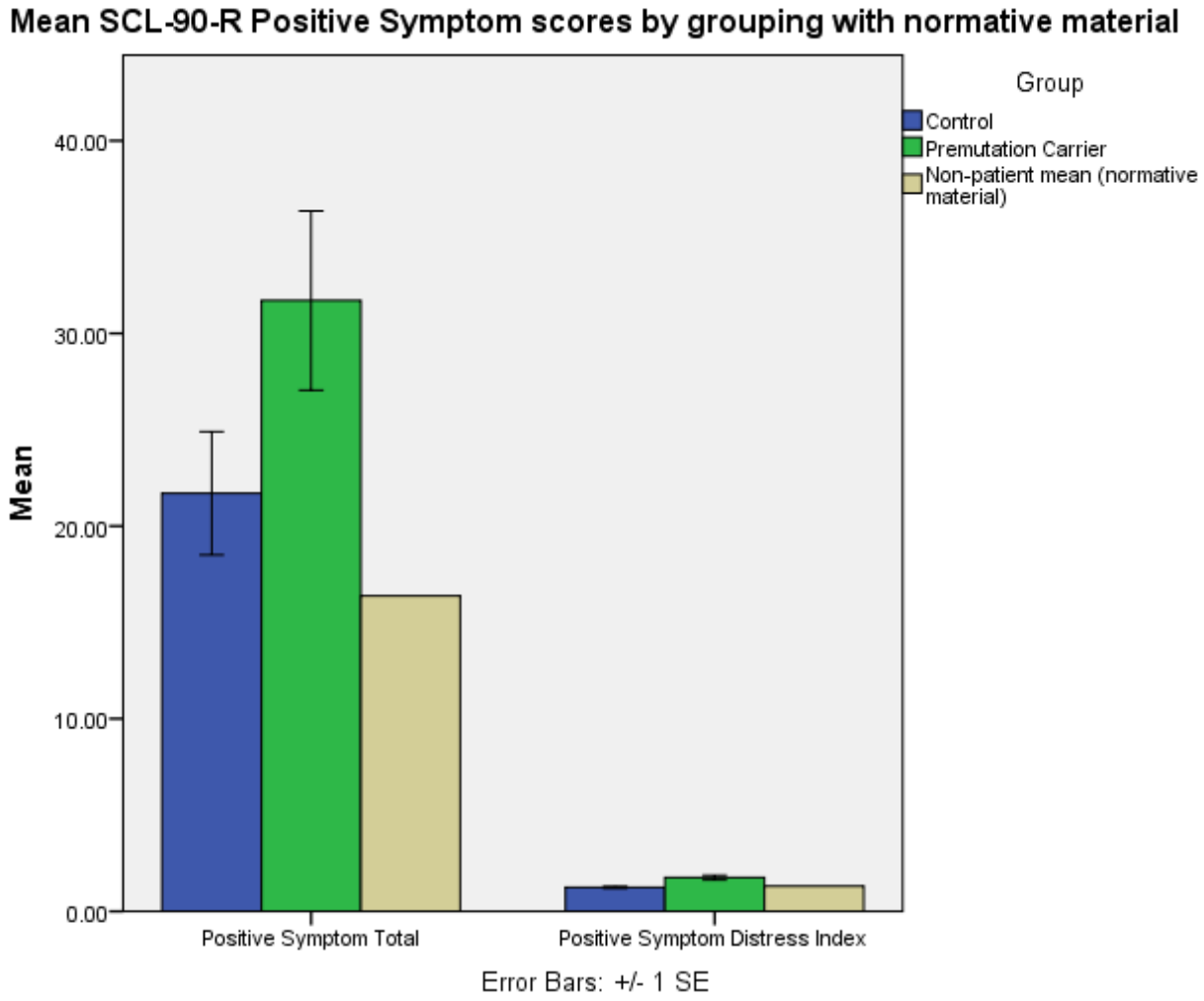

Figure 8.4 SCL-90-R psychiatric data analysed using parametric two-sample t-testing in SPSS **b)** Mean scores of positive symptom total (PST) and positive symptom distress index (PSDI) as measured by the SCL-90-R for the control group and the premutation group with mean scores from SCL-90-R normative non-patient data.

Table 8.2: SCL-90-R psychiatric symptomatology data with normative material

Group	Variable	Mean	Standard deviation
Control	**Somatization**	0.26	0.34
Carrier		0.41	0.41
Non-patient norm		0.29	0.33
Control	**Obsessive-compulsiveness**	0.54	0.49
Carrier		1.33	1.02
Non-patient norm		0.34	0.39
Control	**Interpersonal sensitivity**	0.35	0.29
Carrier		0.6	0.71
Non-patient norm		0.25	0.32
Control	**Depression**	0.39	0.35
Carrier		0.88	0.83
Non-patient norm		0.28	0.32
Control	**Anxiety**	0.21	0.26
Carrier		0.6	0.54
Non-patient norm		0.22	0.27
Control	**Hostility**	0.29	0.24
Carrier		0.67	0.76
Non-patient norm		0.29	0.37
Control	**Phobic anxiety**	0.16	0.35
Carrier		0.24	0.32
Non-patient norm		0.08	0.19
Control	**Paranoid ideation**	0.18	0.27
Carrier		0.50	0.59
Non-patient norm		0.34	0.40
Control	**Psychoticism**	0.12	0.19
Carrier		0.40	0.55
Non-patient norm		0.13	0.22
Control	**Global Severity Index (GSI)**	0.31	0.23
Carrier		0.68	0.55
Non-patient norm		0.25	0.24

Control	**Positive Symptom Total (PST)**	21.71	13.19
Carrier		31.71	19.18
Non-patient norm		16.37	13.85
Control	**Positive Symptom Distress Index (PSDI)**	1.24	0.21
Carrier		1.75	0.51
Non-patient norm		1.31	0.37

Table 8.2 Mean scores and standard deviations of SCL-90-R psychiatric symptom variables for the control group, premutation group and SCL-90-R normative non-patient dataset.

The Ekman 60 Faces Test data analysed in SPSS using an (M)ANOVA indicated that carriers performed significantly worse than control subjects when attempting to recognise facial emotions of anger (p=0.045), disgust (p=0.039) and surprise (p=0.027). Controls and carriers did not perform significantly differently when asked to recognise facial emotions of fear, happiness or sadness (p=0.142, 0.08, 0.161 respectively). Carriers performed worse overall on the test than the control group (p=0.002). Neither group mean score for any Ekman face variable reached the cut-off for impairment as described by the Ekman 60 Faces Test normative sample data. Mean carrier and control scores of the Ekman 60 Faces Test are plotted with normative mean material in figure 8.5 and summarised in table 8.3.

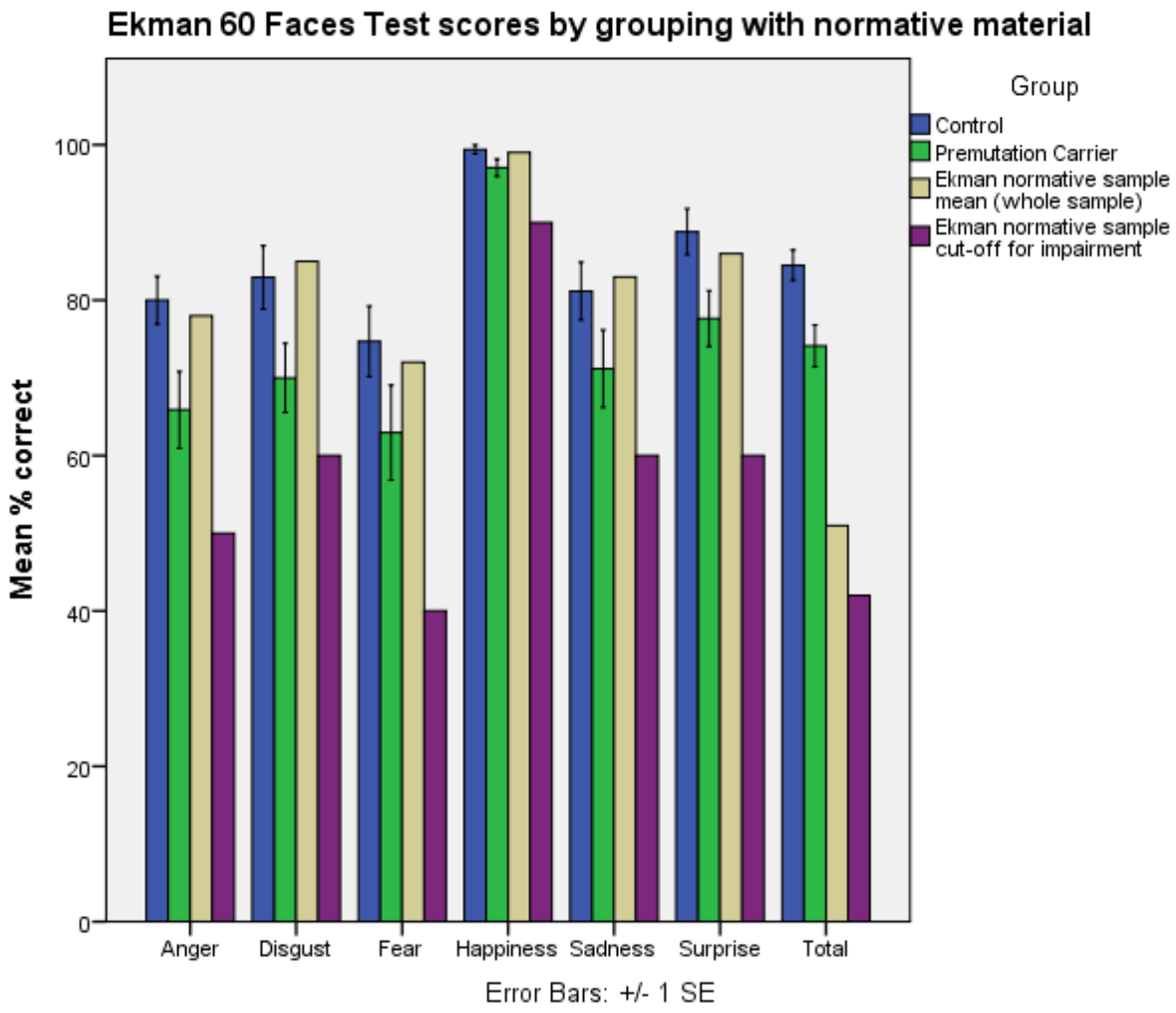

Figure 8.5 Ekman 60 Faces Test analysed in SPSS using an (M)ANOVA. Mean scores of correct recognitions of facial expressions of anger, disgust, fear, happiness, sadness, surprise and total score for the control group and premutation group with mean scores from Ekman 60 Faces Test normative sample data, including normative sample cut-off for impairment scores.

Table 8.3: Ekman 60 Faces Test scoring data with normative material

Group	Variable	Mean	Standard deviation
Control	**Anger**	8.0	1.2
Carrier		6.5	2.0
Normative sample		7.8	
Control	**Disgust**	8.2	1.6
Carrier		7.0	1.8
Normative sample		8.6	
Control	**Fear**	7.4	1.8
Carrier		6.3	2.5
Normative sample		7.2	
Control	**Happiness**	9.9	0.24
Carrier		9.7	0.46
Normative sample		9.9	
Control	**Sadness**	8.1	1.5
Carrier		7.1	2.0
Normative sample		8.3	
Control	**Surprise**	8.8	1.2
Carrier		7.7	1.4
Normative sample		8.6	
Control	**Total**	50.7	4.9
Carrier		44.5	6.6
Normative sample		50.6	

Table 8.3 Mean scores and standard deviations of Ekman 60 Faces Test variables for the control group, premutation group and Ekman 60 Faces Test normative sample dataset.

In the social judgement test, carriers and controls did not score significantly differently on measurements of accurately judged age, approachability, attractiveness, distinctiveness, intelligence and trustworthiness (p=0.292, 0.487, 0.729, 0.521, 0.096, 0.298 respectively). Mean carrier and control scores of the social judgement test are plotted in figure 8.6 and summarised in table 8.4.

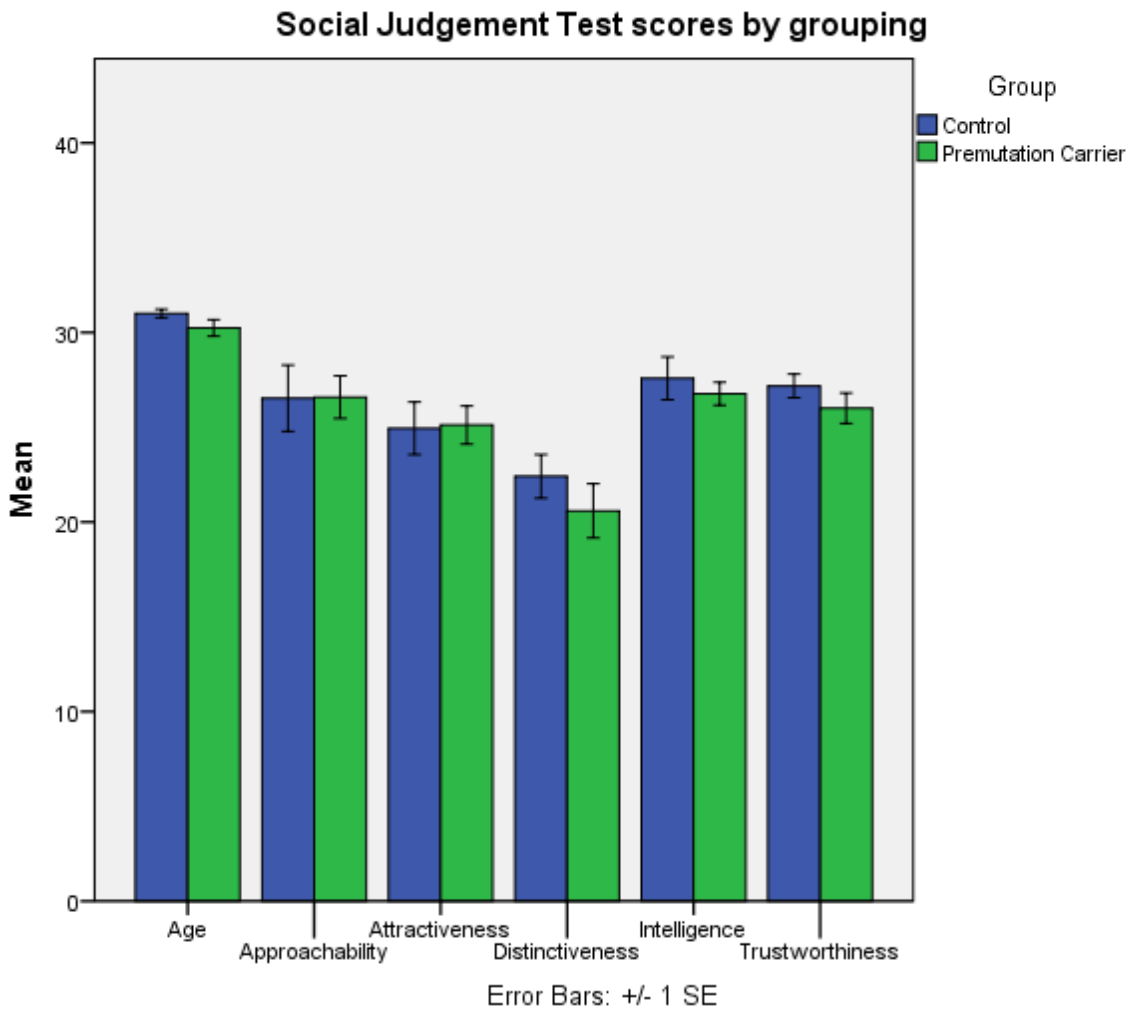

Figure 8.6 Social judgement data analysed using parametric two-sample t-testing in SPSS. Mean scores of correct social judgements of age, approachability, attractiveness, distinctiveness, intelligence and trustworthiness as measured by the social judgement test for the control group and premutation group.

Table 8.4: Social judgement test scoring data

Group	Variable	Mean	Standard deviation
Control	**Age**	31	0.93
Carrier		30.2	1.8
Control	**Approachability**	26.5	7.2
Carrier		26.6	4.7
Control	**Attractiveness**	24.9	5.7
Carrier		25.1	4.1
Control	**Distinctiveness**	22.4	4.7
Carrier		20.6	5.9
Control	**Intelligence**	27.6	4.6
Carrier		26.7	2.5
Control	**Trustworthiness**	27.2	2.5
Carrier		26.0	3.3

Table 8.4 Mean scores and standard deviations of social judgement test variables for the control group and the premutation group.

When investigating autistic traits in the current sample, premutation carriers were seen to display significantly more autistic traits in the AQ than controls ($p=0.015$). Scores of empathy as measured by the EQ were not significantly different between groups however, although a trend towards carriers scoring lower, indicative of less empathy, was evident ($p=0.084$) (Fig. 8.7a). Simple linear regression analyses revealed that AQ and EQ scores were significantly correlated in the control group ($p=0.025$), but not in the carrier group ($p=0.104$) (Fig. 8.7b, Table 8.5). Mean carrier and control scores of the AQ and the EQ are summarised in table 8.6.

a)

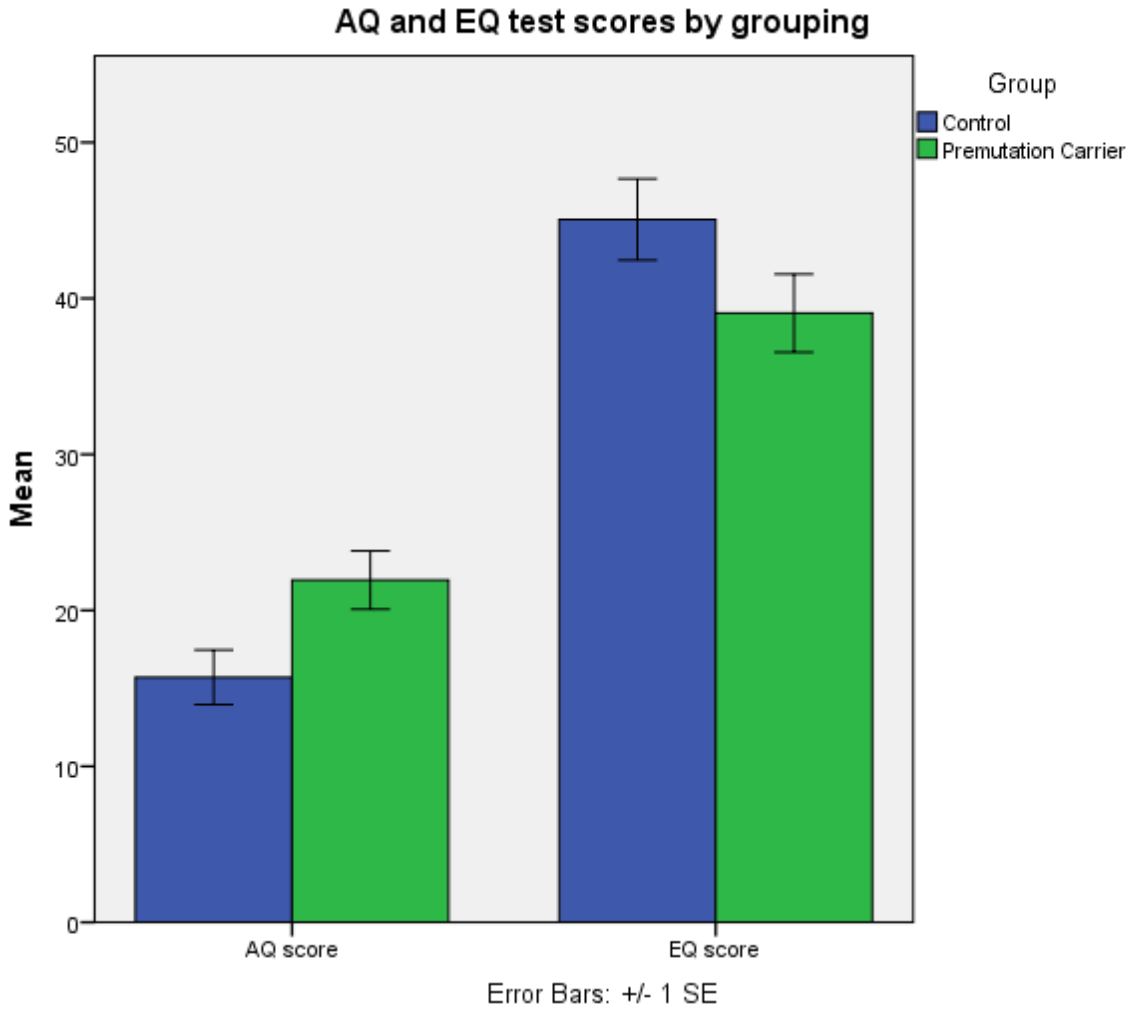

Figure 8.7 AQ and EQ autistic trait and empathy data analysed using parametric two-sample t-testing in SPSS **a)** Mean scores of autistic traits as measured by the AQ and empathy as measured by the EQ for the control group and premutation group.

b)

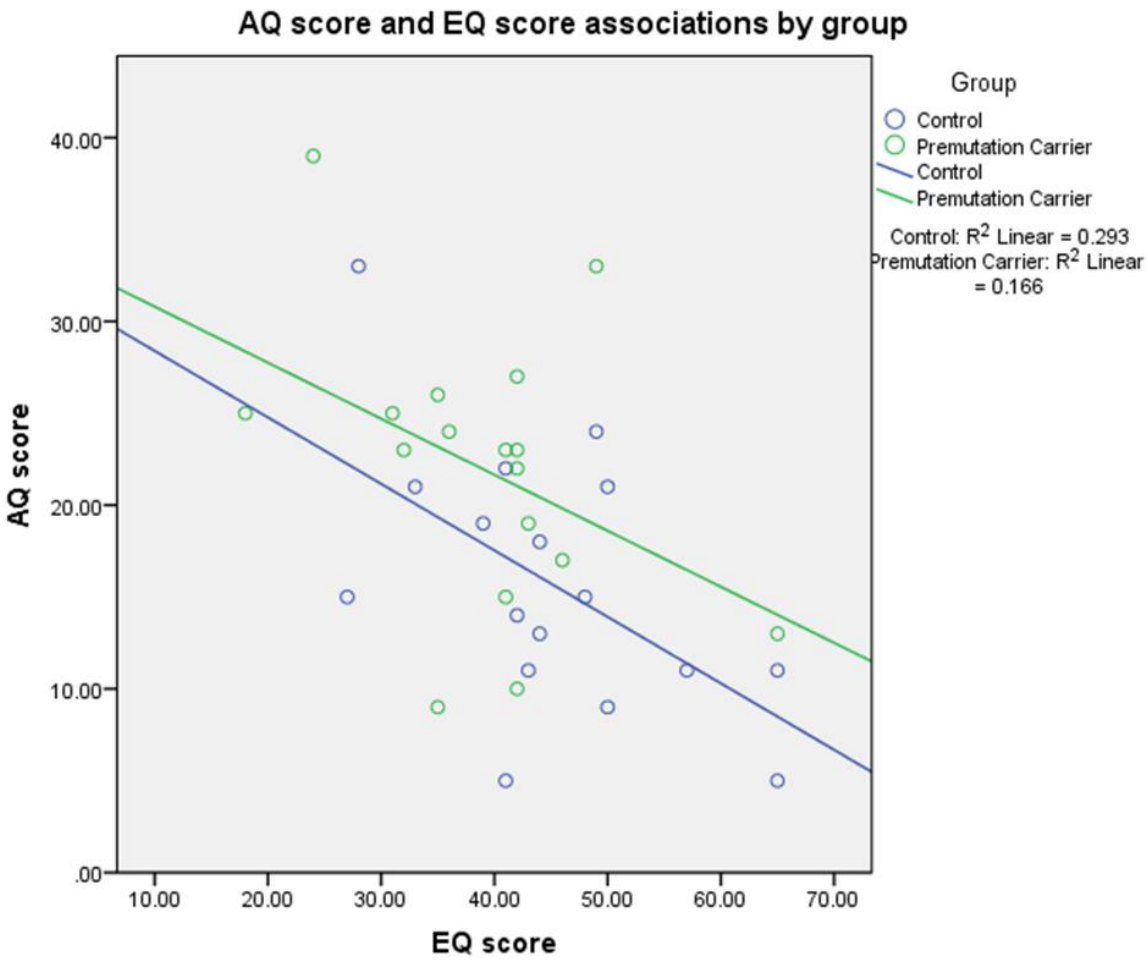

Figure 8.7 AQ and EQ autistic trait and empathy data analysed using parametric two-sample t-testing in SPSS **b)** Association between AQ score and EQ score in the control and carrier groups.

Table 8.5: Within group regression analysis of AQ and EQ scores

Group	DV	IV	β	Standard error	Adjusted R^2	P value
Control	AQ	EQ	-0.541	0.145	0.246	0.25
Premutation	AQ	EQ	-0.408	0.176	0.111	0.104

Table 8.5 Statistical results of within group regression analyses between AQ and EQ scores

Table 8.6: AQ and EQ scoring data

Group	Test	Mean	Standard deviation
Control	**AQ**	15.7	7.2
Carrier		21.9	7.7
Control	**EQ**	45.1	10.8
Carrier		39.1	10.3

Table 8.6 Mean scores and standard deviations of the AQ and EQ measurements of autistic traits for the control group and the premutation group

8.6 Molecular measurements

Western blots imaged in the 800 channel (FMRP only) exhibited multiple additional uncharacterised bands. Due to these bands of unknown identity, subsequent quantification consisted of only the expected 80kDa anti-FMRP band (Fig. 8.8a). Densitometry analysis revealed that carriers and controls did not differ significantly in FMRP levels (p=0.903). Mean carrier and control FMRP levels are plotted in figure 8.8b and summarised in table 8.7.

a)

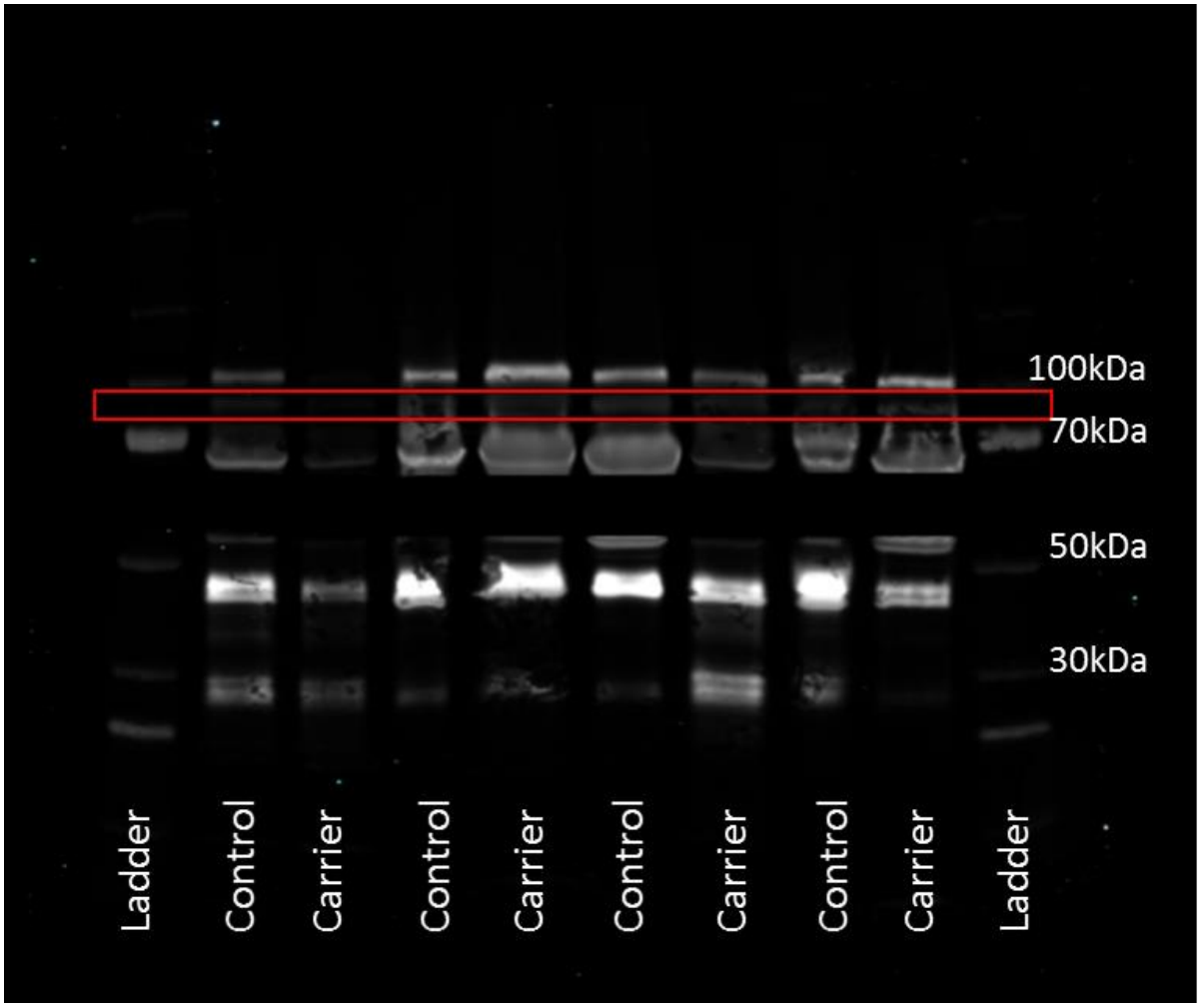

Figure 8.8 a) Example Western blot imaged in the 800 channel at 169µm resolution (FMRP only).

b)

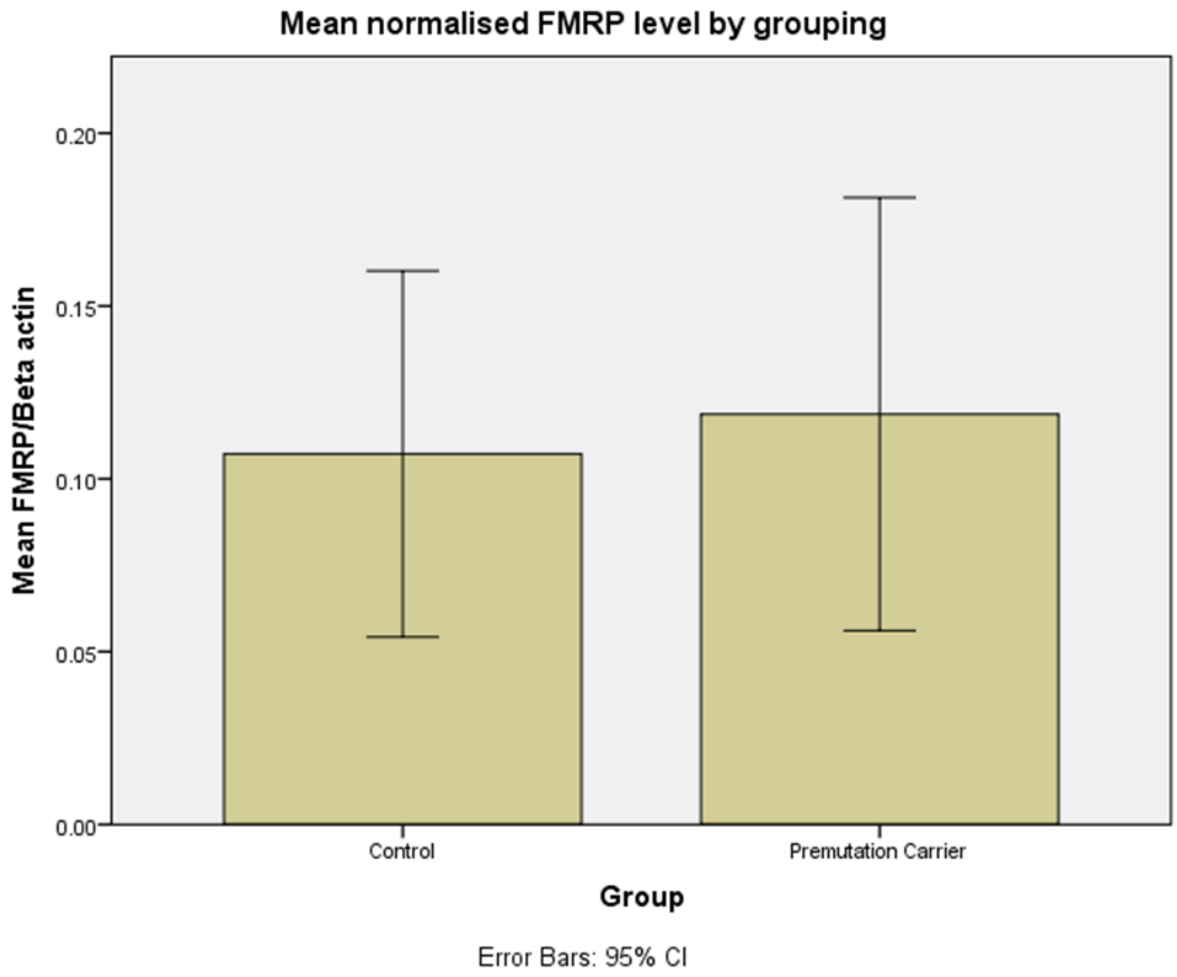

Figure 8.8 FMRP quantification data analysed using parametric two-sample t-testing in SPSS **b)** Group mean FMRP levels normalised to beta actin loading control band quantification.

Table 8.7: FMRP quantification data

Group	Variable	Mean	Standard deviation
Control	**FMRP quantification**	0.107	0.103
Carrier		0.118	0.122

Table 8.7 Mean scores and standard deviations of quantified 80kDa FMRP averaged over 3 runs and normalised to beta actin loading control for the control group and the premutation group

8.7 Linear regression analyses

Simple linear regression analyses were carried out on extracted voxel data from the significant between group BOLD clusters from the imaging analysis against clinical variables of interest that were established to be significantly different between the groups. No significant association was identified between either significant cluster of BOLD response and any of these clinical or neuropsychological variables (Table 8.8).

Similarly, linear regression analysis was carried out on extracted voxel data from the significant between group BOLD clusters against FMRP molecular data, and revealed no significant associations (Table 8.8).

Table 8.8: Within group regression analysis of BOLD response and clinical measurements, neuropsychological measurements and FMRP levels

Group	DV	IV	β	Standard error	Adjusted R^2	P value
Control	BOLD cluster 1	Obsessive-compulsiveness	-2.34	1.85	-0.171	0.098
	BOLD cluster 1	Anxiety	0.02	1.45		0.967
	BOLD cluster 1	GSI	2.75	4.45		0.089
	BOLD cluster 1	PSDI	-1.07	2.00		0.108
	BOLD cluster 1	Anger	-0.24	0.50		0.782
	BOLD cluster 1	Disgust	0.67	0.28		0.316
	BOLD cluster 1	Surprise	0.10	0.28		0.826
	BOLD cluster 1	Total	-0.71	0.19		0.571

	BOLD cluster 1	AQ	-0.01	0.04		0.975
	BOLD cluster 1	FMRP (normalized)	-0.38	3.53		0.452
Premutation	BOLD cluster 1	Obsessive-compulsiveness	-2.49	1.24	0.071	0.178
	BOLD cluster 1	Anxiety	-0.13	2.39		0.940
	BOLD cluster 1	GSI	2.00	2.90		0.373
	BOLD cluster 1	PSDI	0.39	1.13		0.615
	BOLD cluster 1	Anger	0.08	0.19		0.876
	BOLD cluster 1	Disgust	-0.14	0.20		0.781
	BOLD cluster 1	Surprise	-0.18	0.28		0.752
	BOLD cluster 1	Total	-0.01	0.09		0.987
	BOLD cluster 1	AQ	0.19	0.05		0.722
	BOLD cluster 1	FMRP (normalized)	0.11	2.40		0.778
Control	BOLD cluster 2	Obsessive-compulsiveness	-1.25	1.47	0.067	0.473
	BOLD cluster 2	Anxiety	0.58	2.84		0.737
	BOLD cluster 2	GSI	1.22	3.46		0.579
	BOLD cluster 2	PSDI	-0.11	1.34		0.883
	BOLD cluster 2	Anger	0.21	0.23		0.689
	BOLD cluster 2	Disgust	0.03	0.24		0.959

	BOLD cluster 2	Surprise	0.01	0.34		0.979
	BOLD cluster 2	Total	-0.70	0.11		0.409
	BOLD cluster 2	AQ	0.18	0.06		0.735
	BOLD cluster 2	FMRP (normalized)	0.02	2.86		-.967
Premutation	BOLD cluster 2	Obsessive-compulsiveness	-0.07	1.24	0.266	0.938
	BOLD cluster 2	Anxiety	0.23	0.97		0.595
	BOLD cluster 2	GSI	0.10	3.05		0.930
	BOLD cluster 2	PSDI	-0.57	1.35		0.256
	BOLD cluster 2	Anger	-0.42	0.34		0.547
	BOLD cluster 2	Disgust	0.77	0.19		0.161
	BOLD cluster 2	Surprise	0.35	0.19		0.352
	BOLD cluster 2	Total	-0.67	0.13		0.505
	BOLD cluster 2	AQ	0.39	0.03		0.259
	BOLD cluster 2	FMRP (normalized)	0.10	2.36		0.801

Table 8.8 Statistical results of within group regression analyses between significant between group clusters 1 and 2 and measures of clinical, neuropsychological and protein level variables.

Chapter 9: Neurodevelopment in the Fragile X premutation: Discussion

9.1 Within group imaging

When contrasting high and low arousal states as a means of establishing activation patterns in response to images that are arousing across valence ratings, the within group analysis showed no significant clusters of activation in the premutation group and four significant clusters in the control group. The clusters centred in the right intraparietal cortex, left lobules VII and VI of the cerebellum, bilateral superior parietal lobe and right middle and superior frontal gyrus. Previous reports of investigation into emotional arousal in healthy participants utilising the IAPS images have demonstrated similar regions of interest, providing validation of our task design. In an analysis into correlation between participants' own arousal ratings and BOLD activation at a whole brain level, activity was identified at the right superior frontal gyrus, bilateral inferior parietal lobe and left dorsolateral prefrontal gyrus. These findings are indicative of significant activations in this area that are relevant to participants' own judgement of the extent of arousal (Prehn et al. 2015). In addition, it is reported that there is greater activation in response to images with stronger emotional content in the right than in the left parietal regions, which is consistent with the present results exhibiting mainly right hemispheric parietal BOLD responses when observing images of higher arousal ratings (Bradley et al. 2003). The cerebellum has also been connected with social cognition and emotional processing, especially concerning mentalizing more abstract emotions and hypothetical events, which is applicable to this IAPS task presenting a variety of images portraying emotional situations (Van Overwalle et al. 2014). Functional topography of the cerebellum for motor and cognitive tasks demonstrates clear functional connectivity between cerebellar lobules VI and VII and the parietal cortex during cognitively demanding tasks (Stoodley et al. 2012). Moreover, resting state functional connectivity analyses have shown that cerebellar lobule VII is part of a supramodal zone of the cerebellum, which exhibits overlapping connectivity maps for the prefrontal and parietal cortices (O'Reilly et al. 2010b). It is possible that the origin of the cerebellar cluster here in response to high arousal compared to low arousal conditions may have arisen from a strong connectivity between the parietal lobe and lobules VI and VII of the cerebellum and additional mentalizing processing of emotional stimuli.

The two fMRI emotional processing tasks utilised to date in premutation carrier samples have been a fearful and neutral faces paradigm and a facial emotion matching task, both utilising Ekman face images (Hessl et al. 2007; Hessl et al. 2011). The former study carried out a within group analysis comparing fear and control conditions that exhibited significant clusters of activation centring at the orbital gyrus, middle temporal gyri, occipital sulcus, cerebellar lobule VI and middle and inferior frontal gyri in controls. This contrast of fear-control conditions may be seen to somewhat align with the high arousal-low arousal contrast of interest for this study, and clusters at the cerebellum and

middle frontal gyri are concurrent. Also, in a similar manner to the present analysis of emotional processing, the premutation within group analysis of the fear-control contrast exhibited both markedly less overall activation and different activation patterns, with smaller significant clusters than the control group only at the angular gyrus, the bilateral cuneus and the middle occipital gyrus (Hessl et al. 2007). The other fMRI emotional processing study carried out in carriers however did not find overt inconsistency in the within group analysis, with both carriers and control exhibiting robust activations bilaterally in the insula, mid cingulate gyrus, fusiform gyrus, parietal lobe, superior frontal gyrus and middle frontal gyrus (Hessl et al. 2011). Despite the lack of significant clusters in the within group analysis for premutation carriers in the present study, our results are consistent with many of these regions of activation during an emotional processing task. Overall, the results of our within group analyses tally well with some of the previous findings, showing robust areas of emotion-related activation in response to arousing stimuli in controls and exhibiting marked attenuation of BOLD response in carriers. The novelty of the use of an IAPS based task in premutation carrier imaging research and population variance may be a causative factor in the moderate disparity of the present results with previous fMRI findings of emotional processing in premutation groups.

9.2 Between group imaging

Between group analysis of the high arousal-low arousal contrast of interest revealed that premutation carriers showed significantly less activation in a cluster located bilaterally at BA17 (primary visual cortex), right BA18 (visual association area) and the right superior parietal lobe, and another cluster located bilaterally at the superior parietal lobes, right BA2 (primary somatosensory cortex) and right intraparietal area. In previous studies utilising the IAPS, an increase in the extent of visual cortex activation has been found when viewing emotional images that are both pleasant and unpleasant compared to low arousal images (Bradley et al. 2003; Lang et al. 1998). The basis of such increased metabolism at the visual cortex is thought to reflect increased attention towards perceived threat or positive stimuli. Our findings of between group differences at the primary visual cortex and visual association area indicate that this response to high arousal stimuli is significantly attenuated in premutation carriers. The parietal cortex has also been implicated as an area of interest in an IAPS-based fMRI task, with images portraying sadness prompting clusters of BOLD activation at the bilateral parietal cortices including the angular and supramarginal gyri compared to neutral images (Radua et al. 2014). It is possible therefore that extensive clusters of significantly lower activation in carriers at the superior parietal areas is reflective of deficits in the emotional processing of arousing images of a more negative valence.

Like the current study, the two neuroimaging studies to date utilising fMRI emotion-based tasks in premutation carriers, carried out by Hessl et al., demonstrate the existence of between group differences in BOLD response concerning emotional processing (Hessl et al. 2011; Hessl et al. 2007).

In one study, when contrasting fearful and neutral face conditions, the control group showed significantly greater activation at the bilateral amygdalae, bilateral insula, left superior temporal sulcus, bilateral intraparietal sulcus and regions of the left basal ganglia (Hessl et al. 2007). The other study demonstrated no significant differences at a whole brain level when comparing facial stimuli to inanimate stimuli, however subsequent region of interest (ROI) analysis revealed significantly lower activation in the carrier group compared to controls at the left amygdala (Hessl et al. 2011). The present study tallies with these previously identified between group differences in that activation in that carriers exhibited significantly lower activation clusters, not significantly higher. This replicated lower level of activation is indicative of significantly attenuated response to or recognition of emotional stimuli in premutation carriers. Moreover, in the present study there is concurrence with previous findings of the location of between group activation differences at the intraparietal regions during emotional processing contrasts.

However, both previous studies into functional responses to emotional processing in premutation carriers highlight activation differences in the amygdala (Hessl et al. 2007; Hessl et al. 2011). Additionally, multiple studies utilising the IAPS in fMRI investigations show that the amygdala plays an important role in emotional processing, particularly involving arousal and fear. BOLD signal changes have been identified at the amygdala to correlate with participant ratings of arousal for IAPS images at a whole brain level (Prehn et al. 2015) and the amygdala and insula bilaterally demonstrated enhanced responsivity to negative IAPS images of balanced arousal ratings in individuals with social phobia (Shah et al. 2009). Using volume of interest (VOI) analysis in an fMRI study utilising the IAPS, the amygdala was also seen to be involved in emotional discrimination, with amygdala activation preceding activation of the ventrolateral prefrontal cortex, consistent with theories of emotional stimulus detection and integration of information in these areas (Kohno et al. 2015). In the present study however, no differences at the amygdala were discerned in carriers. This disparity may originate from the known heterogeneity of emotional, psychiatric, neuropsychological and autistic trait phenotypes in *FMR1* premutation carriers, therefore causing sample groups to be variable between studies. In addition, our findings indicate that amygdala dysfunction may not be a robustly replicable phenotype of male premutation carriers.

Overall, our results indicate significant between group differences that demonstrate attenuation of the functional response to arousing stimuli in carriers. The locations of the clusters of significantly different activation, at BA17 (primary visual cortex), BA18 (visual association area), the superior parietal lobes, BA2 (primary somatosensory cortex) and intraparietal areas, converge with the results from both other fMRI based emotional processing tasks in carriers and other IAPS based tasks in healthy or psychiatrically affected cohorts.

9.3 Group x age interaction

When group x age interactions were examined at a whole brain level for this emotional processing task, the analysis showed no significant clusters of BOLD activation. This indicates that no areas of the brain differ significantly between the groups in their reactivity to arousing stimuli when considering their interaction with age. It can be drawn from these results therefore, that the lower functional brain response in premutation carriers when contrasting high and low arousal conditions of varying valence is not sensitive to the effects of age. Moreover, not only are the significant differences in BOLD response at BA17 (primary visual cortex), BA18 (visual association area), the superior parietal lobes, BA2 (primary somatosensory cortex) and intraparietal areas not susceptible to age-related changes, neither is any region of the brain's emotional functional response to arousing stimuli.

This is the first study investigating emotional processing in carriers using fMRI that has a cross-sectional design incorporating age as a variable factor, allowing for the collection of neuroimaging evidence supportive of the idea that premutation carriers exhibit neurodevelopmental changes that remain stable over time. Previous findings have indicated the existence of these neurodevelopmental traits in carriers. Most of these findings however concern out of scanner measurements, such as evidence of elevated risk for ASD in carrier populations and increased prevalence of associated seizures (Chonchaiya et al. 2012). Developmental delay, attention problems, aggressiveness, and anxiety have also all been identified as being significantly more common in young carriers than controls (Bailey et al. 2008). However, in previous neuroimaging studies investigating emotional processing in premutation carriers, the participant samples were relatively young, with mean age-matched premutation carrier ages of 32.9 years and 42.9 years (Hessl et al. 2007; Hessl et al. 2011). These sample ages, regarded as low-risk ages for FXTAS onset, combined with the samples being asymptomatic for FXTAS as confirmed by neurological examination, suggest that significantly different BOLD responses during Ekman face-based tasks are both separate from FXTAS and present long prior to expected onset of neurodegeneration. The analysis in the present study probing age-related changes in premutation carriers, is therefore in accord with previous evidence of emotional processing disparities in carriers and we present here novel evidence of *FMR1* premutation carrier phenotypic changes in arousal that may be stable and separate to onset of neurological disease.

9.4 Clinical and neuropsychological measurements

Consistent with the hypotheses of increased levels of psychiatric symptoms and neuropsychological problems in premutation carriers compared to neurotypical individuals, our results show significant differences in carriers pertaining to neurodevelopmental traits. Psychiatric symptomatology as measured by the SCL-90-R self-report questionnaire, facial emotion recognition as measured by the Ekman 60 Faces Test and autistic traits as measured by the AQ all revealed significant deviation from control group norms. Although some measurements did not show any significant differences between

groups, such as the social judgement test and EQ, it is clear that psychiatric and neuropsychological differences exist between carriers and controls.

Here, we report significantly higher neuropsychiatric symptomatology of obsessive-compulsiveness, anxiety, global psychiatric severity and positive symptom distress levels as measured by the SCL-90-R in premutation carriers compared to controls. Control sample results were corroborative with the SCL-90-R normative sample means, suggesting that our control sample is broadly similar to the normative sample. Obsessive-compulsive and anxiety measurements reflect significantly higher levels of these specific symptoms in carriers, whereas measurements of somatization, interpersonal sensitivity, depression, hostility, phobic anxiety, paranoid ideation and psychoticism did not differ significantly between the groups. However, most of these variables did exhibit trends towards being more severe in carriers, which is demonstrated as the measurement of global severity of symptoms is significantly higher in the carrier group. In addition, the positive symptom distress index was also significantly higher in carriers, representing an increased level of psychological distress at the presence of psychiatric symptoms. These results strongly align with previous evidence of psychiatric symptomology in carriers, where outcomes from the SCL-90-R show that obsessive-compulsiveness and global symptom severity are significantly increased in male carriers without FXTAS (Hessl et al. 2005). It is likely that within sample heterogeneity has led to the present sample also exhibiting significantly higher levels of anxiety and positive symptom distress. Our findings are further validated by previous research as higher rates of anxiety and obsessive-compulsive symptoms have been demonstrated in multiple studies of premutation males without FXTAS (S Jacquemont et al. 2004; Dorn et al. 1994).

Participants in the present study also carried out the Ekman 60 Faces Test as an investigation into facial emotion recognition abilities. Our results show that carriers are significantly worse at identifying emotive faces of anger, disgust and surprise, and recognising emotive facial expressions overall as reflected by the total test score. Controls and carriers did not perform significantly differently when asked to recognise facial emotions of fear, happiness or sadness. The mean scores for all variables showed that neither the carrier or control group were reaching cut-off scores for marked impairment of emotive facial recognition, as dictated by the Ekman 60 Faces Test normative dataset. We can therefore infer that carriers are worse at identifying emotional facial expressions, but not to such an extent that denotes significant, clinically relevant impairment. Few prior studies have utilised Ekman faces in investigations into the *FMR1* premutation, however carriers have been shown to exhibit diminished potentiation of the startle response to fearful faces as measured by skin conductance, despite being similar to the control group in their baseline startle responses (Hessl et al. 2007). This lower level of skin conductance reaction to fearful faces in carriers may be a pertinent phenotype, and in a similar manner to the between group neuroimaging attenuated BOLD response to arousing stimuli in premutation carriers, it is possible that when observing Ekman face images,

carriers possess a weakened initial response to facial images demonstrative of heightened arousal, which then manifests as a reduced ability to recognise such facial emotions correctly. Our results are supportive of this theory, as the variables that carriers performed significantly worse on were primarily those that can be considered as typically more threatening or arousing.

All participants took part in testing of social judgement, centred around variables of the perceived age, approachability, attractiveness, distinctiveness, intelligence and trustworthiness of individuals represented in images. In these measurements, mean scores of the carrier and control group were comparable and no significant differences existed between the groups. This is a somewhat unexpected finding, given that carriers have been shown to have higher levels of autistic traits than control populations, and part of the clinical presentation of ASD is social difficulties that may partly arise from lack of accurate social judgement (Shulman et al. 2012; Mathersul et al. 2013). Moreover, investigation into social cognition in young male premutation carriers indicated significantly increased levels of social deficits, particularly pertaining to interpersonal skills that necessitate accurate social perception, such as the recognition of complex emotions from photographs of eyes (Cornish et al. 2005) and our own findings report evidence of emotion processing difficulties. It is of note that research into social cognition in carriers has been carried out in groups of carriers that were younger on average than the sample in this study. It may be the case that older carriers have an increased aptitude for social judgement than younger carriers due to more experience, or that the carriers in the present study were on average more socially able, given that populations of premutation carriers are notably heterogenous.

Investigation into the existence of autistic traits in premutation carriers was carried out in the present study using the AQ and EQ self-report questionnaires. Our results show that carriers have significantly higher levels of autistic traits compared to controls as measured by the AQ. This is supportive of the previous literature reporting *FMR1* premutation carriers as a high-risk ASD cohort. Frequency of ASD in carrier populations has been estimated to be approximately 10-20% in males and 1-7% in females, which is notably elevated compared to the 1% ASD frequency estimation in the general population (Besterman et al. 2014). High rates of social impairment, hyperactivity, delayed receptive and expressive vocabulary and use of social language have also been reported in young males with the premutation (Aziz et al. 2003). Epidemiological data collected through a national survey estimates a 19.3% incidence of autism, a 33% incidence of developmental delay and a 41% incidence of attention problems in male carriers (Bailey et al. 2008). Our data is therefore concurrent with these previous reports of significantly increased ASD attributes in male premutation carrier cohorts. Interestingly however, EQ scores in carriers were not significantly lower than control scores as expected, although mean carrier EQ score was still notably lower. Comparable scores in the EQ between the groups indicate that lack of self-rated empathy is not evident in this group of premutation carriers. Interestingly, the control group in the present study exhibited a significant correlation

between AQ and EQ scores, as previously reported in ASD and neurotypical cohorts (Wheelwright et al. 2006). The carrier group however did not show an association between AQ and EQ scores and deviation from this standard correlation may be indicative of a non-standard autistic presentation in premutation carriers. Indeed, when considering this data in tandem with the aforementioned social judgement scores, which were not significantly different between groups, the present results appear to reveal that impaired social perception and empathic feeling form part of premutation carrier ASD symptomatology to a lesser extent than predicted.

Overall here, we have reported results that show premutation carriers exhibit elevated psychiatric symptoms in the domains of obsessive-compulsiveness, anxiety, total severity and positive symptom distress as hypothesised and concurrent with previous findings. Correct recognition of facial emotions was also seen to be impaired in carriers, particularly for expressions that may be considered as more arousing. Considering neuroimaging data in the present study showing attenuated response to arousing stimuli, it is possible that premutation carriers exhibit a phenotypic loss of response to arousing stimuli and facial expressions, therefore exhibiting lower levels of recognition. Our results also indicate higher levels of autistic traits in male premutation carriers than controls, as shown by the previous research, however comparable between groups results in the social judgement test and EQ indicate that social discernment and empathy remain neurotypical in carriers.

9.5 Molecular measurements

Previous research indicates that levels of FMRP are sometimes lower in premutation carriers. Kenneson et al. reports that reduced FMRP in premutation carriers of intermediate length repeat expansions is proportionally associated with CGG repeat number (Kenneson et al. 2001). Similarly, premutation carriers with more than 100 repeats have been reported to be more likely to possess mild deficits in FMRP and developmental problems than carriers with smaller repeat lengths (Tassone, Hagerman, Taylor, Mills, et al. 2000). Two neuroimaging studies in premutation carrier cohorts to date have utilised additional molecular measurements of FMRP. Both studies quantified FMRP in the same manner, using participant lymphocyte samples and sandwich Enzyme Linked ImmunoSorbent Assays (ELISA) for FMRP (Hessl et al. 2011; J. M. Wang et al. 2012). Unlike Immunocyctochemistry techniques, this ELISA method measures protein level, not just the proportion of lymphocyte cells with detectable staining (Iwahashi et al. 2009). Hessl et al. identified FMRP levels to be reduced by 12% in the premutation group relative to controls after log-transformation to achieve normality, and this difference was statistically significant (Hessl et al. 2011). Wang et al. however reported a 23% reduction of FMRP in carriers compared to controls which did not reach statistical significance, stating high variability within both groups may have been a causative factor (J. M. Wang et al. 2012). The present study utilised a Western blotting technique for protein quantification from samples of peripheral blood mononuclear cells, which revealed that premutation

carrier FMRP levels and control FMRP levels were not significantly different. As referred to in previous reporting of FMRP quantification, the variance in our results was high in both the control and carrier group, even within the same extracted protein sample, which may have contributed to lack of identification of a slight FMRP reduction. Research has previously indicated that it is often carriers of higher CGG repeat expansions (>150 CGG repeats) that exhibit modest reductions in FMRP, and it may be that lower levels of FMRP are not identified in this sample due to the majority of carriers being of lower CGG repeat lengths (Tassone, Hagerman, Taylor, Gane, et al. 2000). Additionally, Western blotting of extracted protein samples originating from peripheral blood mononuclear cell samples produced multiple anti-FMRP specific bands which were of unknown derivation. For this reason, only 80kDa FMRP bands were quantified using densitometry for the analysis, to minimize the chance of quantifying non-FMRP bands. However, this excluded the possibility of quantifying FMRP isoforms that were not 80kDa, of which several have been reported during Western blotting when using Ab17722 as used in the present study, and other commonly used anti-FMRP antibodies with human reactivity. It is likely that lack of quantification of FMRP isoforms has also impacted the accuracy of the present results.

Nevertheless, our results indicate that despite a high variability in both the control and carrier group, that 80kDa FMRP levels equate between the groups. This lack of significant between group difference in FMRP level has been reported before and is therefore not unusual, however this result indicates that, contrary to our original hypotheses, there is no reduction in FMRP, and therefore low levels of FMRP do not appear to be driving neurodevelopmental deficits in premutation carriers in this case (J. M. Wang et al. 2012). While the present results of quantified FMRP levels shed doubt upon the neurodevelopmental hypotheses of FMRP-driven phenotypes, it should be stressed that the Western blotting assay utilised for this study was notably problematic and further limitations and considerations are covered in section 9.7.

9.6 Linear regression analyses

In the present study, no significant associations were identified between significantly decreased clusters of BOLD response in premutation carriers during the emotional processing task and clinical or neuropsychological measures of interest. It was hypothesised that differences between carriers and controls in out of scanner measurements of psychiatric symptoms and neuropsychological variables, such as recognition of facial expressions of emotion, would correlate with neuroimaging differences, indicating a link between functional brain processing during emotional responses and premutation emotional phenotypes. This was not evident however in our analyses, showing no strong connection between differences in BOLD response in carriers and a possible manifestation of symptoms. Conversely, in previous studies, associations between MRI findings and psychiatric or neuropsychological measures have been successfully identified, suggesting structural or functional

brain deficits that may underlie vulnerability to neuropsychiatric phenotypes. Reduced functional activation of the amygdala during an emotion-based task in premutation carriers has been shown to correlate with global psychiatric symptom severity as measured by the SCL-90-R, even with a small sample size of twelve (Hessl et al. 2007). A reduction in volume at the hippocampal complex has been significantly associated with anxiety symptoms in female carriers, and a sample of male carriers exhibited a significant association between reduced hippocampal functional BOLD response during memory recall and higher levels of psychiatric symptoms (Adams et al. 2010; Koldewyn et al. 2008). Given that carriers showed significant differences in both the in scanner and out of scanner measurements of emotional processing in the present study, it is somewhat surprising here that there is no connection between these variables. However, it is possible that the psychiatric and neuropsychological tests were not specific enough to be closely likened to the task contrast of high arousal-low arousal stimuli. In addition, previous studies identifying significant associations between neuroimaging and psychiatric data in carriers have been largely focussed on limbic brain regions. Our results indicate no differences between carriers and controls at the amygdala, hippocampus or other limbic region, so it is possible that significant links between MRI findings and higher levels of psychiatric symptomatology in carriers concerns mainly the limbic system.

In addition, no significant link was identified between levels of FMRP and significantly different clusters of BOLD response during the emotional processing task in either the carrier or control group. It was hypothesised that given the important role of FMRP in neural plasticity and brain development, reported small decreases in FMRP would be a causative factor in the establishment of neurodevelopmental differences between premutation carriers and controls (Hagerman & Hagerman 2013). However, this was not evident in the current sample, and no association was found between attenuated brain response in carriers and levels of FMRP. Previous findings have suggested that such links do exist, with one study in male premutation carriers showing a significant negative correlation between functional activity in the left parahippocampal gyrus during a memory encoding task and FMRP levels as measured by ELISA (J. M. Wang et al. 2012). Another study found that FMRP levels, also quantified by ELISA, were positively correlated with right and left amygdala BOLD response in premutation carriers during an emotion processing task (Hessl et al. 2011). This previous research is supportive of the theory that neurodevelopmental deficits in carriers is driven, at least partly, by FMRP expression. Our results are not supportive of this however, but it is notable in this case that the present study quantified FMRP levels using a different methodology to the two aforementioned studies, which may be reflective of different isoform and total FMRP quantification. Moreover, our results do not indicate any significant difference between the carrier and control group in FMRP expression, as has been shown in prior research, so it is possible that no association exists due to comparative FMRP levels in the present sample and lack of initial moderate protein reduction (Hessl et al. 2011; Kenneson et al. 2001). In a similar manner to the previous reports of associations

between clinical symptoms and neuroimaging data, FMRP and fMRI data correlations have been identified only in limbic regions to date. Therefore, it may be possible that it is mainly the limbic regions that exhibit sensitivity to lower levels of FMRP, causing aberrant BOLD responses and linking to vulnerability to psychiatric phenotypes.

Overall therefore, we can surmise that in the present premutation carrier sample, FMRP levels are not influencing significantly lower clusters of BOLD response in response to emotional stimuli and in turn, these functional brain differences do not necessarily infer psychiatric or neuropsychological premutation phenotypes. Nevertheless, the possible influencing factors on why such associations may not have been statistically identified in this sample should be taken into account.

9.7 Limitations and conclusions

An important limitation when investigating neuropsychological and psychiatric phenotypes in any cohort is the large influence of environmental factors, including life stressors, traumatic life events and socioeconomic background (Klengel & Binder 2015; Fatori et al. 2013). In addition, drug and alcohol abuse can both result from and exacerbate psychiatric difficulties (Indlekofer et al. 2009). Environmental factors are of especial import when considering psychiatric symptoms in carrier populations, as both male and female carriers have been documented to have higher levels of alcohol abuse which may be suggestive of a heightened sensitivity to social and psychological stress (Seltzer et al. 2012). In a group of FXTAS patients with dementia, 21% reported alcohol abuse or dependence (Seritan et al. 2016). In addition to affecting individuals psychiatrically, a recent case study suggests that drug use, specifically narcotics, may greatly increase risk for, onset of and speed of progression in FXTAS, causing exacerbated white matter disease through RNA toxicity (Muzar et al. 2015). Carriers of the *FMR1* premutation are also at increased risk for endocrinological medical conditions, which can contribute to the development of psychiatric disorders (Hunter et al. 2010). For example, women with the premutation have a 20% risk of experiencing premature ovarian insufficiency, which can lead to infertility and early menopause (Sullivan et al. 2011). As a result of the associated decrease in oestrogen and potential emotional stress, risk for mood disorders in this group is elevated (McConkie-Rosell et al. 2012). Premutation carriers also have an increased risk for hypothyroidism, with reported incidence being as high as 8.84% in carriers compared to 0.93% in the general population, which characteristically increases risk for mood and affective disorders (Merino et al. 2016). In the present study of neurodevelopmental differences in premutation carriers, co-morbidities or environmental factors were not addressed and so could not be controlled for or investigated in the analyses. It may be pertinent for future study to gain complete drug histories for this sample group, and to consider more environmental and co-morbidity factors in prospective study design and analyses.

Another limitation in the present study methodology is the use of peripheral blood mononuclear cell samples to obtain relative quantifications of FMRP with the assumption that these levels will reflect

brain expression levels. It is known however that FMRP levels are higher in the brain compared to other tissues, with moderate expression in lymphocytes, which form part of the mononuclear cell group, and that within brain tissue FMRP expression can also be variable between regions (Hinds et al. 1993). It is therefore not ideal to utilise blood-based measurements as a reflection of brain protein expression levels, but venepuncture and subsequent analysis of peripheral blood mononuclear cells remain the safest, least invasive and most ethically sound methodology for a clinical research setting. Moreover, some research has shown support for robust association between blood and brain measures of FMRP, for example, full mutation males and females exhibit a significant correlation between FMRP levels and full-scale intelligence quotient scores (LaFauci et al. 2013). Another study found that FMRP expression was similar between peripheral blood mononuclear cells and fibroblast samples as measured by Western blot (Pretto et al. 2014). We can therefore infer that FMRP measured from peripheral blood mononuclear cells can be cautiously treated as relative to brain expression levels, although further research should be carried out to characterise this relationship.

Western blotting-based methodology to obtain quantifications of FMRP relative to a loading control has also been a limiting factor in this study. The blots revealed multiple FMRP specific bands of unknown origin between approximately 10-100kDa. Cross-reactivity of secondary antibodies and IgG reactivity was ruled out by control blots. Extensive splicing of the *FMR1* gene has previously been reported using RT-PCR and several FMRP isoforms have been demonstrated using Western blotting (Ashley et al. 1993; Verheij et al. 1993; Verkerk et al. 1993). These isoforms do not appear to be tissue specific, with similar FMRP isoform expression profiles being seen in multiple foetal tissues, brain and testis (Verkerk et al. 1993). Splice variant molecular function remains unknown to date, but four or five isoforms of FMRP, ranging in weight from 70 to 80kDa have been identified using Western blotting and FMRP-specific antibodies (LaFauci et al. 2016; Verheij et al. 1995). Our blots did not replicate these isoform expression patterns, and variability was high both within and between samples. Given the unknown source of variance and the extra banding in our blots, only 80kDa FMRP was quantified, as the stated expected molecular weight. It is important however for future research to establish the identify of extra FMRP-specific bands when Western blotting peripheral blood mononuclear cell-derived protein samples, and for this method to be validated using additional control samples.

Overall, we find in this study multiple differences in premutation carriers compared to controls in several modes of measurement. Our neuroimaging analysis revealed that carriers exhibit significantly attenuated response at bilateral BA17 (primary visual cortex), right BA18 (visual association area) bilateral superior parietal lobes, right BA2 (primary somatosensory cortex) and right human intraparietal area 1 when contrasting high arousal and low arousal images. Previous research utilising fMRI and the IAPS indicates that the visual system is an early regulator of arousal response, and exhibits localised increased BOLD response during high arousal stimuli compared to low arousal

(Bradley et al. 2003). Significantly lower activation in carriers at the visual cortex and visual association area therefore indicates diminution of this response and a possible reduction in the ability to heighten attentional control during arousing events. In addition, no group x age interaction was identified for this task, showing that changes to emotional processing concerning arousal in carriers are not sensitive to age in a way that deviates from the normative sample. In general, we demonstrate a significantly reduced functional emotional response in premutation carriers which appears to be stable and neurodevelopmental in nature.

We also show that carriers have significantly increased measures of psychiatric symptomatology, reduced performance when recognising facial emotions and increased levels of autistic features. Firstly, higher levels of psychiatric features in carriers was both hypothesised and closely replicates previous studies. Secondly, a poorer ability for the recognition of facial expressions of emotion in carriers, particularly those that can be considered to be more arousing, links to the differences in response to arousal in the neuroimaging analysis. These combined findings imply that a reduction in functional brain response to arousing stimuli may cause a downstream reduction in the ability to correctly recognise emotionally arousing expressions, such as anger, disgust and surprise. Lastly, the absence of any significant differences between carriers and controls in measures of social judgement and EQ scores, but significantly increased levels of autistic traits as measured by the AQ, is suggestive of an autistic profile in carriers that may deviate from normal ASD presentation, as social perception and empathy remain typical.

Analysis of FMRP levels in the present sample revealed no significant between group differences, not a reduction in *FMR1* protein product as hypothesised and previously reported (Tassone, Hagerman, Taylor, Mills, et al. 2000). However, the present sample of carriers tended towards lower premutation allele repeat sizes, which may be an explanatory factor, as higher CGG repeat regions appear to produce lower FMRP expression levels (Tassone, Hagerman, Taylor, Mills, et al. 2000). Additionally, as discussed, the Western blotting assay used here would benefit from further protocol refinement and validation.

Simple linear regression analyses of neuroimaging significant between group cluster data and clinical or neuropsychological measurements yielded no statistical associations, as did regression analyses of imaging data and FMRP levels. These findings appear to show that the functional reduction in BOLD response in carriers is not related to higher levels of psychiatric symptoms, autistic traits or performance in the Ekman 60 Faces Test, contrary to the original hypotheses. However, it is possible that out of scanner measurements of emotional processing were not specific enough to accurately map to brain responses of arousal, or that lack of limbic involvement in the fMRI analysis meant that previously reported results were not replicated.

In all, we report here evidence in keeping with neurodevelopmental symptomatology in premutation carriers at both a functional brain imaging and clinical level. Age-related analyses show that the attenuated emotional BOLD response in carriers is stable in nature, and increased levels of psychiatric involvement and neuropsychological differences are supportive of the hypothesis that premutation carriers exhibit neuropsychiatric and emotional problems throughout their life-span, regardless of FXTAS development.

Chapter 10: Study discussion

10.1 Limitations of the study design

The present study was designed to utilise fMRI, clinical, neuropsychological and molecular measurements to probe both neurodegenerative and neurodevelopmental aspects of the *FMR1* premutation phenotype. We report here new insights into both features, which are predominantly supportive of previous findings in the field and our original hypotheses. The study has limitations however, which are important to acknowledge.

A possible limitation may be statistical power. Whilst some studies report that to reach a statistical power of 80% in a functional neuroimaging study, approximately 13 subjects are required when data is FWE corrected, other studies report that a minimum of 18 subjects are necessary to reach a statistical power of 80%, regardless of length of condition blocks, which when lengthened can increase power (Hayasaka et al. 2007; Mumford & Nichols 2008). Some studies cite even higher sample size requirements, despite liberal thresholding at 0.05 necessitating just 12 subjects to reach 80% statistical power, realistic thresholds and correction for multiple comparison require double this sample size to reach statistical power (Desmond & Glover 2002). It seems reasonable therefore to infer that a sample size of 17 subjects in the present study falls somewhere in the middle of these estimations, and is likely to be adequately powered, although still at the lower end of the spectrum. When considering the present two-sample analysis, and the non-clinical nature of both the control and premutation group however, it is possible that the observed effect size may be relatively small.

A cross-sectional design also is a limit to the study's ability to establish neurodevelopmental or neurodegenerative aspects of the premutation. Whilst using age as a variable to investigate the possible existence of abnormal brain development and degeneration may be insightful, because the study is not longitudinal inferences of change over time cannot fully be made. In addition, factors such as relative compensation in older carriers and individual differences in ability level may drive or mask age-related associations.

Cluster-wise inference using statistical parametric methods, as used in this analysis, has additionally been reported to yield high rates of Type I error in some cases (Eklund et al. 2012). Voxel-wise inference on the other hand has been identified as a stringent estimate of significance, with family-wise error rates often falling below 5% (Eklund et al. 2016). Given possible limitations concerning power of this study, as previously discussed, and reported over-stringency of voxel-wise inference, the present results nevertheless remain promising.

An additional limitation of the present study is that the design did not incorporate a neurological examination or a FXTAS rating scale, which could have been used to fully confirm asymptomatic carrier status. Although no carriers presented with any overt FXTAS symptoms, or had a diagnosis of

FXTAS, verification of FXTAS status would have allowed certainty of the nature of the sample group. It should also be acknowledged that the sample of premutation carriers taking part in this study had a mean age of 50.4 years, with an age range of 24-68 years old. Penetrance of FXTAS is age-related; 40% of male carriers over the age of 50 develop the disease and FXTAS penetrance in male carriers over 80 years old is 75% (Sébastien Jacquemont et al. 2004). Considering that none of the premutation carriers in this study had a FXTAS diagnosis, it is possible that this sample had a bias towards a lower FXTAS penetrance, and older individuals in the sample were at a lower risk for FXTAS development than a group that had been selected regardless of disease status. The results presented from this study therefore characterise a cross-sectional group of carriers without FXTAS, and may not be accurately representative of a cross-section of all premutation carriers.

10.2 Future directions

Fragile X-associated Tremor/Ataxia Syndrome and the effects of the *FMR1* premutation were only uncovered in the last two decades, and research into this field is quickly developing. Many methodologies have yet to be utilised in premutation carrier samples, and there is much room for advancement in the characterisation of phenotypes, with the aim of creating more effective, targeted treatments for FXTAS and neurodevelopmental premutation traits.

The scanner protocol for this study involved a DTI sequence for all participants, which can be analysed in the future. Functional connectivity analyses may also be carried out on the existing fMRI data. Previous studies utilising DTI in premutation carrier cohorts have shown minimal differences between non-FXTAS and control groups, but robust differences between controls and FXTAS groups. In carriers with FXTAS, fractional anisotropy was significantly reduced in multiple white matter tracts, including the MCP, superior cerebellar peduncle, cerebral peduncle and the fornix and stria terminalis (Hashimoto, Srivastava, et al. 2011). Structural connectivity loss was identified in motor, limbic, association and callosal fiber tracts in carriers with FXTAS compared to controls, with greater age-related decline in connectivity in all tracts analysed (J. Y. Wang et al. 2012; Wang, Hessl, et al. 2013). Premutation carriers with FXTAS also showed significantly reduced diffusion-weighted signal compared to controls in the bilateral thalamus, caudate, putamen and right pallidus and significantly reduced diffusion-weighted signal compared to asymptomatic carriers in the bilateral putamen, right thalamus and left caudate (Wang, Hagerman, et al. 2013). In one study, the no significant differences in structural connectivity were identified between non-FXTAS carriers and controls, however connectivity strength of the superior cerebellar peduncles in premutation carriers without FXTAS exhibited a negative association with CGG repeat expansion length and *FMR1* mRNA levels. Structural connectivity measurements from the corpus callosum and superior cerebellar peduncles also showed a robust correlation with motor symptoms in all participants (Wang, Hessl, et al. 2013). Abnormalities at the MCPs were also indicated in carriers without FXTAS in a study showing

significant elevation in axial and radial diffusivities here, with an additional clear relationship between axial and radial diffusivity and CGG repeat size (Hashimoto, Srivastava, et al. 2011). Another study reported no significant alterations in structural fiber tractography in older carrier without FXTAS (J. Y. Wang et al. 2012). Given these results in carriers asymptomatic for FXTAS, we may expect analysis of DTI data in our sample to show no structural differences or some mild changes in connectivity or integrity at the MCPs. Previous correlative analyses indicate molecular and DTI measurement associations, so we may expect to see replication of relationships between imaging measurements at the MCPs, superior cerebellar peduncles and corpus callosum and CGG repeat size or *FMR1* mRNA expression levels. Our sample indicated significantly lower functional BOLD response in the motor task carriers compared to controls at the cerebellum, and an age-related reduction in activation in the temporo-parietal region, which we may predict to see reflected in a DTI analysis.

Another future investigation of interest would be into expression patterns of *FMR1* mRNA isoforms. It has been shown that in premutation carriers compared to age-matched control tissue all groups of *FMR1* mRNA isoforms are significantly increased in both peripheral blood mononuclear cell samples and derived brain tissue. The majority of isoform groups were approximately 2-fold higher in carriers, however isoforms *10* and *10b* were disproportionately increased up to 6-fold in premutation samples. Isoform transcript levels were also shown to correlate positively with increasingly large CGG repeat lengths (Pretto et al. 2015). Additionally, the skipping of Exon 12 (isoforms *7-12*) during transcription of *FMR1* is more frequent than its inclusion (isoforms *1-6*). It appears that inclusion of Exon 12 is greatly increased in the premutation compared to typical expression profiles. A developmental switch, demonstrated in the developing mouse brain, chiefly involving the presence or absence of Exon 12, is suggestive of a shift in the RNA-binding properties of FMRP during neural development (Brackett et al. 2013). A future question of interest is therefore whether isoform expression patterns, in particular the large relative increases in the skipping of Exon 12 and isoforms *10* and *10b*, are related to measures related to neurodegeneration, such as loss of brain connectivity and integrity as measured by DTI or motor symptoms. Isoform expression profiles may also be reflective of neurodevelopmental traits also, given the role of developmental switching in the transcript expression patterns.

The further development and validation of Western blotting techniques for FMRP quantification is also a relevant future direction of the current research. Western blotting has previously been reported as an effective method of measuring FMRP levels against a GAPDH loading control using peripheral blood mononuclear cell and lymphocyte clinical samples in the study of the Fragile X full mutation (Pretto et al. 2014; LaFauci et al. 2013). As previously mentioned however, the blots in the current study revealed multiple bands ranging from 10-100kDa molecular weight of unknown origin. To make steps to further validate and characterise the nature of this method, control samples should be run in the future under tightly controlled venepuncture and storage circumstances, where sample

processing and freezing is immediate. Subsequent Western blotting of these samples should reveal whether extra banding has resulted from partial sample degradation, and human-derived sample handling can be informed by this in later clinical research.

The *FMR1* premutation gene also produces RAN protein products, the most toxic among them being FMRpolyG, which possesses the translated CGG repeat region as a repetitive glycine amino acid chain in the protein (Todd et al. 2013). Large, ubiquitinated aggregates found throughout the brain and brainstems of FXTAS patients appear to strongly implicate a role for protein-mediated neurodegeneration. FMRpolyG is seen to aggregate in FXTAS fly and mouse models as well as in human autopsy tissue, especially in the hippocampus, frontal cortex and cerebellum, strongly suggesting a role in the development and progression of FXTAS pathology (Cleary & Ranum 2014). To date, RAN translation of the *FMR1* gene has not been investigated in a clinical setting, mainly due to fact that the strong propensity of FMRpolyG to aggregate causes inefficient quantification using Western blotting and ELISA and anti-FMRpolyG antibodies are not recommended for these methodological uses at this time. The development of an FMRpolyG specific antibody in the future however that is effective in Western blotting and ELISA techniques may allow for accurate FMRpolyG quantification in prospective clinical research, and its role in premutation and FXTAS humans can be characterised more thoroughly. Alternatively, mass spectrometry is an effective method that may be used currently to examine the presence of FMRpolyG in human-derived samples (Cleary & Ranum 2014).

Structural equation modelling is a statistical technique that has been employed in multiple psychiatrically- and psychologically-based studies to elucidate effect sizes and associations between multiple variables (Whalley et al. 2013; Hart et al. 2005). This type of analysis would fit well with the neurodevelopmental hypotheses of the *FMR1* premutation, as here we present numerous neuropsychological, psychiatric and molecular measures in our sample that are likely interconnected, however links and effect sizes are not established between these variables. A structural equation model may aid in identifying which variables are associated, and whether measurements of FMRP and CGG repeat length influence neurodevelopmental traits. However, the sample size in the present study is relatively small compared to some cohorts analysed using structural equation modelling and the sample size requirement is not satisfied as reported by evaluations of power and bias for this type of investigation (Wolf et al. 2013). As addressed previously, environmental factors have a large influence on neuropsychiatric manifestations, and individuals with the premutation may be particularly vulnerable to the effects of environmental influences and stressors (Seltzer et al. 2012). The participant groups for this study were all consented for future follow-up contact, and it therefore would be possible and relatively simple to utilise self-report measures to obtain information about medical co-morbidities, socio-economic background and environmental stressors which could be added to a potential structural equation model. This would allow for a novel analysis in a premutation

cohort to examine the interactions between *FMR1* molecular function, psychiatric and neuropsychological traits and environmental influence.

Second hit hypotheses are commonly cited in the study of neuropsychiatric disorders (Bonnet-Brilhault et al. 2016; Jozwiak & Jozwiak 2005). A recent pilot study has also revealed a possible role of second genetic variant hits in the manifestation of premutation carrier phenotypes. The study identified that additional copy number variants, both deleterious and duplicative, located at 10q26 and Xp22.3 and not seen in any individuals in the control group, were more commonly observed in carriers with neurological involvement and ASD (Lozano, Hagerman, et al. 2014). These results suggest that genetic hits secondary to the *FMR1* CGG repeat expansion may instigate more severe neurodevelopmental and neurological phenotypes. Further study in this area, utilising genome-wide mapping or focussed investigation of psychiatrically implicated gene groups, may reveal further support for this hypothesis.

10.3 Concluding remarks

Significant differences between carrier and control groups during a finger-tapping task demonstrated diminished cerebellar activity when responding to increased motor-related demand. In addition, group x age interaction analyses for this task revealed that carriers deviate from compensatory activation in response to higher task demand displayed during normative aging. Motor symptom measurements also reveal that carriers have significantly worse but sub-clinical tremor and co-ordination than observed in the control group and molecular measures of *FMR1* mRNA are increased in carriers but not significantly so. We presently report the first motor fMRI task carried out in a premutation carrier group, and our results show neuroimaging and clinical indications of possible neurodegeneration prior to overt FXTAS onset.

Premutation carriers displayed a significantly attenuated response in the visual and superior parietal regions to arousing stimuli during an emotional processing task compared to controls, and group x age interaction analyses revealed differences to be stable in this cross-sectional sample. Moreover, recognition of emotive faces was significantly poorer in carriers, which is suggestive of impairment to the neurotypical response to and detection of emotional arousal. As expected, psychiatric symptomatology in premutation carriers was also significantly higher than in controls. Social judgement and empathy scores were comparative between the carrier and control group, despite carriers showing significantly more autistic traits, indicative of a non-classical ASD presentation without impairment of social perception and responsiveness in carriers. FMRP levels also appear to be similar between the groups. Overall here, we report new findings of altered emotional, neuropsychological and psychiatric states in premutation carriers and our results are supportive of the hypotheses that carriers exhibit neurodevelopmental traits throughout their life-span in addition to FXTAS-related neurodegeneration.

The findings of this study are in keeping with hypotheses of primarily separate mechanisms of altered brain development and degeneration in *FMR1* premutation carriers.

Chapter 11: References

Adams, J.S. et al., 2007. Volumetric brain changes in females with fragile X-associated tremor/ataxia syndrome (FXTAS). *Neurology*, 69(9), pp.851–9. Available at: http://www.ncbi.nlm.nih.gov/pubmed/17724287 [Accessed April 30, 2016].

Adams, P.E. et al., 2010. Psychological symptoms correlate with reduced hippocampal volume in fragile X premutation carriers. *American journal of medical genetics. Part B, Neuropsychiatric genetics : the official publication of the International Society of Psychiatric Genetics*, 153B(3), pp.775–85. Available at: http://www.ncbi.nlm.nih.gov/pubmed/19908235 [Accessed April 29, 2016].

Aguilar, D. et al., 2008. A quantitative assessment of tremor and ataxia in FMR1 premutation carriers using CATSYS. *American journal of medical genetics. Part A*, 146A(5), pp.629–35. Available at: http://doi.wiley.com/10.1002/ajmg.a.32211 [Accessed January 23, 2017].

Allen, E.G. et al., 2008a. Detection of early FXTAS motor symptoms using the CATSYS computerised neuromotor test battery. *Journal of Medical Genetics*, 45(5), pp.290–297. Available at: http://jmg.bmj.com/cgi/doi/10.1136/jmg.2007.054676 [Accessed January 6, 2017].

Allen, E.G. et al., 2008b. Detection of early FXTAS motor symptoms using the CATSYS computerised neuromotor test battery. *Journal of medical genetics*, 45(5), pp.290–7. Available at: http://jmg.bmj.com/cgi/doi/10.1136/jmg.2007.054676 [Accessed January 6, 2017].

Allen, E.G. et al., 2005. Examination of the effect of the polymorphic CGG repeat in the FMR1 gene on cognitive performance. *Behavior genetics*, 35(4), pp.435–45. Available at: http://link.springer.com/10.1007/s10519-005-2792-4 [Accessed January 17, 2017].

Apartis, E. et al., 2012. FXTAS: New insights and the need for revised diagnostic criteria. *Neurology*, 79(18), pp.1898–1907. Available at: http://www.ncbi.nlm.nih.gov/pubmed/23077007 [Accessed February 17, 2017].

Ashley, C.T. et al., 1993. FMR1 protein: conserved RNP family domains and selective RNA binding. *Science (New York, N.Y.)*, 262(5133), pp.563–6. Available at: http://www.ncbi.nlm.nih.gov/pubmed/7692601 [Accessed April 7, 2017].

Assaf, Y. & Pasternak, O., 2008. Diffusion Tensor Imaging (DTI)-based White Matter Mapping in Brain Research: A Review. *Journal of Molecular Neuroscience*, 34(1), pp.51–61. Available at: http://www.ncbi.nlm.nih.gov/pubmed/18157658 [Accessed January 8, 2017].

Aziz, M. et al., 2003. Clinical features of boys with fragile X premutations and intermediate alleles. *American Journal of Medical Genetics*, 121B(1), pp.119–127. Available at:

http://doi.wiley.com/10.1002/ajmg.b.20030 [Accessed April 5, 2017].

Bacalman, S. et al., 2006. Psychiatric phenotype of the fragile X-associated tremor/ataxia syndrome (FXTAS) in males: newly described fronto-subcortical dementia. *The Journal of clinical psychiatry*, 67(1), pp.87–94. Available at: http://www.ncbi.nlm.nih.gov/pubmed/16426093 [Accessed April 27, 2016].

Bailey, D.B. et al., 2008. Co-occurring conditions associated with *FMR1* gene variations: Findings from a national parent survey. *American Journal of Medical Genetics Part A*, 146A(16), pp.2060–2069. Available at: http://www.ncbi.nlm.nih.gov/pubmed/18570292 [Accessed April 4, 2017].

Baron-Cohen, S. et al., 2001. The autism-spectrum quotient (AQ): evidence from Asperger syndrome/high-functioning autism, males and females, scientists and mathematicians. *Journal of autism and developmental disorders*, 31(1), pp.5–17. Available at: http://www.ncbi.nlm.nih.gov/pubmed/11439754 [Accessed January 17, 2017].

Baron-Cohen, S. & Wheelwright, S., 2004. The empathy quotient: an investigation of adults with Asperger syndrome or high functioning autism, and normal sex differences. *Journal of autism and developmental disorders*, 34(2), pp.163–75. Available at: http://www.ncbi.nlm.nih.gov/pubmed/15162935 [Accessed January 20, 2017].

Bartenstein, P. et al., 1997. Central motor processing in Huntington's disease. A PET study. *Brain : a journal of neurology*, pp.1553–67. Available at: http://www.ncbi.nlm.nih.gov/pubmed/9313639 [Accessed January 11, 2017].

Battistella, G. et al., 2013. Brain structure in asymptomatic FMR1 premutation carriers at risk for fragile X-associated tremor/ataxia syndrome. *Neurobiology of aging*, 34(6), pp.1700–7. Available at: http://www.ncbi.nlm.nih.gov/pubmed/23298734 [Accessed April 30, 2016].

Berns, G.S., Song, A.W. & Mao, H., Continuous Functional Magnetic Resonance Imaging Reveals Dynamic Nonlinearities of " Dose–Response " Curves for Finger Opposition.

Berry-Kravis, E., Abrams, L., et al., 2007. Fragile X-associated tremor/ataxia syndrome: clinical features, genetics, and testing guidelines. *Movement disorders : official journal of the Movement Disorder Society*, 22(14), p.2018–30, quiz 2140. Available at: http://www.ncbi.nlm.nih.gov/pubmed/17618523 [Accessed April 27, 2016].

Berry-Kravis, E., Goetz, C.G., et al., 2007. Neuropathic features in fragile X premutation carriers. *American journal of medical genetics. Part A*, 143A(1), pp.19–26. Available at: http://www.ncbi.nlm.nih.gov/pubmed/17152065 [Accessed April 27, 2016].

Berry-Kravis, E. & Hall, D.A., 2011. Executive dysfunction in young FMR1 premutation carriers: forme fruste of FXTAS or new phenotype? *Neurology*, 77(7), pp.612–3. Available at: http://www.ncbi.nlm.nih.gov/pubmed/21775737 [Accessed May 3, 2016].

Besterman, A.D. et al., 2014. Towards an Understanding of Neuropsychiatric Manifestations in Fragile X Premutation Carriers. *Future neurology*, 9(2), pp.227–239. Available at: http://www.ncbi.nlm.nih.gov/pubmed/25013385 [Accessed April 27, 2016].

Bigler, E.D., 2015. Structural Image Analysis of the Brain in Neuropsychology Using Magnetic Resonance Imaging (MRI) Techniques. *Neuropsychology Review*, 25(3), pp.224–249. Available at: http://www.ncbi.nlm.nih.gov/pubmed/26280751 [Accessed January 8, 2017].

Bonnet-Brilhault, F. et al., 2016. GABA/Glutamate synaptic pathways targeted by integrative genomic and electrophysiological explorations distinguish autism from intellectual disability. *Molecular Psychiatry*, 21(3), pp.411–418. Available at: http://www.ncbi.nlm.nih.gov/pubmed/26055424 [Accessed April 11, 2017].

Bonnet, L. et al., 2015. The role of the amygdala in the perception of positive emotions: an "intensity detector". *Frontiers in behavioral neuroscience*, 9, p.178. Available at: http://www.ncbi.nlm.nih.gov/pubmed/26217205 [Accessed January 16, 2017].

Boraxbekk, C.J., Hagkvist, F. & Lindner, P., 2016. Motor and mental training in older people: Transfer, interference, and associated functional neural responses. *Neuropsychologia*, 89, pp.371–7. Available at: http://linkinghub.elsevier.com/retrieve/pii/S0028393216302640 [Accessed January 12, 2017].

Bourgeois, J.A. et al., Cognitive, anxiety and mood disorders in the fragile X-associated tremor/ataxia syndrome. *General hospital psychiatry*, 29(4), pp.349–56. Available at: http://www.ncbi.nlm.nih.gov/pubmed/17591512 [Accessed April 27, 2016].

Bourgeois, J.A. et al., 2006. Dementia with mood symptoms in a fragile X premutation carrier with the fragile X-associated tremor/ataxia syndrome: clinical intervention with donepezil and venlafaxine. *The Journal of neuropsychiatry and clinical neurosciences*, 18(2), pp.171–7. Available at: http://www.ncbi.nlm.nih.gov/pubmed/16720793 [Accessed April 27, 2016].

Bourgeois, J.A. et al., 2011. Lifetime prevalence of mood and anxiety disorders in fragile X premutation carriers. *The Journal of clinical psychiatry*, 72(2), pp.175–82. Available at: http://www.ncbi.nlm.nih.gov/pubmed/20816038 [Accessed April 27, 2016].

Braak, H. & Braak, E., 1991. Neuropathological stageing of Alzheimer-related changes. *Acta neuropathologica*, 82(4), pp.239–59. Available at: http://www.ncbi.nlm.nih.gov/pubmed/1759558 [Accessed December 30, 2016].

Brackett, D.M. et al., 2013. FMR1 transcript isoforms: association with polyribosomes; regional and developmental expression in mouse brain. D. L. Silver, ed. *PloS one*, 8(3), p.e58296. Available at: http://dx.plos.org/10.1371/journal.pone.0058296 [Accessed February 24, 2017].

Bradley, M.M. et al., 2003. Activation of the visual cortex in motivated attention. *Behavioral neuroscience*, 117(2), pp.369–80. Available at: http://www.ncbi.nlm.nih.gov/pubmed/12708533 [Accessed January 17, 2017].

Brasa, S. et al., 2016. Reciprocal changes in DNA methylation and hydroxymethylation and a broad repressive epigenetic switch characterize FMR1 transcriptional silencing in fragile X syndrome. *Clinical epigenetics*, 8, p.15. Available at: http://www.ncbi.nlm.nih.gov/pubmed/26855684 [Accessed January 10, 2017].

Brega, A.G. et al., 2008. The primary cognitive deficit among males with fragile X-associated tremor/ataxia syndrome (FXTAS) is a dysexecutive syndrome. *Journal of clinical and experimental neuropsychology*, 30(8), pp.853–69. Available at: http://www.ncbi.nlm.nih.gov/pubmed/18608667 [Accessed April 27, 2016].

Broersma, M. et al., 2016. Bilateral cerebellar activation in unilaterally challenged essential tremor. *NeuroImage. Clinical*, 11, pp.1–9. Available at: http://linkinghub.elsevier.com/retrieve/pii/S2213158215300504 [Accessed February 20, 2017].

Brunberg, J.A. et al., 2002. Fragile X premutation carriers: characteristic MR imaging findings of adult male patients with progressive cerebellar and cognitive dysfunction. *AJNR. American journal of neuroradiology*, 23(10), pp.1757–66. Available at: http://www.ncbi.nlm.nih.gov/pubmed/12427636 [Accessed April 29, 2016].

Buijink, A.W.G. et al., 2015. Motor network disruption in essential tremor: a functional and effective connectivity study. *Brain*, 138(10), pp.2934–2947. Available at: http://www.ncbi.nlm.nih.gov/pubmed/26248468 [Accessed December 30, 2016].

Buxton, R.B., 2013. The physics of functional magnetic resonance imaging (fMRI). *Reports on Progress in Physics*, 76(9), p.96601. Available at: http://www.ncbi.nlm.nih.gov/pubmed/24006360 [Accessed January 8, 2017].

Capelli, L.P. et al., 2010. The fragile x-associated tremor and ataxia syndrome (FXTAS). *Arquivos de Neuro-Psiquiatria*, 68(5), pp.791–798. Available at: http://www.scielo.br/scielo.php?script=sci_arttext&pid=S0004-282X2010000500023&lng=en&nrm=iso&tlng=en [Accessed February 17, 2017].

Chonchaiya, W. et al., 2012. Increased prevalence of seizures in boys who were probands with the FMR1 premutation and co-morbid autism spectrum disorder. *Human Genetics*, 131(4), pp.581–

589. Available at: http://www.ncbi.nlm.nih.gov/pubmed/22001913 [Accessed April 4, 2017].

Cleary, J.D. & Ranum, L.P.W., 2014. Repeat associated non-ATG (RAN) translation: new starts in microsatellite expansion disorders. *Current opinion in genetics & development*, 26, pp.6–15. Available at: http://linkinghub.elsevier.com/retrieve/pii/S0959437X14000082 [Accessed January 24, 2017].

Coffey, S.M. et al., 2008. Expanded clinical phenotype of women with the FMR1 premutation. *American journal of medical genetics. Part A*, 146A(8), pp.1009–16. Available at: http://www.ncbi.nlm.nih.gov/pubmed/18348275 [Accessed April 27, 2016].

Cohen, S. et al., 2006. Molecular and imaging correlates of the fragile X-associated tremor/ataxia syndrome. *Neurology*, 67(8), pp.1426–31. Available at: http://www.ncbi.nlm.nih.gov/pubmed/17060569 [Accessed April 29, 2016].

Cornish, K. et al., 2005. The emerging fragile X premutation phenotype: evidence from the domain of social cognition. *Brain and cognition*, 57(1), pp.53–60. Available at: http://www.ncbi.nlm.nih.gov/pubmed/15629215 [Accessed April 27, 2016].

Cornish, K.M. et al., 2008. Age-dependent cognitive changes in carriers of the fragile X syndrome. *Cortex; a journal devoted to the study of the nervous system and behavior*, 44(6), pp.628–36. Available at: http://www.ncbi.nlm.nih.gov/pubmed/18472033 [Accessed April 27, 2016].

Danish Product Development Ltd., *CATSYS 2000 User's Manual*,

Deiber, M.P. et al., 1993. Thalamic stimulation and suppression of parkinsonian tremor. Evidence of a cerebellar deactivation using positron emission tomography. *Brain : a journal of neurology*, pp.267–79. Available at: http://www.ncbi.nlm.nih.gov/pubmed/8453462 [Accessed January 11, 2017].

Desmond, J.E. & Glover, G.H., 2002. Estimating sample size in functional MRI (fMRI) neuroimaging studies: statistical power analyses. *Journal of neuroscience methods*, 118(2), pp.115–28. Available at: http://www.ncbi.nlm.nih.gov/pubmed/12204303 [Accessed February 21, 2017].

Dombrowski, C. et al., 2002. Premutation and intermediate-size FMR1 alleles in 10572 males from the general population: loss of an AGG interruption is a late event in the generation of fragile X syndrome alleles. *Human molecular genetics*, 11(4), pp.371–8. Available at: http://www.ncbi.nlm.nih.gov/pubmed/11854169 [Accessed April 27, 2016].

Dorn, M.B., Mazzocco, M.M. & Hagerman, R.J., 1994. Behavioral and psychiatric disorders in adult male carriers of fragile X. *Journal of the American Academy of Child and Adolescent Psychiatry*, 33(2), pp.256–64. Available at:

http://linkinghub.elsevier.com/retrieve/pii/S0890856709644920 [Accessed January 16, 2017].

Duarte, J.V. et al., 2016. Parametric fMRI of paced motor responses uncovers novel whole-brain imaging biomarkers in spinocerebellar ataxia type 3. *Human Brain Mapping*, 37(10), pp.3656–3668. Available at: http://www.ncbi.nlm.nih.gov/pubmed/27273236 [Accessed January 11, 2017].

Eklund, A. et al., 2012. Does parametric fMRI analysis with SPM yield valid results?—An empirical study of 1484 rest datasets. *NeuroImage*, 61(3), pp.565–578. Available at: http://www.ncbi.nlm.nih.gov/pubmed/22507229 [Accessed February 23, 2017].

Eklund, A., Nichols, T.E. & Knutsson, H., 2016. Cluster failure: Why fMRI inferences for spatial extent have inflated false-positive rates. *Proceedings of the National Academy of Sciences*, 113(28), pp.7900–7905. Available at: http://www.ncbi.nlm.nih.gov/pubmed/27357684 [Accessed January 8, 2017].

Eshed, I. et al., 2007. Claustrophobia and premature termination of magnetic resonance imaging examinations. *Journal of Magnetic Resonance Imaging*, 26(2), pp.401–404. Available at: http://www.ncbi.nlm.nih.gov/pubmed/17610281 [Accessed January 8, 2017].

Fatori, D. et al., 2013. Influence of psychosocial risk factors on the trajectory of mental health problems from childhood to adolescence: a longitudinal study. *BMC Psychiatry*, 13(1), p.31. Available at: http://www.ncbi.nlm.nih.gov/pubmed/23327711 [Accessed April 6, 2017].

Franke, P. et al., 1998. Genotype-phenotype relationship in female carriers of the premutation and full mutation of FMR-1. *Psychiatry research*, 80(2), pp.113–27. Available at: http://www.ncbi.nlm.nih.gov/pubmed/9754690 [Accessed April 27, 2016].

Garcia-Arocena, D. & Hagerman, P.J., 2010. Advances in understanding the molecular basis of FXTAS. *Human molecular genetics*, 19(R1), pp.R83-9. Available at: http://www.ncbi.nlm.nih.gov/pubmed/20430935 [Accessed May 3, 2016].

Garin-Muga, A. & Borro, D., 2014. Review and Challenges of Brain Analysis through DTI Measurements. *Studies in health technology and informatics*, 207, pp.27–36. Available at: http://www.ncbi.nlm.nih.gov/pubmed/25488208 [Accessed January 8, 2017].

Glover, G.H., 2011. Overview of Functional Magnetic Resonance Imaging. *Neurosurgery Clinics of North America*, 22(2), pp.133–139. Available at: http://www.ncbi.nlm.nih.gov/pubmed/21435566 [Accessed January 8, 2017].

Gountouna, V.-E. et al., 2010. Functional Magnetic Resonance Imaging (fMRI) reproducibility and variance components across visits and scanning sites with a finger tapping task. *NeuroImage*,

49(1), pp.552–560. Available at: http://www.ncbi.nlm.nih.gov/pubmed/19631757 [Accessed January 23, 2017].

Greco, C.M. et al., 2002. Neuronal intranuclear inclusions in a new cerebellar tremor/ataxia syndrome among fragile X carriers. *Brain : a journal of neurology*, 125(Pt 8), pp.1760–71. Available at: http://www.ncbi.nlm.nih.gov/pubmed/12135967 [Accessed January 5, 2017].

Greco, C.M. et al., 2005. Neuropathology of fragile X-associated tremor/ataxia syndrome (FXTAS). *Brain*, 129(1), pp.243–255. Available at: http://www.ncbi.nlm.nih.gov/pubmed/16332642 [Accessed January 5, 2017].

Greco, C.M. et al., 2006. Neuropathology of fragile X-associated tremor/ataxia syndrome (FXTAS). *Brain : a journal of neurology*, 129(Pt 1), pp.243–55. Available at: http://brain.oxfordjournals.org/cgi/doi/10.1093/brain/awh683 [Accessed January 6, 2017].

Grigsby, J. et al., 2007. Impairment of executive cognitive functioning in males with fragile X-associated tremor/ataxia syndrome. *Movement Disorders*, 22(5).

Grodd, W. et al., 2001. Sensorimotor mapping of the human cerebellum: fMRI evidence of somatotopic organization. *Human Brain Mapping*, 13(2), pp.55–73. Available at: http://doi.wiley.com/10.1002/hbm.1025 [Accessed January 27, 2017].

De Guio, F. et al., 2012. Functional magnetic resonance imaging study comparing rhythmic finger tapping in children and adults. *Pediatric neurology*, 46(2), pp.94–100. Available at: http://www.ncbi.nlm.nih.gov/pubmed/22264703 [Accessed January 27, 2017].

Hägele, C. et al., 2016. Affective responses across psychiatric disorders-A dimensional approach. *Neuroscience letters*, 623, pp.71–8. Available at: http://linkinghub.elsevier.com/retrieve/pii/S0304394016302506 [Accessed January 16, 2017].

Hagerman, P.J. & Hagerman, R.J., 2004. The fragile-X premutation: a maturing perspective. *American journal of human genetics*, 74(5), pp.805–16. Available at: http://www.ncbi.nlm.nih.gov/pubmed/15052536 [Accessed May 3, 2016].

Hagerman, R. & Hagerman, P., 2013. Advances in clinical and molecular understanding of the FMR1 premutation and fragile X-associated tremor/ataxia syndrome. *The Lancet. Neurology*, 12(8), pp.786–98. Available at: http://www.ncbi.nlm.nih.gov/pubmed/23867198 [Accessed April 27, 2016].

Hagerman, R.J. et al., 2004. Fragile-X-associated tremor/ataxia syndrome (FXTAS) in females with the FMR1 premutation. *American journal of human genetics*, 74(5), pp.1051–6. Available at: http://www.ncbi.nlm.nih.gov/pubmed/15065016 [Accessed April 27, 2016].

Hagerman, R.J. et al., 2001. Intention tremor, parkinsonism, and generalized brain atrophy in male carriers of fragile X. *Neurology*, 57(1), pp.127–30. Available at: http://www.ncbi.nlm.nih.gov/pubmed/11445641 [Accessed April 27, 2016].

Hagerman, R.J. & Hagerman, P., 2016. Fragile X-associated tremor/ataxia syndrome — features, mechanisms and management. *Nature Reviews Neurology*, 12(7), pp.403–412. Available at: http://www.ncbi.nlm.nih.gov/pubmed/27340021 [Accessed January 8, 2017].

Hall, D.A. et al., 2005. Initial diagnoses given to persons with the fragile X associated tremor/ataxia syndrome (FXTAS). *Neurology*, 65(2), pp.299–301. Available at: http://www.ncbi.nlm.nih.gov/pubmed/16043804 [Accessed April 27, 2016].

Hall, D.A. et al., 2006. Symptomatic treatment in the fragile X-associated tremor/ataxia syndrome. *Movement disorders : official journal of the Movement Disorder Society*, 21(10), pp.1741–4. Available at: http://www.ncbi.nlm.nih.gov/pubmed/16773616 [Accessed April 27, 2016].

Hall, J. et al., 2004. Social cognition and face processing in schizophrenia. *The British Journal of Psychiatry*, 185(2). Available at: http://bjp.rcpsych.org/content/185/2/169/F1 [Accessed May 10, 2017].

Harlow, E.G. et al., 2010. Critical period plasticity is disrupted in the barrel cortex of FMR1 knockout mice. *Neuron*, 65(3), pp.385–98. Available at: http://www.ncbi.nlm.nih.gov/pubmed/20159451 [Accessed January 10, 2017].

Hart, C.L. et al., 2005. Childhood IQ of parents related to characteristics of their offspring: linking the Scottish Mental Survey 1932 to the Midspan Family Study. *Journal of biosocial science*, 37(5), pp.623–39. Available at: http://www.journals.cambridge.org/abstract_S0021932004006923 [Accessed April 10, 2017].

Hashimoto, R., Javan, A.K., et al., 2011. A voxel-based morphometry study of grey matter loss in fragile X-associated tremor/ataxia syndrome. *Brain : a journal of neurology*, 134(Pt 3), pp.863–78. Available at: http://www.ncbi.nlm.nih.gov/pubmed/21354978 [Accessed April 30, 2016].

Hashimoto, R., Backer, K.C., et al., 2011. An fMRI study of the prefrontal activity during the performance of a working memory task in premutation carriers of the fragile X mental retardation 1 gene with and without fragile X-associated tremor/ataxia syndrome (FXTAS). *Journal of psychiatric research*, 45(1), pp.36–43. Available at: http://www.ncbi.nlm.nih.gov/pubmed/20537351 [Accessed April 29, 2016].

Hashimoto, R., Srivastava, S., et al., 2011. Diffusion tensor imaging in male premutation carriers of the fragile X mental retardation gene. *Movement disorders : official journal of the Movement Disorder Society*, 26(7), pp.1329–36. Available at:

http://www.ncbi.nlm.nih.gov/pubmed/21484870 [Accessed April 29, 2016].

Hayasaka, S. et al., 2007. Power and sample size calculation for neuroimaging studies by non-central random field theory. *NeuroImage*, 37(3), pp.721–30. Available at: http://www.ncbi.nlm.nih.gov/pubmed/17658273 [Accessed February 21, 2017].

Hessl, D. et al., 2005. Abnormal elevation of FMR1 mRNA is associated with psychological symptoms in individuals with the fragile X premutation. *American journal of medical genetics. Part B, Neuropsychiatric genetics : the official publication of the International Society of Psychiatric Genetics*, 139B(1), pp.115–21. Available at: http://www.ncbi.nlm.nih.gov/pubmed/16184602 [Accessed April 27, 2016].

Hessl, D. et al., 2007. Amygdala dysfunction in men with the fragile X premutation. *Brain : a journal of neurology*, 130(Pt 2), pp.404–16. Available at: http://www.ncbi.nlm.nih.gov/pubmed/17166860 [Accessed April 29, 2016].

Hessl, D. et al., 2011. Decreased fragile X mental retardation protein expression underlies amygdala dysfunction in carriers of the fragile X premutation. *Biological psychiatry*, 70(9), pp.859–65. Available at: http://www.ncbi.nlm.nih.gov/pubmed/21783174 [Accessed April 29, 2016].

Hinds, H.L. et al., 1993. Tissue specific expression of FMR-1 provides evidence for a functional role in fragile X syndrome. *Nature genetics*, 3(1), pp.36–43. Available at: http://www.nature.com/doifinder/10.1038/ng0193-36 [Accessed January 5, 2017].

Hochgräfe, K., Sydow, A. & Mandelkow, E.-M., 2013. Regulatable transgenic mouse models of Alzheimer disease: onset, reversibility and spreading of Tau pathology. *FEBS Journal*, 280(18), pp.4371–4381. Available at: http://www.ncbi.nlm.nih.gov/pubmed/23517246 [Accessed December 30, 2016].

Hunter, J., Rohr, J. & Sherman, S., 2010. Co-occurring diagnoses among *FMR1* premutation allele carriers. *Clinical Genetics*, 77(4), pp.374–381. Available at: http://www.ncbi.nlm.nih.gov/pubmed/20059484 [Accessed April 6, 2017].

Hutchinson, S. et al., 2002. Age-related differences in movement representation. *NeuroImage*, 17(4), pp.1720–8. Available at: http://www.ncbi.nlm.nih.gov/pubmed/12498746 [Accessed January 12, 2017].

Indlekofer, F. et al., 2009. Reduced memory and attention performance in a population-based sample of young adults with a moderate lifetime use of cannabis, ecstasy and alcohol. *Journal of Psychopharmacology*, 23(5), pp.495–509. Available at: http://www.ncbi.nlm.nih.gov/pubmed/18635709 [Accessed April 6, 2017].

Ismail, Z. et al., 2016. Neuropsychiatric symptoms as early manifestations of emergent dementia: Provisional diagnostic criteria for mild behavioral impairment. *Alzheimer's & dementia : the journal of the Alzheimer's Association*, 12(2), pp.195–202. Available at: http://www.ncbi.nlm.nih.gov/pubmed/26096665 [Accessed January 10, 2017].

Iwahashi, C. et al., 2009. A quantitative ELISA assay for the fragile x mental retardation 1 protein. *The Journal of molecular diagnostics : JMD*, 11(4), pp.281–9. Available at: http://www.pubmedcentral.nih.gov/articlerender.fcgi?artid=2710703&tool=pmcentrez&rendertype=abstract.

Jacquemont, S. et al., 2004. Aging in individuals with the FMR1 mutation. *American journal of mental retardation : AJMR*, 109(2), pp.154–64. Available at: http://www.ncbi.nlm.nih.gov/pubmed/15000674 [Accessed January 16, 2017].

Jacquemont, S. et al., 2003a. Fragile X premutation tremor/ataxia syndrome: molecular, clinical, and neuroimaging correlates. *American journal of human genetics*, 72(4), pp.869–78. Available at: http://www.ncbi.nlm.nih.gov/pubmed/12638084 [Accessed April 27, 2016].

Jacquemont, S. et al., 2003b. Fragile X premutation tremor/ataxia syndrome: molecular, clinical, and neuroimaging correlates. *American journal of human genetics*, 72(4), pp.869–78. Available at: http://www.ncbi.nlm.nih.gov/pubmed/12638084 [Accessed April 29, 2016].

Jacquemont, S. et al., 2004. Penetrance of the fragile X-associated tremor/ataxia syndrome in a premutation carrier population. *JAMA*, 291(4), pp.460–9. Available at: http://www.ncbi.nlm.nih.gov/pubmed/14747503 [Accessed April 28, 2016].

Jozwiak, J. & Jozwiak, S., 2005. Giant Cells: Contradiction to Two-Hit Model of Tuber Formation? *Cellular and Molecular Neurobiology*, 25(5), pp.795–806. Available at: http://www.ncbi.nlm.nih.gov/pubmed/16133934 [Accessed April 11, 2017].

Juncos, J.L. et al., 2011. New clinical findings in the fragile X-associated tremor ataxia syndrome (FXTAS). *Neurogenetics*, 12(2), pp.123–35. Available at: http://www.ncbi.nlm.nih.gov/pubmed/21279400 [Accessed April 29, 2016].

Kandiah, N. et al., 2014. Hippocampal volume and white matter disease in the prediction of dementia in Parkinson's disease. *Parkinsonism & related disorders*, 20(11), pp.1203–8. Available at: http://linkinghub.elsevier.com/retrieve/pii/S1353802014003228 [Accessed January 8, 2017].

Kazui, H. et al., 2016. Differences of Behavioral and Psychological Symptoms of Dementia in Disease Severity in Four Major Dementias. *PloS one*, 11(8), p.e0161092. Available at: http://www.ncbi.nlm.nih.gov/pubmed/27536962 [Accessed January 10, 2017].

Kenneson, A. et al., 2001. Reduced FMRP and increased FMR1 transcription is proportionally associated with CGG repeat number in intermediate-length and premutation carriers. *Human molecular genetics*, 10(14), pp.1449–54. Available at: http://www.ncbi.nlm.nih.gov/pubmed/11448936 [Accessed February 17, 2017].

Keysor, C.S. & Mazzocco, M.M.M., 2002. A developmental approach to understanding Fragile X syndrome in females. *Microscopy research and technique*, 57(3), pp.179–86. Available at: http://www.ncbi.nlm.nih.gov/pubmed/12112455 [Accessed April 28, 2016].

Khalil, A.M. et al., 2008. A novel RNA transcript with antiapoptotic function is silenced in fragile X syndrome. V. Bajic, ed. *PloS one*, 3(1), p.e1486. Available at: http://dx.plos.org/10.1371/journal.pone.0001486 [Accessed January 5, 2017].

Kim, S.-Y. et al., 2014. Altered neural activity in the "when" pathway during temporal processing in fragile X premutation carriers. *Behavioural brain research*, 261, pp.240–8. Available at: http://www.ncbi.nlm.nih.gov/pubmed/24398265 [Accessed April 12, 2017].

Kim, S.-Y. et al., 2013. Altered neural activity of magnitude estimation processing in adults with the fragile X premutation. *Journal of psychiatric research*, 47(12), pp.1909–16. Available at: http://www.ncbi.nlm.nih.gov/pubmed/24045061 [Accessed April 29, 2016].

Klengel, T. & Binder, E.B., 2015. Epigenetics of Stress-Related Psychiatric Disorders and Gene × Environment Interactions. *Neuron*, 86(6), pp.1343–1357. Available at: http://www.ncbi.nlm.nih.gov/pubmed/26087162 [Accessed April 6, 2017].

Kloppel, S. et al., 2009. Functional compensation of motor function in pre-symptomatic Huntington's disease. *Brain*, 132(6), pp.1624–1632. Available at: http://brain.oxfordjournals.org/cgi/doi/10.1093/brain/awp081 [Accessed January 11, 2017].

Kohno, S. et al., 2015. Emotional discrimination during viewing unpleasant pictures: timing in human anterior ventrolateral prefrontal cortex and amygdala. *Frontiers in human neuroscience*, 9, p.51. Available at: http://www.ncbi.nlm.nih.gov/pubmed/25713527 [Accessed January 16, 2017].

Koldewyn, K. et al., 2008. Reduced Hippocampal Activation During Recall is Associated with Elevated FMR1 mRNA and Psychiatric Symptoms in Men with the Fragile X Premutation. *Brain imaging and behavior*, 2(2), pp.105–116. Available at: http://www.ncbi.nlm.nih.gov/pubmed/19430586 [Accessed April 29, 2016].

Ladd, P.D. et al., 2007. An antisense transcript spanning the CGG repeat region of FMR1 is upregulated in premutation carriers but silenced in full mutation individuals. *Human molecular genetics*, 16(24), pp.3174–87. Available at: http://www.ncbi.nlm.nih.gov/pubmed/17921506 [Accessed May 3, 2016].

LaFauci, G. et al., 2016. Detection and Quantification of the Fragile X Mental Retardation Protein 1 (FMRP). *Genes*, 7(12), p.121. Available at: http://www.ncbi.nlm.nih.gov/pubmed/27941672 [Accessed April 7, 2017].

LaFauci, G. et al., 2013. Fragile X Screening by Quantification of FMRP in Dried Blood Spots by a Luminex Immunoassay. *The Journal of Molecular Diagnostics*, 15(4), pp.508–517. Available at: http://www.ncbi.nlm.nih.gov/pubmed/23660422 [Accessed April 7, 2017].

Lang, P.J. et al., 1998. Emotional arousal and activation of the visual cortex: an fMRI analysis. *Psychophysiology*, 35(2), pp.199–210. Available at: http://www.ncbi.nlm.nih.gov/pubmed/9529946 [Accessed January 17, 2017].

Lang, P.J. et al., 2005. International Affective Picture System (IAPS): Technical Manual and Affective Ratings. *International Affective Picture System (IAPS)*. Available at: https://www2.unifesp.br/dpsicobio/adap/instructions.pdf [Accessed March 2, 2017].

Leehey, M.A. et al., 2008. FMR1 CGG repeat length predicts motor dysfunction in premutation carriers. *Neurology*, 70(16 Pt 2), pp.1397–402. Available at: http://www.ncbi.nlm.nih.gov/pubmed/18057320 [Accessed April 27, 2016].

Leehey, M.A. et al., 2003. The fragile X premutation presenting as essential tremor. *Archives of neurology*, 60(1), pp.117–21. Available at: http://www.ncbi.nlm.nih.gov/pubmed/12533098 [Accessed February 17, 2017].

Lewis, M.M. et al., 2011. Differential involvement of striato- and cerebello-thalamo-cortical pathways in tremor- and akinetic/rigid-predominant Parkinson's disease. *Neuroscience*, 177, pp.230–9. Available at: http://linkinghub.elsevier.com/retrieve/pii/S0306452210016994 [Accessed January 11, 2017].

Li, Y. & Jin, P., 2012. RNA-mediated neurodegeneration in fragile X-associated tremor/ataxia syndrome. *Brain research*, 1462, pp.112–7. Available at: http://www.ncbi.nlm.nih.gov/pubmed/22459047 [Accessed May 3, 2016].

Loesch, D.Z. et al., 2008. A low symptomatic form of neurodegeneration in younger carriers of the FMR1 premutation, manifesting typical radiological changes. *Journal of medical genetics*, 45(3), pp.179–81. Available at: http://www.ncbi.nlm.nih.gov/pubmed/18057083 [Accessed April 29, 2016].

Loesch, D.Z. et al., 2005. Evidence for, and a spectrum of, neurological involvement in carriers of the fragile X pre-mutation: FXTAS and beyond. *Clinical genetics*, 67(5), pp.412–7. Available at: http://www.ncbi.nlm.nih.gov/pubmed/15811008 [Accessed April 29, 2016].

Lozano, R., Hagerman, R.J., et al., 2014. Genomic studies in fragile X premutation carriers. *Journal of Neurodevelopmental Disorders*, 6(1), p.27. Available at: http://www.ncbi.nlm.nih.gov/pubmed/25170347 [Accessed April 11, 2017].

Lozano, R., Rosero, C.A. & Hagerman, R.J., 2014. Fragile X spectrum disorders. *Intractable & Rare Diseases Research*, 3(4), pp.134–146. Available at: http://www.ncbi.nlm.nih.gov/pubmed/25606363 [Accessed January 8, 2017].

Mak, M.K.Y. et al., 2016. Increased Cognitive Control During Execution of Finger Tap Movement in People with Parkinson's Disease. *Journal of Parkinson's Disease*, 6(3), pp.639–650. Available at: http://www.ncbi.nlm.nih.gov/pubmed/27372216 [Accessed December 30, 2016].

Mathersul, D., McDonald, S. & Rushby, J.A., 2013. Psychophysiological correlates of social judgement in high-functioning adults with autism spectrum disorder. *International Journal of Psychophysiology*, 87(1), pp.88–94. Available at: http://www.ncbi.nlm.nih.gov/pubmed/23183316 [Accessed April 7, 2017].

McConkie-Rosell, A., Heise, E.M. & Spiridigliozzi, G.A., 2012. Influence of Genetic Risk Information on Parental Role Identity in Adolescent Girls and Young Women from Families with Fragile X Syndrome. *Journal of Genetic Counseling*, 21(1), pp.59–71. Available at: http://www.ncbi.nlm.nih.gov/pubmed/21826579 [Accessed April 6, 2017].

Merino, S. et al., 2016. Associated Clinical Disorders Diagnosed by Medical Specialists in 188 FMR1 Premutation Carriers Found in the Last 25 Years in the Spanish Basque Country: A Retrospective Study. *Genes*, 7(10), p.90. Available at: http://www.ncbi.nlm.nih.gov/pubmed/27775646 [Accessed April 6, 2017].

Minkova, L. et al., 2015. Detection of Motor Changes in Huntington's Disease Using Dynamic Causal Modeling. *Frontiers in human neuroscience*, 9, p.634. Available at: http://www.ncbi.nlm.nih.gov/pubmed/26635585 [Accessed January 11, 2017].

Moore, C.J. et al., 2004. The effect of pre-mutation of X chromosome CGG trinucleotide repeats on brain anatomy. *Brain : a journal of neurology*, 127(Pt 12), pp.2672–81. Available at: http://www.ncbi.nlm.nih.gov/pubmed/15483045 [Accessed April 30, 2016].

Mumford, J.A. & Nichols, T.E., 2008. Power calculation for group fMRI studies accounting for arbitrary design and temporal autocorrelation. *NeuroImage*, 39(1), pp.261–268.

Murta, T. et al., 2016. Phase–amplitude coupling and the BOLD signal: A simultaneous intracranial EEG (icEEG) - fMRI study in humans performing a finger-tapping task. *NeuroImage*. Available at: http://www.ncbi.nlm.nih.gov/pubmed/27554531 [Accessed January 12, 2017].

Muzar, Z. et al., 2015. Methadone use in a male with the FMRI premutation and FXTAS. *American journal of medical genetics. Part A*, 167(6), pp.1354–9. Available at: http://doi.wiley.com/10.1002/ajmg.a.37030 [Accessed April 6, 2017].

Narcisa, V. et al., 2011. A Quantitative Assessment of Tremor and Ataxia in Female FMR1 Premutation Carriers Using CATSYS. *Current gerontology and geriatrics research*, 2011, p.484713. Available at: http://www.ncbi.nlm.nih.gov/pubmed/23008705 [Accessed February 17, 2017].

Nolin, S.L. et al., 2003. Expansion of the fragile X CGG repeat in females with premutation or intermediate alleles. *American journal of human genetics*, 72(2), pp.454–64. Available at: http://www.ncbi.nlm.nih.gov/pubmed/12529854 [Accessed April 28, 2016].

Nolin, S.L. et al., 1996. Familial transmission of the FMR1 CGG repeat. *American journal of human genetics*, 59(6), pp.1252–61. Available at: http://www.ncbi.nlm.nih.gov/pubmed/8940270 [Accessed April 28, 2016].

Nunomura, A. et al., 2012. The earliest stage of cognitive impairment in transition from normal aging to Alzheimer disease is marked by prominent RNA oxidation in vulnerable neurons. *Journal of neuropathology and experimental neurology*, 71(3), pp.233–41. Available at: http://www.ncbi.nlm.nih.gov/pubmed/22318126 [Accessed December 30, 2016].

O'Reilly, J.X. et al., 2010a. Distinct and Overlapping Functional Zones in the Cerebellum Defined by Resting State Functional Connectivity. *Cerebral Cortex*, 20(4), pp.953–965. Available at: http://www.ncbi.nlm.nih.gov/pubmed/19684249 [Accessed February 20, 2017].

O'Reilly, J.X. et al., 2010b. Distinct and Overlapping Functional Zones in the Cerebellum Defined by Resting State Functional Connectivity. *Cerebral Cortex*, 20(4), pp.953–965. Available at: https://academic.oup.com/cercor/article-lookup/doi/10.1093/cercor/bhp157 [Accessed February 20, 2017].

Oh, S.Y. et al., 2015. RAN translation at CGG repeats induces ubiquitin proteasome system impairment in models of fragile X-associated tremor ataxia syndrome. *Human Molecular Genetics*, 24(15), pp.4317–4326.

Van Overwalle, F. et al., 2014. Social cognition and the cerebellum: A meta-analysis of over 350 fMRI studies. *NeuroImage*, 86, pp.554–572. Available at: http://www.ncbi.nlm.nih.gov/pubmed/24076206 [Accessed May 12, 2017].

Penagarikano, O., Mulle, J.G. & Warren, S.T., 2007. The pathophysiology of fragile x syndrome. *Annual review of genomics and human genetics*, 8, pp.109–29. Available at: http://www.ncbi.nlm.nih.gov/pubmed/17477822 [Accessed April 28, 2016].

Prehn, K. et al., 2015. The neural correlates of emotion alignment in social interaction. *Social cognitive and affective neuroscience*, 10(3), pp.435–43. Available at: https://academic.oup.com/scan/article-lookup/doi/10.1093/scan/nsu066 [Accessed January 16, 2017].

Pretto, D. et al., 2014. Clinical and molecular implications of mosaicism in FMR1 full mutations. *Frontiers in genetics*, 5, p.318. Available at: http://journal.frontiersin.org/article/10.3389/fgene.2014.00318/abstract [Accessed April 7, 2017].

Pretto, D.I. et al., 2015. Differential increases of specific *FMR1* mRNA isoforms in premutation carriers. *Journal of Medical Genetics*, 52(1), pp.42–52. Available at: http://www.ncbi.nlm.nih.gov/pubmed/25358671 [Accessed February 24, 2017].

Primerano, B. et al., 2002. Reduced FMR1 mRNA translation efficiency in fragile X patients with premutations. *RNA (New York, N.Y.)*, 8(12), pp.1482–8. Available at: http://www.ncbi.nlm.nih.gov/pubmed/12515381 [Accessed January 8, 2017].

Qurashi, A. et al., 2011. Nuclear accumulation of stress response mRNAs contributes to the neurodegeneration caused by Fragile X premutation rCGG repeats. *PLoS genetics*, 7(6), p.e1002102. Available at: http://www.ncbi.nlm.nih.gov/pubmed/21655086 [Accessed January 10, 2017].

Radua, J. et al., 2014. Common and specific brain responses to scenic emotional stimuli. *Brain Structure and Function*, 219(4), pp.1463–1472. Available at: http://www.ncbi.nlm.nih.gov/pubmed/23700105 [Accessed January 16, 2017].

Sabatinelli, D. et al., 2005. Parallel amygdala and inferotemporal activation reflect emotional intensity and fear relevance. *NeuroImage*, 24(4), pp.1265–1270. Available at: http://www.ncbi.nlm.nih.gov/pubmed/15670706 [Accessed January 17, 2017].

Sabatinelli, D. et al., 2007. Pleasure Rather Than Salience Activates Human Nucleus Accumbens and Medial Prefrontal Cortex. *Journal of Neurophysiology*, 98(3), pp.1374–1379. Available at: http://www.ncbi.nlm.nih.gov/pubmed/17596422 [Accessed January 17, 2017].

Saul, R.A. & Tarleton, J.C., 1993. *FMR1-Related Disorders*, University of Washington, Seattle. Available at: http://www.ncbi.nlm.nih.gov/pubmed/20301558 [Accessed January 17, 2017].

Sellier, C. et al., 2010. Sam68 sequestration and partial loss of function are associated with splicing alterations in FXTAS patients. *The EMBO journal*, 29(7), pp.1248–61. Available at: http://emboj.embopress.org/cgi/doi/10.1038/emboj.2010.21 [Accessed January 17, 2017].

Selmeczy, D. et al., 2011. Investigation of amygdala volume in men with the fragile X premutation. *Brain imaging and behavior*, 5(4), pp.285–94. Available at: http://www.ncbi.nlm.nih.gov/pubmed/21786216 [Accessed April 29, 2016].

Seltzer, M.M. et al., 2012. Differential sensitivity to life stress in FMR1 premutation carrier mothers of children with Fragile X Syndrome. *Health Psychology*, 31(5), pp.612–622. Available at: http://www.ncbi.nlm.nih.gov/pubmed/22149120 [Accessed April 6, 2017].

Seritan, A.L. et al., 2008. Dementia in fragile X-associated tremor/ataxia syndrome (FXTAS): comparison with Alzheimer's disease. *American journal of medical genetics. Part B, Neuropsychiatric genetics : the official publication of the International Society of Psychiatric Genetics*, 147B(7), pp.1138–44. Available at: http://www.ncbi.nlm.nih.gov/pubmed/18384046 [Accessed April 27, 2016].

Seritan, A.L. et al., 2016. Risk Factors for Cognitive Impairment in Fragile X-Associated Tremor/Ataxia Syndrome. *Journal of Geriatric Psychiatry and Neurology*, 29(6), pp.328–337. Available at: http://www.ncbi.nlm.nih.gov/pubmed/27647792 [Accessed April 6, 2017].

Serrano-Pozo, A. et al., 2011. Neuropathological alterations in Alzheimer disease. *Cold Spring Harbor perspectives in medicine*, 1(1), p.a006189. Available at: http://www.ncbi.nlm.nih.gov/pubmed/22229116 [Accessed December 30, 2016].

Sévin, M. et al., 2009. Penetrance of marked cognitive impairment in older male carriers of the FMR1 gene premutation. *Journal of medical genetics*, 46(12), pp.818–24. Available at: http://jmg.bmj.com/cgi/doi/10.1136/jmg.2008.065953 [Accessed January 6, 2017].

Shah, S.G. et al., 2009. Amygdala and insula response to emotional images in patients with generalized social anxiety disorder. *Journal of psychiatry & neuroscience : JPN*, 34(4), pp.296–302. Available at: http://www.ncbi.nlm.nih.gov/pubmed/19568481 [Accessed April 2, 2017].

Sharma, N. & Baron, J.-C., 2014. Effects of Healthy Ageing on Activation Pattern within the Primary Motor Cortex during Movement and Motor Imagery: An fMRI Study X.-N. Zuo, ed. *PLoS ONE*, 9(6), p.e88443. Available at: http://dx.plos.org/10.1371/journal.pone.0088443 [Accessed January 12, 2017].

Shulman, C. et al., 2012. Moral and Social Reasoning in Autism Spectrum Disorders. *Journal of Autism and Developmental Disorders*, 42(7), pp.1364–1376. Available at: http://www.ncbi.nlm.nih.gov/pubmed/21960456 [Accessed April 7, 2017].

Soontarapornchai, K. et al., 2008. Abnormal nerve conduction features in fragile X premutation carriers. *Archives of neurology*, 65(4), pp.495–8. Available at: http://www.ncbi.nlm.nih.gov/pubmed/18413472 [Accessed April 27, 2016].

Stoodley, C.J., Valera, E.M. & Schmahmann, J.D., 2012. Functional topography of the cerebellum for motor and cognitive tasks: An fMRI study. *NeuroImage*, 59(2), pp.1560–1570. Available at: http://www.ncbi.nlm.nih.gov/pubmed/21907811 [Accessed January 27, 2017].

Sullivan, S.D., Welt, C. & Sherman, S., 2011. FMR1 and the continuum of primary ovarian insufficiency. *Seminars in reproductive medicine*, 29(4), pp.299–307. Available at: http://www.thieme-connect.de/DOI/DOI?10.1055/s-0031-1280915 [Accessed April 6, 2017].

Tassone, F. et al., 2008. A rapid polymerase chain reaction-based screening method for identification of all expanded alleles of the fragile X (FMR1) gene in newborn and high-risk populations. *The Journal of molecular diagnostics : JMD*, 10(1).

Tassone, F., Adams, J., Berry-Kravis, E.M., et al., 2007. CGG repeat length correlates with age of onset of motor signs of the fragile X-associated tremor/ataxia syndrome (FXTAS). *American Journal of Medical Genetics Part B: Neuropsychiatric Genetics*, 144B(4), pp.566–569. Available at: http://www.ncbi.nlm.nih.gov/pubmed/17427188 [Accessed January 6, 2017].

Tassone, F., Adams, J., Berry-Kravis, E.M., et al., 2007. CGG repeat length correlates with age of onset of motor signs of the fragile X-associated tremor/ataxia syndrome (FXTAS). *American journal of medical genetics. Part B, Neuropsychiatric genetics : the official publication of the International Society of Psychiatric Genetics*, 144B(4), pp.566–9. Available at: http://www.ncbi.nlm.nih.gov/pubmed/17427188 [Accessed April 27, 2016].

Tassone, F., Hagerman, R.J., Taylor, A.K., Mills, J.B., et al., 2000. Clinical involvement and protein expression in individuals with the FMR1 premutation. *American journal of medical genetics*, 91(2), pp.144–52. Available at: http://www.ncbi.nlm.nih.gov/pubmed/10748416 [Accessed April 5, 2017].

Tassone, F., Hagerman, R.J., Taylor, A.K., Gane, L.W., et al., 2000. Elevated levels of FMR1 mRNA in carrier males: a new mechanism of involvement in the fragile-X syndrome. *American journal of human genetics*, 66(1), pp.6–15. Available at: http://www.ncbi.nlm.nih.gov/pubmed/10631132 [Accessed May 3, 2016].

Tassone, F. & Berry-Kravis, E.M., 2010. *The Fragile X-Associated Tremor Ataxia Syndrome (FXTAS)*, New York, NY: Springer .

Todd, P.K. et al., 2013. CGG repeat-associated translation mediates neurodegeneration in fragile X tremor ataxia syndrome. *Neuron*, 78(3), pp.440–55. Available at: http://www.ncbi.nlm.nih.gov/pubmed/23602499 [Accessed May 3, 2016].

Todd, P.K. et al., 2010. Histone deacetylases suppress cgg repeat-induced neurodegeneration via transcriptional silencing in models of Fragile X Tremor Ataxia Syndrome. *PLoS Genetics*, 6(12).

Tzeng, C.-C. et al., 2005. Prevalence of the FMR1 mutation in Taiwan assessed by large-scale screening of newborn boys and analysis of DXS548-FRAXAC1 haplotype. *American journal of medical genetics. Part A*, 133A(1), pp.37–43. Available at: http://www.ncbi.nlm.nih.gov/pubmed/15637705 [Accessed April 28, 2016].

Verheij, C. et al., 1993. Characterization and localization of the FMR-1 gene product associated with fragile X syndrome. *Nature*, 363(6431), pp.722–724. Available at: http://www.ncbi.nlm.nih.gov/pubmed/8515814 [Accessed April 7, 2017].

Verheij, C. et al., 1995. Characterization of FMR1 proteins isolated from different tissues. *Human molecular genetics*, 4(5), pp.895–901. Available at: http://www.ncbi.nlm.nih.gov/pubmed/7633450 [Accessed April 7, 2017].

Verkerk, A.J. et al., 1993. Alternative splicing in the fragile X gene FMR1. *Human molecular genetics*, 2(4), pp.399–404. Available at: http://www.ncbi.nlm.nih.gov/pubmed/8504300 [Accessed April 7, 2017].

Wang, J.M. et al., 2012. Male carriers of the FMR1 premutation show altered hippocampal-prefrontal function during memory encoding. *Frontiers in human neuroscience*, 6, p.297. Available at: http://www.ncbi.nlm.nih.gov/pubmed/23115550 [Accessed April 30, 2016].

Wang, J.Y. et al., 2012. Age-dependent structural connectivity effects in fragile x premutation. *Archives of neurology*, 69(4), pp.482–9. Available at: http://www.ncbi.nlm.nih.gov/pubmed/22491193 [Accessed April 29, 2016].

Wang, J.Y., Hessl, D., et al., 2013. Fragile X–Associated Tremor/Ataxia Syndrome. *JAMA Neurology*, 70(8), p.1022. Available at: http://archneur.jamanetwork.com/article.aspx?doi=10.1001/jamaneurol.2013.2934 [Accessed April 29, 2016].

Wang, J.Y., Hagerman, R.J. & Rivera, S.M., 2013. A multimodal imaging analysis of subcortical gray matter in fragile X premutation carriers. *Movement disorders : official journal of the Movement Disorder Society*, 28(9), pp.1278–84. Available at: http://www.ncbi.nlm.nih.gov/pubmed/23649693 [Accessed April 30, 2016].

Whalley, L.J. et al., 2013. Genetic and environmental factors in late onset dementia: possible role for early parental death. *International Journal of Geriatric Psychiatry*, 28(1), pp.75–81. Available at: http://www.ncbi.nlm.nih.gov/pubmed/22821632 [Accessed April 10, 2017].

Wheelwright, S. et al., 2006. Predicting Autism Spectrum Quotient (AQ) from the Systemizing Quotient-Revised (SQ-R) and Empathy Quotient (EQ). *Brain research*, 1079(1), pp.47–56. Available at: http://linkinghub.elsevier.com/retrieve/pii/S0006899306000722 [Accessed January

20, 2017].

Wolf, E.J. et al., 2013. Sample Size Requirements for Structural Equation Models: An Evaluation of Power, Bias, and Solution Propriety. *Educational and psychological measurement*, 76(6), pp.913–934. Available at: http://www.ncbi.nlm.nih.gov/pubmed/25705052 [Accessed April 10, 2017].

Woodbury-Smith, M.R. et al., 2005. Screening adults for Asperger Syndrome using the AQ: a preliminary study of its diagnostic validity in clinical practice. *Journal of autism and developmental disorders*, 35(3), pp.331–5. Available at: http://www.ncbi.nlm.nih.gov/pubmed/16119474 [Accessed January 17, 2017].

Yang, J.-C. et al., 2013. Neural substrates of executive dysfunction in fragile X-associated tremor/ataxia syndrome (FXTAS): a brain potential study. *Cerebral cortex (New York, N.Y. : 1991)*, 23(11), pp.2657–66. Available at: http://www.ncbi.nlm.nih.gov/pubmed/22918986 [Accessed April 27, 2016].

Young, A. et al., 2002. Facial Expressions of Emotion: Stimuli and Tests(FEEST). *Psychology manual*, (January).

Zapparoli, L. et al., 2013. Mental images across the adult lifespan: a behavioural and fMRI investigation of motor execution and motor imagery. *Experimental brain research*, 224(4), pp.519–40. Available at: http://link.springer.com/10.1007/s00221-012-3331-1 [Accessed January 12, 2017].

Appendix

4.1.

Instructions for the scanner tasks

1. The pictures task

- This task is approximately 7 minutes long.
- The task uses pictures from the 'International Affective Picture System' and is designed to look at your emotional responses to the pictures.
- Please look at each picture and use the LEFT and RIGHT trigger buttons to indicate your responses to the pictures. The responses will be categorised as "Face" or "No Face", where "Face" refers to the presence of a face in the picture.
- In this task, animals are also classified as having faces.
- During the task there will be some black screens with a cross-hair in the middle, please just focus on the cross-hair during these screens. The screen will go blank at the end of the task.
- The pictures will stay up for approximately 3 seconds each, and will change regardless of whether you indicate a "Face"/"No Face" answer, so please answer within this time frame if you can.
- As this task is designed to elicit emotional responses, you may find some of the images slightly distressing.

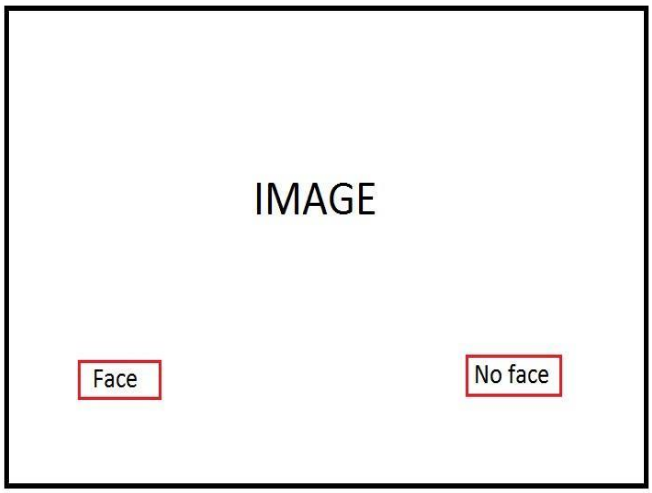

2. The finger-tapping task

- This task is approximately 6 minutes long.
- The task asks you to tap your fingers (on trigger buttons in the scanner) and is designed to look at movement processing in the brain.

- There are two different types of tapping you will be asked to do, ‘sequential’ and ‘random’, and there are also rest periods.
    - In the ‘sequential’ condition, the task requires you to tap your fingers in a row in time with a flashing **#** symbol – ie. Left thumb, left finger, right thumb, right finger.
    - In the random condition, you will be asked to tap the buttons in a random order in time with a flashing **?** symbol – ie. Left thumb, right thumb.
    - In the rest condition, you are asked to simply watch the flashing **+** symbol. There will be a prompt before each condition, reminding you of these instructions.

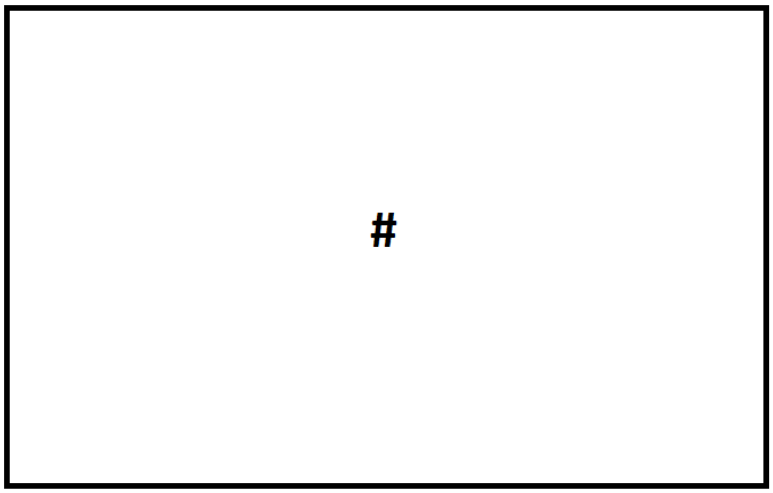

4.2

Motor task behavioural test form

This task for use in an fMRI scanner is approximately 6 minutes long.

The task asks you to tap your fingers (on a keyboard or trigger buttons in the scanner) and is designed to look at movement processing in the brain. For these tests, the buttons on the keyboard that you will use are **1 and 2** for your left hand and **9 and 0** for your right hand. In the 'sequential' condition, the task requires you to tap your fingers in a row in time with a flashing **#** symbol – ie. 1, 2, 9, 0. In the random condition, you will be asked to tap the buttons in a random order in time with a flashing **?** symbol – ie. 1, 9, 9, 2. In the rest condition, you are asked to simply watch the flashing **+** symbol. The screen will go blank at the end of the task.

Your feedback from these tasks will help to determine whether they are suitable for use in an fMRI scan. Thank you ☺

1. Were you clear on how to do the task, or did you find it confusing?

(Not really, it was confusing) 1 2 3 4 5 (Yes, it was simple)

2. How engaged were you in the task?

(Not much) 1 2 3 4 5 (A lot)

3. How did you find the 'sequential' tapping condition? (i.e. was it easy to do, were you able to keep up with the flashing symbol?)

_____

_____

4. How did you find the 'random' tapping condition? (i.e. was it easy to do, were you able to keep up with the flashing symbol?)

_____

_____

5. Did you find that you began to lose interest in the task towards the end? Yes / No

If so, to what extent? (Please describe) _____

6. Do you have any other comments?

_____

_____

4.3

CATSYS formula relating performance index to performance below average:

$$\boldsymbol{PI = 1 \div \ominus \left((P - Pm) \div s\,(Pm)\right)}$$

CATSYS formula relating performance index to performance above average:

$$\boldsymbol{PI = 2 - \ominus\,(1 \div (P - Pm) \div s\,(Pm))}$$

PI = performance index

P = performance as measured and calculated by CATSYS

Pm = Mean performance of large, sound population defined in the test battery

s (Pm) = standard deviation of normal human performance defined in the test

7.1

	Description	Slide No.	Valence Mean	Arousal Mean
	High pleasure, low arousal			
1	Family	2332	7.18	4.2
2	Children	2341	6.78	3.59
3	Man	2357	5.33	3.06
4	Woman	2372	5.35	3.39
5	Band	2373	6.8	4.92
6	Girl	2381	5.54	3.76
7	Fish	1900	6.4	3.04
8	Medical worker	2394	5.36	3.85
9	Porpoise	1920	7.83	4.21
10	Baby	2070	7.69	4.02
11	Balloons	2791	6.02	3.58
12	Couple	2501	6.33	2.67
13	Woman	2506	5.8	4.14
14	Couple	2550	7.37	4.15
15	Shadow	2880	5.13	2.68
16	Food basket	2980	5.48	3.09
17	Mountains	5631	7.08	4.31
18	Cave	5661	6.02	4.36
19	Beach	5836	7.08	4.47
20	Romance	4622	6.7	4.11

	Description	Slide No.	Valence Mean	Arousal Mean
	High pleasure, high arousal			
1	Teens	2389	6.38	5.26
2	Dancer	2616	6.13	5.06
3	Woman	2030	7.51	6.24
4	Bride	2209	7.12	5.04
5	Erotic female	4220	7.81	6.64
6	Attractive fem	4250	8.39	7.02
7	Attractive fem	4275	7.51	6
8	Couple	4598	6.55	5.25
9	Romance	4599	7.02	5.73
10	Romance	4606	6.37	5.1
11	Shark	5622	6.44	5.38
12	Windsurfers	5623	7.12	5.56
13	Earth	5890	6.6	5.17
14	Fireworks	5910	7.41	5.37
15	Wedding	4626	7.36	5.45
16	Erotic couple	4645	6.56	5.56
17	Waterfall	5260	7.47	6

18	Skydivers	5621	7.28	6.96
19	Turkey	7230	7.42	5.81
20	Sky	5982	7.38	5.25

	Description	**Slide No.**	**Valence Mean**	**Arousal Mean**
	Low pleasure, low arousal			
1	Boy	2410	4.72	3.83
2	Sad girls	2455	3.32	4.26
3	Elderly man	2480	4.76	2.8
4	Toddler	2095	2.16	4.69
5	Angry face	2100	4.3	3.77
6	Angry face	2120	3.65	4.93
7	Fingerprint	2206	3.91	3.56
8	Girl	2276	3.17	4.02
9	Mother	2312	4	3.77
10	Disabled child	3300	3.14	4.14
11	Erotic male	4538	4.59	2.9
12	Beach boys	4542	4.92	3.75
13	Police	2682	3.98	4.43
14	Refugees	2695	4.49	4.26
15	Woman	2700	3.33	4.52
16	Alcoholic	2753	3.37	3.93
17	Actor	2780	4.75	4.7
18	Tourist	2850	4.69	2.58
19	Crying boy	2900	2.76	4.76
20	Tornado	5970	4.31	4.65

	Description	**Slide No.**	**Valence Mean**	**Arousal Mean**
	Low pleasure, high arousal			
1	Baby	2661	3.22	5.18
2	Open chest	3250	3.92	6.1
3	Dental exam	3280	3.83	5.72
4	Injury	3550	3.1	5.69
5	Bomb	2692	4.02	5.11
6	Sad children	2703	2.33	5.73
7	Drug addict	2710	3.04	5.29
8	Pipe	2716	3.48	5.21
9	Gun	2811	2.84	6.31
10	Deer head	2981	3.55	5.54
11	Scream	3022	4.28	5.61
12	Surgery	3210	4.83	5.27
13	Medical assist	3216	3.6	5.3
14	Lava	5940	4.79	6.42
15	Tornado	5972	4.11	6.38

16	Electric chair	6020	4.1	5.23
17	Aimed gun	6200	3.36	5.8
18	Attack	6211	4.25	5.38
19	Terrorist	6213	3.75	5.25
20	Gang	6242	3.28	5.09

	Description	**Slide No.**	**Valence Mean**	**Arousal Mean**
	Neutral pleasure, low arousal			
1	Men	2397	5.06	3.12
2	Neutral girl	2441	4.95	3.48
3	Man	2512	4.96	3.63
4	Neutral woman	2038	5.08	2.98
5	Woman	2830	5.09	3.93
6	Chess	2840	4.92	2.31
7	Plant	5740	5.07	2.36
8	Plate	7233	5.01	2.51
9	Mug	7009	4.96	2.69
10	Fan	7020	5.02	2.15
11	Baskets	7041	4.96	2.68
12	Tool	7056	4.98	3.24
13	Keyring	7059	5.04	2.96
14	Book	7090	4.95	2.3
15	Fabric	7160	4.98	3.06
16	Pole	7161	4.99	2.79
17	Abstract art	7184	4.94	3.44
18	Abstract art	7186	4.98	3.48
19	Beads	7207	5	3.31
20	Clock	7211	4.98	3.7

	Description	**Slide No.**	**Valence Mean**	**Arousal Mean**
	Neutral pleasure, high arousal			
1	Shark	1931	4.51	6.88
2	Shark	1932	4.81	6.21
3	Male fale	2220	5.21	5.04
4	Sick baby	3302	5	5.69
5	Surgery	3210	4.83	5.27
6	Lava	5940	4.79	6.42
7	Aimed gun	6410	4.43	5.6
8	Freeway	7560	4.42	5
9	Skyscraper	7640	5.31	6.21
10	Police	6840	4.43	5.96
11	Aircraft	6900	5.15	6.02
12	Missiles	6930	4.46	5.17
13	Tank	6940	4.77	5.17

14	Boy	9411	4.99	5.61
15	Rock climber	8160	5.54	6.9
16	Boxer	8231	4.6	5.17
17	Nudists	8466	5.45	5.04
18	Biking/train	8475	5.57	5.04
19	Biker on fire	8480	4.5	5.83
20	Soldiers	2704	5.25	5.24

7.2

IAPS behavioural test form

This task for use in an fMRI scanner is approximately 7 minutes long.

The task uses pictures from the 'International Affective Picture System' and is designed to look at your emotional responses to the pictures. Please look at each picture and use the LEFT and RIGHT arrow buttons on the keyboard to indicate your responses to the pictures. The responses will be categorised as "Face" or "No Face", where "Face" refers to the presence of a face in the picture. In this task, animals are also classified as having faces. During the task there will be some black screens with a cross-hair in the middle, please just focus on the cross-hair during these screens. The screen will go blank at the end of the task. The pictures will stay up for approximately 3 seconds each, and will change regardless of whether you indicate a "Face"/"No Face" answer, so please answer within this time frame if you can.

Your feedback from these tasks will help to determine whether they are suitable for use in an fMRI scan. Thank you ☺

1. How much did you focus on the content of the pictures during the task?

(Not much) 1 2 3 4 5 (A lot)

2. Did you find that choosing "Face" or "No Face" distracted you from looking properly at the images?

(No, not at all) 1 2 3 4 5 (Yes, a lot)

3. Did you find choosing "Face" or "No Face" at all confusing or difficult?

(No, not at all) 1 2 3 4 5 (Yes, a lot)

If so, please describe:

_____

_____

4. Were you clear on how to do the task, or did you find it confusing?

(Not really, it was confusing) 1 2 3 4 5 (Yes, it was simple)

5. Did you think that some of the images were quite emotional?

(No, they were not emotional) 1 2 3 4 5 (Yes, they were emotional)

6. Did you find any of the pictures that were shown particularly disturbing? Yes / No

If so, which ones? (Please describe)

_____

7. Would you object to being shown these particular pictures without first being informed of their nature? Yes / No

8. Did you find that you began to lose interest in the task towards the end? Yes / No

If so, to what extent? (Please describe) _____

9. Do you have any other comments?

_____

_____